2003-12

Final Report

The Effects of Transverse Stiffener Beams on Shear Transfer

Minnesota Local Road Research Board

Research

Technical Report Documentation Page

1. Report No.	2.	3. Recipients Accession No.
MN/RC – 2003-12		

4. Title and Subtitle	5. Report Date
THE EFFECT OF TRANSVERSE STIFFENER BEAMS ON SHEAR TRANSFER	January 2003
	6.

7. Author(s)	8. Performing Organization Report No.
Henryk Stolarski, Paul Bergson, Khalid Obeidat, Carol Shield	

9. Performing Organization Name and Address	10. Project/Task/Work Unit No.
University of Minnesota Department of Civil Engineering 500 Pillsbury Drive S.E. Minneapolis, MN 55455	11. Contract (C) or Grant (G) No. (c) 74708 (wo) 65

12. Sponsoring Organization Name and Address	13. Type of Report and Period Covered
Minnesota Department of Transportation Office of Research Services 395 John Ireland Boulevard Mail Stop 330 St. Paul, Minnesota 55155	Final Report
	14. Sponsoring Agency Code

15. Supplementary Notes

http://www.lrrb.gen.mn.us/PDF/200312.pdf

16. Abstract (Limit: 200 words)

There are many wooden bridges in the United States. Their decks are often built of timber beams nailed together and covered with asphalt. The asphalt plays a mechanical role, and it provides environmental protection for the wood deck. The asphalt layer deteriorates and requires replacement. That leads to a faster deterioration of the deck, increased maintenance, and shorter bridge life.

The flexibility of the deck is a probable cause of the fast deterioration of the asphalt. Low temperatures lead to deformations of the deck and may lead to cracks, which are propagated by mechanical and environmental effects.

This project investigates stiffening the bridge deck by connecting a beam perpendicularly to the deck planks with metal bolts to reduce deformations of the deck. The additional beam is called a "Transverse Stiffener Beam" (or TSB). It can be incorporated as a part of new bridges or be attached to existing bridges.

The investigations show the TSB significantly reduces deformations of the deck in most cases. The study indicates the positive effects of the TSB's should be expected in other applications. The magnitude of the effects can be analyzed with the computer program developed during this project.

17. Document Analysis/Descriptors		18.Availability Statement
Transverse Stiffener Beam TSB Wooden Bridge	Deterioration Asphalt	No restrictions. Document available from: National Technical Information Services, Springfield, Virginia 22161

19. Security Class (this report)	20. Security Class (this page)	21. No. of Pages	22. Price
Unclassified	Unclassified	101	

THE EFFECT OF TRANSVERSE STIFFENER BEAMS ON SHEAR TRANSFER

FINAL REPORT

Paul Bergson
Khalid Obeidat
Carol Shield
Henryk Stolarski

University of Minnesota
Department of Civil Engineering
500 Pillsbury Drive S.E.
Minneapolis, MN 55455

January 2003

Minnesota Department of Transportation
Office of Research Services
200 Ford Building Mail Stop 330
117 University Avenue
St Paul Minnesota 55155-1899

TABLE OF CONTENTS

Executive Summary

There are many wooden bridges on the country roads in the state of Minnesota and in the greater United States, and new wooden bridges are constantly erected. Often, their decks are built of timber beams, nailed together against their wider face, and covered with a layer of asphalt that, in addition to playing a mechanical role in the system, is expected to provide environmental protection for the wooden deck. Although these bridges serve very well in general, the asphalt layer deteriorates quickly and needs to be replaced frequently. This problem not only increases a bridge's maintenance cost, but leads to faster deterioration of the deck and, consequently, to shorter bridge life.

The asphalt layer probably deteriorates quickly due to the high flexibility of the deck on which it rests. Asphalt can be very brittle, particularly at low temperatures. Excessive deformations of the deck may lead to cracking which then propagate and magnify as a result of both mechanical and environmental effects.

This project investigates the idea of stiffening the deck by adding a beam perpendicular to the planks of the deck and connected to it by metal bolts. This beam would reduce deformations of the deck and alleviate the asphalt-cracking problem. The additional beam, called here the "Transverse Stiffener Beam" (TSB), can be easily attached to the existing bridges (underneath their decks) and even more easily incorporated as a part of the newly constructed bridges. So, it is a viable method of retrofitting existing bridges.

The results of the investigations, described in this report, show that addition of the TSB to a bridge does indeed reduce deformations of its deck. Depending on the position of the load (at the center or side of the bridge) the influence of the TSB varies, but in each case it is positive, and in most practical cases it can be classified as significant. While the study described here does not cover many practical situations, it clearly indicates that in those cases not covered here the TSB's positive effects should be expected. In each specific design case, the computer program developed as a result of this project can be used to analyze the magnitude of those effects.

CHAPTER 1
INTRODUCTION

Longitudinally nail laminated (LNL) timber bridge decks are commonly used on low-traffic, rural routes throughout the USA (1). They consist of a series of wood timbers nailed together against their wide face, with a single nail typically spanning the width of three timbers, although other nailing patterns may also exist. The individual timbers are usually 2-4 in. wide and 4-12 in. deep, and deck dimensions are on the order of 30 ft. in span and 24 ft. in width (2). The deck is typically simply supported on a pair of piers. The deck tested within this project was fabricated by Wheeler Corporation. Its dimensions and the nailing pattern are provided in the sequel.

Many of the existing LNL decks are now 30-50 years old and placed on county roads. Over time, they have become notorious for poor long-term performance and consequent high maintenance costs (3). One of the main problems is the surprisingly quick deterioration of asphalt forming the top surface of wooden bridges. A primary reasons for adding asphalt is protecting the wood. Unfortunately, quickly deteriorating asphalt surface not only fails to protect the deck's wood, it makes the surface uneven, which imparts additional dynamic forces to the structure. This accelerates the negative effects of fatigue and shortens the bridge's life causing negative financial implications.

One of the principal reasons for the rapid deterioration of asphalt layers on wooden bridges is the relatively high flexibility (or small stiffness) of the deck. This flexibility leads to highly localized deformations, associated with large differential movement between the planks, that the asphalt layer cannot withstand. This might be particularly true in low temperatures, when asphalt becomes quite stiff and brittle. It is farther hypothesized that such high flexibility occurs primarily because of the inadequate coupling between individual planks, which, in existing bridges, is provided only by the nails. This is further exacerbated by the fact that the nail laminations have shown low resistance to fatigue, causing the nail connections to loosen (1). This reduces the deck plank's ability to distribute the load across the bridge.

The fatigue process is accelerated when asphalt deterioration progresses to a point where the surface of the bridge becomes rough. The additional vibration that this causes magnifies the negative effects of fatigue. Under those conditions, just replacing the asphalt on the bridge,

without some additional stiffening of the deck, is bound to lead to an increasingly frequent asphalt layer replacement.

The methods, results, and conclusions of a research program addressing this situation are described in this report. The hypothesis leading to this research state that the durability of LNL timber bridges can be improved by adding one or more Transverse Stiffener Beam (TSB) running in the direction perpendicular to the laminates (or planks). Figure 1.1 depicts the general configuration of a LNL deck with attached TSBs. It was hypothesized that such beams would increase overall stiffness of the deck, by distributing a bigger fraction of the load, which is typically quite local, to the laminations located farther away from the point of load application. This would reduce internal forces in the bridge, as well as its total deformation, and would, therefore, mitigate stress-related negative effects, such as quick deterioration of asphalt. To the authors' best knowledge, a solution of this kind has not been rigorously analyzed in the past, although the TSBs were used. Its simplicity and low cost, as well as perceived benefits, seem to justify research on the influence of TSBs on response of LNL bridges.

The attachment of TSBs to the underside of the deck can be easily used as a retrofit for existing LNL decks and would compensate for weakened nail laminations. On a newly built deck, they would perhaps reduce wear and prevent loosening of the connections.

If TSBs can be proven efficient and effective in improving the performance of LNL timber bridge decks, they would be an economical solution to problems posed by deterioration. They are inexpensive to fabricate, because they can be made of the same material and approximately the same dimensions as the deck timbers themselves. They can be easily attached to the deck using three or more bolts per TSB and only standard bridge equipment.

The objective of this research is to assess the benefits of TSBs to an LNL deck. The goal was pursued in two complementary ways: numerical and experimental. Development of a numerical model of the problem was to facilitate future exploration of with different design and retrofit options without need for costly and time consuming experiments. Given the complexity of the system, which is seriously magnified by the geometric irregularities ubiquitous in timber, the reliability of the computer model can only be assessed by simultaneous numerical and experimental analysis of at least one problem. Thus, in this project, both numerical modeling and experimental investigations are conducted in parallel for the same bridge.

In order to observe the changes in deck behavior with the addition of TSBs, a typical LNL deck, constructed by Wheeler Corporation, was tested in the Civil Engineering Structures Lab. Displacement measurements were used to evaluate the behavior of the deck under three loading conditions and three TSB configurations. The deck was then subjected to cyclic loading, with the number of cycles corresponding approximately to 30 years of traffic loading. After cycling tests, the effects of the TSBs on the bridge were tested in a static manner. For reasons described in the subsequent sections, the load for static and fatigue testing was of different magnitude.

The bridge configuration used in the experimental investigations was also analyzed numerically, using the computer program developed expressly for that purpose. Comparison of the results and extensive discussion is provided in Section 4.2.

The following report outlines both the basic features of the numerical model and the experimental procedure used in analysis. The results of static testing before, during, and after cyclic loading are presented and, when appropriate, compared to the values obtained from simulations. The authors' interpretation of those results and findings, both from the point of view of the methodology used and in regards to the benefits of TSB members, is also given.

CHAPTER 2
BASIC FEATURES OF NUMERICAL MODEL

Technical aspects of the finite element model developed to simulate the behavior of longitudinally laminated wood bridge decks are described in this section.

The model of the deck pursued in this project assumes that each plank behaves as a beam that, in addition to bending in the vertical plane, undergoes torsion. Torsion occurs as a result of interaction between the planks provided by the nail connections, Fig. 2.3. Each of the nail connections is assumed to act as a spring (or system of springs), which resists the relative motion between the neighboring planks in each of the three spatial directions. As a result, there are three constants characterizing each nail connection, one for each of the coordinate directions. These constants are obtained from experiments conducted in parallel with the experiments on the entire bridge assembly. The material used in those experiments was the same as the material of the deck (Douglas fir) and was provided by the Wheeler Corporation along with the deck. Experiments conducted to obtain the properties of the nail connections are described in the following sections of the report. Properties of the planks are described by the standard values used in analysis for Douglas fir.

The TSB, if present, is also modeled as a beam but, in variance with the model of the planks, its torsional effects have been assumed to be negligible. This assumption appears appropriate in view of the fact that the TSBs are suspended underneath the deck, have free ends, and only a small number (three in the present project) of screws connecting it to the deck. Thus, the only mechanism by which TSBs provide additional stiffness to the system is their bending which is activated as a result of common displacements with the deck.

A computer program to analyze the bridge was written using Matlab as a computer language and the finite element method as a numerical tool. The basic technical ingredients of the program are described in the subsequent sections. The program also contains a graphical used interface, which described in Appendix A.

2.1 Coordinate System and Nodal Numbering Scheme

The coordinate system is defined so that the x-axis is parallel to the axis of the planks. The origin of the coordinate system lies on the first end of the first plank. The z-axis lies in the plane of the bridge, and the y-axis is defined in such a way as to produce a right-handed coordinate system (x,y,z). There is a node at each nail connection and at both ends of the planks. The coordinate axes and the nodal numbering system are shown on Fig. 2.1a.

The planks are numbered so that plank number one coincides with the x-axis. Plank numbers increases with increasing z coordinate. The nodal numbering scheme starts at the beginning of the first plank (i.e., the origin of the coordinate system) and progresses along the plank until the end of that plank, then moves consecutively to the subsequent planks.

The nodal and elemental numbering scheme is shown in Fig. 2.1. Numbering of the connector elements is shown in Fig. 2.2.

2.2 The Finite Element Model.

For the purpose of modeling the bridge is divided into three components, Fig. 2.3. These are:

1. The wood laminations or planks.
2. Nail connections.
3. Transverse beams.

The whole system has been assumed to act as a grid, in which nails and, if present, transverse beams are agents forcing planks to interact. Consequently, it has been assumed that three displacements (degrees of freedom) describe deformation of the bridge. Those are vertical displacement and two rotations about axes located within the plane of the deck, one parallel and the other is perpendicular to the planks.

2.3 Plank Elements

The wood laminations were modeled as grid elements (beams undergoing bending and torsion) lumped along the centroids of the planks. The planks were discretized into finite elements whose length is equal to the distance between the neighboring nails. The stiffness matrix of plank element is:

$$k_{plank} = \begin{bmatrix} \frac{12EI}{L^3} & 0 & \frac{6EI}{L^2} & -\frac{12EI}{L^3} & 0 & \frac{6EI}{L^2} \\ 0 & C_T & 0 & 0 & -C_T & 0 \\ \frac{6EI}{L^2} & 0 & \frac{4EI}{L} & -\frac{6EI}{L^2} & 0 & \frac{2EI}{L} \\ -\frac{12EI}{L^3} & 0 & -\frac{6EI}{L^2} & \frac{12EI}{L^3} & 0 & -\frac{6EI}{L^2} \\ 0 & -C_T & 0 & 0 & C_T & 0 \\ \frac{6EI}{L^2} & 0 & \frac{2EI}{L} & -\frac{6EI}{L^2} & 0 & \frac{4EI}{L} \end{bmatrix} \qquad (2.1)$$

The above matrix corresponds to the following arrangement of the element degrees of freedom

$$d = \begin{bmatrix} w_I & \theta_{XI} & \theta_{ZI} & w_J & \theta_{XJ} & \theta_{ZJ} \end{bmatrix} \qquad (2.2)$$

with *w* representing displacement perpendicular to the deck (directed along vertical axis y), θ_X being rotations about the axis of the plank (x-axis, that is) and θ_z standing for rotations about the z-axis (horizontal axis perpendicular to planks), while the indices I and J represent two ends of the plank element.

In equation (2.1) ***E*** is the Young modulus of the timber (modulus of elasticity), ***I*** is the moment of inertia of the plank about the z-axis and *L* is the length of the plank element (equal to the nail spacing). C_T is defined as:

$$C_T = \beta a b^3 G \qquad (2.3)$$

Where G is shear modulus parallel to the grains, a is plank depth, b is plank width and β is computed from the following table (this computation is done automatically in the program):

a/b	β
1	0.141
1.5	0.196
2	0.229
2.5	0.249
3	0.263
4	0.281
5	0.291
10 >	0.312

2.4. Nail Connection

The nails were modeled as linear springs (or system of springs), connecting neighboring planks, and resisting relative motion of the planks in all three spatial directions, (x, y and z). These springs model only one aspect of the load transfer mechanism between the adjacent plank laminations; the other aspect is related to the transverse shear beams, if present, which is described next. The action of the nails is illustrated on Fig. 2.4 and Fig. 2.5.

The resulting stiffness matrix for the nails (both) the upper part of the plank as well as in the lower part) is:

$$k_n = \begin{bmatrix} k_q & -k_q W & 0 & -k_q & -k_q W & 0 \\ -k_q W & k_w H^2 + k_q W^2 & 0 & k_q W & -k_w H^2 + k_q W^2 & 0 \\ 0 & 0 & k_p H^2 & 0 & 0 & -k_p H^2 \\ -k_q & k_q W & 0 & k_q & k_q W & 0 \\ -k_q W & -k_w H^2 + k_q W^2 & 0 & k_q W & k_w H^2 + k_q W^2 & 0 \\ 0 & 0 & -k_p H^2 & 0 & 0 & k_p H^2 \end{bmatrix} \quad (2.4)$$

The above matrix is related to the set of degrees of freedom given in equation (2.2) with I, J being the ends of the connector, and k_P is the shear stiffness of the nail connection parallel to grains (x direction), k_q is the shear stiffness of the nail connection perpendicular to grains (y-direction), whereas k_w is nail withdrawal stiffness (z direction), H is the vertical distance from the neutral axis of the plank to the nail location, and W is the plank's half width of the plank as automatically selected by the program.

2.5. Transverse Beams

As described earlier, the transverse beams (TSB) are used to aid in distributing the load between the planks and reduce the differential deflections of the planks. The stiffness matrix for the transverse beam element is:

$$k_{TSB} = \begin{bmatrix} \frac{12EI}{L^3} & \frac{-6EI}{L^2} & 0 & -\frac{12EI}{L^3} & \frac{-6EI}{L^2} & 0 \\ -\frac{6EI}{L^2} & \frac{4EI}{L} & 0 & \frac{6EI}{L^2} & \frac{2EI}{L} & 0 \\ 0 & 0 & 0 & 0 & 0 & 0 \\ -\frac{12EI}{L^3} & \frac{6EI}{L^2} & 0 & \frac{12EI}{L^3} & \frac{6EI}{L^2} & 0 \\ -\frac{6EI}{L^2} & \frac{2EI}{L} & 0 & \frac{6EI}{L^2} & \frac{4EI}{L} & 0 \\ 0 & 0 & 0 & 0 & 0 & 0 \end{bmatrix} \quad (2.4)$$

As can be seen, it has been assumed that the effects of torsional stiffness of the TSB are negligible. This matrix refers to a displacement vector analogical to the one given in equation (2.2), but for properly selected I, J.

2.6. Computation of Internal Forces (Post-processing)

2.6.1. Calculation of Plank Forces

Bending moment, torsional moment, and shear forces in the plank finite elements are computed following the procedure outlined below:

a. Obtain the local displacement vector ***d*** for a plank element, as presented in equation (2.2)
b. Compute local stiffness matrix described by equation (2.1)
c. Compute the force vector:

$$f = k_{plank} d \tag{2.5}$$

2.6.2. Calculation of Forces in the Nails

The forces in the nails are computed as follows:

a. Identify the end nodes of the nail element and retrieve the displacement vector *d,* of equation (2.2)

b. Compute relative displacements:

$$\begin{Bmatrix} \Delta x \\ \Delta y \\ \Delta z \end{Bmatrix} = \begin{Bmatrix} -\theta_{XJ}\dfrac{W_{pl}}{2} + \theta_{XI}\dfrac{W_{pl}}{2} \\ w_J - w_I + (\theta_{XJ} + \theta_{XI}) * W_{pl} \\ \vartheta_{XJ}\dfrac{W_{pl}}{2} - \theta_{XI}\dfrac{W_{pl}}{2} \end{Bmatrix} \tag{2.6}$$

Where W_{pl} is the width of the plank.

c. Compute forces in the nail:

$$\begin{Bmatrix} f_x \\ f_y \\ f_z \end{Bmatrix} = \begin{Bmatrix} k_p \Delta x \\ k_q \Delta y \\ k_w \Delta z \end{Bmatrix} \tag{2.7}$$

The resultant shear and axial forces are:

$$shear = \sqrt{f_y{}^2 + f_x{}^2}$$
$$axial = f_z \tag{2.8}$$

2.6.3. TSB Forces

a. Retrieve local degrees of freedom (displacements) associated with a TSB element, as specified in the equation (2.2).
b. Recreate k_{TSB} for a TSB element of the equation (2.4).
c. Compute forces:

$$kd = \begin{Bmatrix} T_I \\ M_I \\ 0 \\ T_J \\ M_J \\ 0 \end{Bmatrix} \tag{2.9}$$

The forces computed using equations (2.5)-(2.9), as well as displacements and rotations, can be displayed graphically, as illustrated in the section containing some representative results.

CHAPTER 3
EXPERIMENTAL INVESTIGATIONS

There have been two types of experiments conducted within this project. The goal of the experiment of the first type was to identify the three properties of the nail connections (k_p , k_q and k_w) needed in the numerical modeling of the bridge. Three groups of experiments where needed in this regard, corresponding to the three constants needed to characterize the nail connections; these experiments were conducted in the U of M's Department of Wood and Forest Products. The goal of experiments of the second type was to investigate behavior of the entire bridge, and contrast this behavior with the results obtained by numerical modeling; these experiments were conducted in the structural engineering laboratory of the U of M's Department of Civil Engineering. Both types of experiments are described below.

3.1 Determination of Properties for the Nail Connections

Nail Pull Test (k_w)

Nails were pulled from wood blocks to find the axial stiffness of the nail connections. Diameter of the nails was 3/8 in. and they were driven into 5/16 in. diameter holes, predrilled in 4 in. wood blocks. Thus, the test conditions were very similar to those in the real bridge deck. The experimental setup is illustrated in Fig 3.1 Typical axial load-displacement curves emerging from this test are illustrated in Fig. 3.2. (See next paragraph for some comments regarding that figure.) The calculated axial stiffness of the nail connection (denoted in Chapter 2 by k_w) was found to be 16,750 lb/in. This value, although representative for the conditions in the lab, is expected to vary slightly with moisture and temperature fluctuations. Thus, to capture the behavior of a bridge in specific conditions, the experiments aimed at characterization of the nail connections should, ideally, be conducted in those conditions. However, given a large variety of conditions a typical bridge is subjected to, an average value like the one reported earlier in this paragraph is likely to be satisfactory in all practical applications.

Figures 3.2, 3.4, and 3.5 may leave the reader with an incorrect impression that some nails slipped substantially before their load carrying capacity was activated. However, the perceived slip is actually related to the manual repositioning of the plotting pen to a new origin prior to the start of some new experiments. It was done to avoid excessive overlapping of the curves obtained from different experiments and to increase clarity with which individual curves can be identified. In fact, the results obtained from different experiments were quite reproducible.

NailShear Test (k_p and k_q)

For this test the nails were driven into the timber in exactly the same way as for the pull-out test, but the experimental setup was like the one shown on Fig. 3.3. This set-up was identical for investigating the shear stiffness in both directions, parallel (k_p, x direction) and perpendicular to grain (k_q, y direction). The load-displacement curves obtained in this experiment are shown in Fig. 3.4 (for the test in direction parallel to grain) and in Fig. 3.5 (for the test perpendicular to grain). The corresponding values of the stiffness were, correspondingly k_p = 25,000 lbs/in. and k_q = 11,750 lbs/in. Just like axial stiffness, the shear stiffness values will fluctuate with the moisture and temperature of wood.

3.2 Experiments with the Bridge Deck

The timber deck specimen was designed to be a scale replica of typical timber bridge decks existing in the field. It was assembled and furnished by the Wheeler Lumber in South Dakota. The deck, three transverse stiffener beams, and the accompanying bolts were then shipped for testing in the Civil Engineering Structures Laboratory.

3.2.1. Description of Test Specimen

LNL Timber Bridge Deck

The longitudinal nail laminated bridge deck (LNL deck) was made of 21 Douglas fir planks. Each timber was 4 in. wide, 12 in. deep, and 20 ft. long. The assembled deck had planar dimensions 7 ft. by 20 ft., and it was 12 in. thick. The scale of the test deck was approximately two-thirds of a typical deck used in bridges (typical LNL decks in the field have dimensions on the order of 24 ft. by 30 ft.).

The nail laminations between timbers were such that each nail penetrated three timbers, and the nails were staggered between lower and upper positions of the depth along the length of the deck, as shown in Fig. 3.6. The spikes used were 3/8 in. in diameter and 12 in. long.

The timber deck was simply supported on 2.5 in. diameter steel rollers placed within 4 in. by 2 in. steel channels. The steel channels were spot welded to a W27x94 steel section that was in turn bolted to the strong floor of the lab using 1.5 in. diameter threaded rod. The W27x94s were braced with a 3 in. x 3 in. x 5/16 in. tube mounted on steel plates and bolted to the floor at an angle of 27^{o}. They were also stiffened with 0.5 in. plates welded to the cross-section of the beams near the brace locations. All steel sections were ASTM A36 and the threaded rods were of high strength steel. Fig. 3.7 is a photo of the support structures.

For convenience of discussion, the deck can be described by its orientation relative to the structures lab. Its length ran in the north-south direction, and accordingly, the transverse stiffener beams ran in the east-west direction. The timbers were numbered from 1 to 21 in ascending order from east to west, as shown in Fig. 3.8.

It was discovered after disassembly that the four timbers on the west side of the deck were connected to the rest of the deck with a slightly weaker spike configuration. Nails between Timber 17 and Timber 18 were omitted at alternating top and bottom positions, so that these timbers had only two-thirds the nails that they should have. This was probably because, in the manufacturing process, nailing of timber started from one side of the deck and ended at the other (as opposed to adding the planks on both sides of the initial plank). Under those circumstances, it is understandable that the side at which nailing started could have fewer nails. Upon testing, the

effects of these missing spikes were apparent in a reduced initial stiffness of the west side over the east side and center portions of the deck, as documented in Section 4.1.2.

Stiffener beams

The transverse stiffener beams (TSB) were also made of Douglas fir cut to a size of 6 in. wide, 12 in. deep, and 7 ft. long. Each had three pre-drilled holes located at the center and at 18 in. from either end. This corresponds to holes drilled in the deck in the center of Timbers 5, 11, and 17. The 0.75 in. diameter bolts used for connection were 26 in. in length and made of galvanized steel. The head diameters were 3 in., and there were 2.5 in. x 2.5 in. x 0.25 in. plate washers for the bottom.

The TSBs were placed at the exact center and quarter spans of the deck, corresponding to 5 ft., 10 ft., and 15 ft. along the length, as can be seen in Figure 3.8. The "attached" position meant that the TSB bolts were hand-tightened to a snug fit, as would be the expected field procedure. When unattached, the bolts were loosened and the TSB left to hang about 2 in. from the bottom of the deck.

Complications with assembly

When the stiffener beams and deck arrived, it contained the holes drilled in both the deck and the TSBs for mounting. However, the TSBs had warped considerably with the holes drilled in only roughly the correct locations. The fits were tight. On the north beam, one of the holes had to be expanded in order to align with the deck. It may be noted that due to warping of wood and the thickness of the beams, it would be beneficial in field applications to drill both the deck and beam holes at the same time to avoid complications with assembly.

3.2.2. Loading System

The bridge deck was loaded using three 77 kip (350kN) hydraulic actuators suspended over the center of the deck. They were attached to the deck using 0.75 in. diameter lag screws that were fed through the actuator swivel and into the deck where 0.5 in. holes had been drilled

10 in. deep in the deck timbers. The actuators were centered on the 2nd timbers from the edges, Timbers 2 and 20, and the center timber, Timber 11. The lag screws were in the approximate centers of the adjacent timbers. At the center location (Timber 11) a plate with a 3 in. diameter hole cut in the center was placed between the actuator swivel and the deck to make room for the TSB bolt attachment. The actuator swivels had a 9.5 in. x 9.5 in. cross-section. The 9.5 in. width is on the same order as the width of a tire for a small truck.

The load frame was made of a W24x131 steel spreader beam with 0.5 in. stiffeners located at each of the actuator mount locations. The spreader was mounted on two braced W12x65 columns that were bolted to the strong floor of the lab with 1.5 in. diameter high-strength threaded rod. The braces were connected to the column with six 0.75 in. bolts at approximately 6 ft. from the floor. They were attached to floor beams with six more bolts, and the floor beams then bolted to the strong floor. The actuators were braced at their free ends with a W18x71 section mounted to the columns. Figure 3.9 is an elevation of the load frame assembly, and Figure 3.10 shows the entire test set-up.

3.2.3. Instrumentation

The instrumentation consisted of Linear Variable Differential Transformers (LVDT's) placed at regular intervals across the deck to measure relative displacements. Separation LVDT's were installed near the load points, but the data they produced was noisy and of very low magnitude. All gages were wired to the central data acquisition system in the CE lab (National Instruments SCXI System). Dial gages were placed at the corners of each support to measure support settlement at peak loading during testing.

Displacement LVDT's

LVDT's for measuring displacement were mounted on every third timber, beginning on Timber 2, in three lines along the length of the deck: midspan line, 2.5 ft. from midspan, and 6 ft. from midspan. On the 2.5 ft. and 6 ft. lines, the LVDT's on Timber 5 were omitted due to lack of available instrumentation. These points were chosen because Timber 5 was not directly beneath any load point, and it was relatively far from the position of cyclic loading on the west

side of the deck. Two LVDT's were placed on the center timber (Timber 11) in corresponding positions 2.5 ft. and 6 ft. from midspan on the far side of the deck to verify symmetrical behavior along the deck length. Each LVDT was labeled according to its timber number and longitudinal location. For example, the name of the LVDT placed on the center timber at midspan was 11C. The LVDT's on the same timber at 2.5 ft. from midspan on the south side of the deck was named 11MS and at 6 ft. from midspan was named 11S.

The displacement LVDT's were mounted to the deck using an aluminum plate with a threaded hole in the center. An aluminum rod was screwed into both the plate and the core of the transducer. The plates were connected to the centers of the timbers with wood screws. On the floor, four small I-beams were placed along the instrumentation lines. Holes were drilled into the flanges at 12 in. intervals (every third beam), and pressed wood clamps were bolted to the beams to hold the LVDT's. The steel beams were heavy enough to hold the LVDT's securely in place during testing, so the displacement of the deck timber relative to the floor was measured. The majority of displacement LVDT's were 1-in. LVDT's, however, some 2-in. LVDT's were used in positions underneath the actuators, and one 0.5-in LVDT was used at a distant location. The names, locations, and sizes of all LVDT's can be seen in Figure 3.11. Figure 3.12 shows the mounting for displacement LVDT's.

Separation LVDT's

Three LVDT's were mounted between timbers to measure separation underneath the center and west load points and next to the west actuator. They were mounted in a similar way as the displacement LVDT's, using the same clamps and aluminum plates. In this case, a bent aluminum section with a threaded hole was connected to one timber using wood screws. The LVDT clamp was mounted on another aluminum plate and screwed to the adjacent timber, so that the system would measure the relative separation between the timbers. Separation was measured with 0.1 in. size LVDT's. Figure 3.13 shows the mounting for separation LVDT's.

Dial Gages

Two dial gages, each with a magnetic base, were mounted on the support beams at the corners of the deck. A 2 in. x 4 in. wood section was nailed to the corner in order to provide enough space for the gage so that the displacement of the corner relative to the support could be monitored, as shown in Figure 3.14. The position of the two gages was alternated between the north and south corners of the deck. The measurements were taken at peak loads for each actuator and were intended to indicate any motion of the deck off of the supports.

3.2.4. Testing Procedure

Static testing of the bridge deck with actuators run under load control provided the basis for analysis of displacements based on the TSB configuration (zero, one, or three) and the variation between loading points. The deck was then subject to cyclic loading (1.2 million cycles) on the west edge with the intention of simulating approximately 30 years of traffic (assuming 400,000 cycles per year) to loosen the nail laminations. Selection of the load for cycling testing is described in the sequel. Finally, another set of static tests, identical to the first, was run to assess the effects of the cyclic loading.

Static Testing

Several preliminary static tests were to provide the basis for determining the required load range for each actuator to achieve the prescribed displacement of $2L/500$ (0.91 in.) for the 20 ft. deck. This limit is typically imposed by the codes as a serviceability limit for beams under bending. Here it was used somewhat arbitrarily only to establish loading conditions that would be somewhat related to practice. That was deemed sufficient to determine the TSBs' effect on the overall behavior of the bridge. Of course, the real loads on the bridges are different not only in terms of their magnitude, but also in terms of the number of loads. Those real loads have to be considered in designing the actual bridges. Although it would be difficult to reproduce them exactly in the laboratory, the computer program prepared within this project can handle arbitrary

load configurations and can be used to investigate various design options under very realistic loading conditions.

The load-stroke curve from one of these tests for each actuator (west, center, and east), as shown in Figure 3.15, was used to determine the correct load for each individual actuator to achieve the required displacement. The loads were found to be 17 kips for the west actuator, 18.2 kips for the east actuator, and 34 kips for the center actuator. For simplicity, it was decided to use the value of 17 kips, or half of 34 kips, for both west and east actuators.

The dial gage readings during the preliminary tests also indicated that the deck would rotate off the support when loaded on the east or west side, so each actuator was set with a constant 2 kips to simulate dead load. As a result, the load range used for all static tests was 2-19 kips for the east and west actuators, and 2-36 kips for the center actuator. The three actuators were run consecutively in a single test, from east to west, for each TSB configuration. The first tests were on the bare deck; then one TSB was attached at midspan. The two TSBs at quarter points were then added for a total of three stiffeners, and then tests were done on the initial condition without TSBs. Table 3.1 shows the sequence in which the various combinations of load points and TSB placements were tested.

At least two data sets were taken for each location, resulting in at least eight initial static data sets. The test numbers in Table 3.1 indicate the name of the data set used for analysis. Test trials were numbered beginning at 001, but not all tests yielded a full set of data.

Cyclic Loading

The deck was subjected to cyclic loading on the west side only and without TSBs. Initially, the load range was set at 2-16 kips at 0.75 Hz under the assumption that the full deflection of 0.9 in. was not necessary for the cyclic conditioning. However, after 9,500 cycles, it was determined by inspection that even the reduced load range was producing too much deflection. The cycling was not meant to bring about failure, but a large crack had formed through a knot (defect!) in Timber 21, directly under the west actuator. The range was cut in half at that point, and the deck was cycled from 2-9 kips for the remaining 1.2 million cycles, lasting

about 12 days. This level provided reasonable deflections, and the propagation of the crack soon slowed and stopped. Static tests were taken periodically to monitor the effect of the cyclic loading.

Final Static Tests

The final set of the static tests were run in a sequence identical to the first. Data was taken for loading at all three points and under all three TSB placements. Again, two data sets were taken for each configuration and dial gage readings taken at peak loads.

CHAPTER 4
RESULTS

4.1. Observed Deck Behavior

The deck behavior during each stage of loading was observed through a record of the maximum displacements that occurred at peak loads. During testing, it was clear that the attachment of TSBs did change the values of displacements at each LVDT location. The magnitude of those changes and the resulting profiles of deflections are described below.

4.1.1. Assumptions

During testing, it was assumed that the deck would act as a simply supported beam in the longitudinal direction, and therefore, would deflect symmetrically along the 20 ft. span. In this case, instrumentation on both halves would be redundant. Figure 4.1 shows the deflections at four points along the Timber 11. LVDTs 11N and 11S were located 6 ft. from either side the deck's midspan, and 11MN and 11MS were 2.5 ft. from either side of the deck midspan. The load-deflection curves shown were taken from static tests on the virgin deck. The load was applied at the center of the deck and repeated for the cases with zero, one, and three attached TSBs.

The two pairs of LVDT's at locations situated symmetrically with respect to the midspan symmetry line followed identical paths on the load-deflection curves both with and without attached TSBs. The identical response on either half of the deck shows that the deck behaved symmetrically on both sides of the midspan line of symmetry. Thus, there was no hidden asymetry associated, for example, with the nailing pattern (as was the case with respect to the longitudinal line of symmetry described elsewhere in this report). Consequently, only one half of the deck had to be instrumented, and the data from that one half of the deck can be assumed to be accurate for the points located symmetrically with respect to midspan line of deck.

In addition, the linearity of the load-displacement curves in Figure 4.1 indicate that the deck behaved linear-elastically, as expected for the range of loads applied.

Data from the separation LVDT's is not included in the following sections describing the deck behavior. Little change in separation was measured, and the data that was collected was inconsistent. Furthermore, the information from the displacement LVDT's was clear and provided a complete picture of the deck behavior, as described in the following sections.

4.1.2. Effect of Transverse Stiffeners on the Virgin Deck

The initial static test on the virgin deck without stiffeners resulted in maximum deflections of 1.0 in., 1.05 in. and 1.17 in. at the midspan east, center, and west locations of the load, respectively. From these first observations, it can be seen that the displacements of the virgin deck were greater on the west side in the transverse direction. This result was consistent with the discovery that there were fewer connecting nails between Timbers 18-21 on this side. With fewer nail laminations to promote sharing the load between timbers, those directly under the load point carried more load and had higher deflections. It will be seen that this skew towards the west side remained constant throughout testing.

Figure 4.2 shows the maximum deflections at midspan for the timbers directly beneath the load points. The deflections shown were a function of the loading location, shown along the top axis, and the number of TSBs attached, shown along the bottom axis. On the bare deck, it is clear that the loads remained concentrated on the timbers adjacent to the load points. Deflections four to five timbers transversely away from the load points were minimal, approximately one-tenth of those directly under the load.

After the attachment of the TSB at midspan, maximum defections at the load points were considerably reduced, approximately 0.2 in. at each location. Simultaneously, deflections four to five timbers transverse from the load point increased on the same order that the maximums decreased, indicating improved load sharing between timbers. Furthermore, when the deck was loaded on an edge, the opposite side rose off the support significantly more than without the TSB. Although the maximum negative deflections underneath the load points were not identical after the attachment of one TSB, the rotation off the support was almost identical for the east and west sides.

Figure 4.3 shows the displacements of every third timber at midspan, resulting in a profile of the deck deformation at this cross-section. From this figure, it can be seen that the

profile became more linear with the addition of one TSB. The rotation off the supports during loading on the east or west side is also illustrated. When loaded on the west side, Timber 6 has no displacement, and Timber 1 to Timber 5 have a negative deflection. The opposite is true for loading on the east side; Timber 16 has no displacement, and Timber 17 to Timber 21 show deflection away from the supports.

The transverse behavior of the deck at locations closer to the supports was similar to the patterns shown at midspan. Figures 4.4 and 4.5 illustrate the maximum displacements at lines 2.5 ft. (L/10) away from midspan and 6 ft. (L/3.33) away from midspan. The changes after the addition of the single TSB were proportional to those at the center. The maximum displacements were reduced, and the positive displacements were increased. There was a slight variation when loaded in the center, with the response slightly more symmetrical in the transverse direction than those at midspan.

The addition of two TSBs at the quarter points had almost no additional effect beyond the deflection reductions due to the single TSB attached at midspan. The maximum deflections at midspan were reduced by less than 0.04 in. at all locations in both the positive and negative directions. The changes at 2.5 ft. and 6 ft. from midspan were proportionally smaller.

4.1.3 Effect of Cyclic Loading on the Deck

The objective of the cyclic loading was to simulate traffic usage on the bare deck. The west side of the deck was loaded for approximately 1.2 million cycles at 0.75Hz with a load range of 2-9 kips. The cyclic loading on this side was expected to result in more nail loosening and to reveal effects of cycling loading more clearly, because the west timbers held fewer nails. Cycling experiment on the east side was not performed due to the considerable amount of time it requires; it was assumed that cyclic loading on the west side is representative.

Figures 4.6 and 4.7 illustrate the softening of the deck stiffness during cycling. Effective stiffnesses were determined from static tests that were taken at several points during cycling. The stiffness was taken as the slope of the load-deflection curve and was calculated for points along Timber 20, directly under the west actuator, and at the midspan of Timber 11. It can be seen from these figures that the majority of softening on the loaded timber due to cycling occurred within the first 300,000 cycles. By this time, a crack had formed through a knot on the

far west timber (Timber 21), but its propagation had stopped. However, the stiffenesses shown were calculated for Timber 20, so the effects of this crack on the results would be minimal.

The remaining million cycles showed almost no further change in stiffness, indicating with good confidence that continued cycling would not have damaged the nail laminations further. The effects of the cycling were localized to the four to five timbers on the west side approximately 3 ft. from the loading point along their lengths. The effective stiffness of the center timber remained constant throughout, indicating that nail laminations remained intact and unaffected by the cyclic loading. This result is consistent with initial static tests on the bare deck showing little load sharing beyond the five timbers adjacent to the load location.

4.1.4 Effect of Transverse Stiffeners After Cyclic Loading

The effects of load cycling were localized to the west side of the deck, so the response in the center and east locations should have been, and was, almost identical to previous tests. Figure 4.8 illustrates that the maximum deflections at midspan were high when no stiffeners were attached, decreased considerably with one TSB at midspan, and remained effectively constant with the addition of quarter-span TSBs. The deformed shapes of the deck, as illustrated in Figure 4.9, closely resemble the profiles observed before cycling, shown in Figure 4.3.

The west side had a slightly larger initial maximum deflection than before cycling at 1.21 in. With the addition of the midspan TSB, however, the reduction in the maximum was actually slightly greater than before, while the response of the east and center for the west side load remained constant. In addition, the west side of the deck now displayed slightly higher rise from the support for east side loading.

The center loading condition showed more transverse asymmetry than before cycling. With the midspan TSB attached, the east side of the deck experienced more deflection as the west side of the deck experienced less. It seems that although the TSB could compensate for weakened nail laminations directly under the load point, the sharing from a distant load point was not improved. As a result, the east side of the deck carried more load in response to loosened laminations of the west timbers.

Again, similar patterns occurred at locations 2.5 ft. and 6 ft. longitudinally from the midspan in that deflections were considerably reduced with the addition of one TSB and essentially the same after the attachment of the quarter-point TSBs, as shown in Figures 4.10 and 4.11. The deflections at points away from the loading location appeared proportional to those at midspan. However, the values of the maximum deflections at 2.5 ft. and 6 ft. from midspan were essentially unchanged from the previous tests, even on the west side of the deck. This result is curious considering that the effective stiffenesses all along Timber 20 were shown to have reduced during the cyclic loading.

When loaded in the center with one attached TSB, the displacements appeared even more asymmetrical in the transverse direction than those at midspan. The east side of the deck experienced considerably more deflection than the west side of the deck at 6 ft. from midspan. The change from before cycling is especially apparent at this location, because previously, there was near-perfect transverse symmetry for this condition.

At all locations both transverse and longitudinal, the effects of the two quarter-point TSBs were marginal, with almost no change in maximum deflections.

The response of the LNL deck to the addition of transverse stiffener beams was consistent with predicted behaviors. The assumptions made were proven to be correct, and the measured deflections gave a clear picture of the changes resulting from the addition of TSBs.

4.1.5. Discussion of Experimental Results

Based on the behavior outlined in the previous section, it is clear that TSBs do indeed reduce vertical (perpendicular to the deck) deflections on both new and worn LNL decks. This is evident from Figs 4.3 and 4.9. Those figures also show that slopes of the vertical displacements across the bridge are also smaller when the TSB is added. Smaller slopes of total displacements indicate reduction in differential displacements between the planks achieved by addition of the TSB. Consequently, bridges with the TSBs are likely to need less maintenance than those without them. This finding is confirmed by the numerical results discussed later. However, in determining how TSBs should be applied in practice, various effects need further examination. For example, the behavior of the deck is different when looking at the center timbers versus those located on the edges. Furthermore, the behavior looks different when examining the points

directly beneath the applied load and the TSB locations than looking at the points away from the applied load and TSB locations.

The following sections examine some of these effects based on the maximum deflections at each load point, as well as a factor called the effective width (b_E). The effective width is a calculation of the width of a solid timber deck that would yield the same deflection under the same load as the LNL deck experienced. It was obtained by solving the deflection equation for a simply supported beam for the width, given the depth, length, deflection, and modulus of elasticity.

At the midspan of the deck

$$b_E = PL^3/(4h^3E\delta) \qquad (4.1)$$

At length x from the support

$$b_E = Px(3L^2-4x^2)/(4h^3E\delta) \qquad (4.2)$$

Where P is the applied load, L is the span length, h is the deck thickness and E is the modulus of elasticity. The modulus of elasticity, E, was taken to be 2000 ksi, a typical value for wood.

The effective width is useful in representing the extent to which the load is transferred through the nail laminations. A solid deck would not experience the slip or the losses of shear transfer that occurs on the nail-laminated deck. A solid deck could experience shear lag so that the effective b of the solid deck may not exactly equal the actual width of the deck (b_{act}) of 7 ft., but these losses would be small compared to the losses in shear transfer through the nail laminations. Accordingly, the closer the effective width is to the actual width (b_{act}) of the deck, the more efficiently the load is being distributed across the deck width.

4.1.5a Deck Response Near the Applied Load and TSB

The effectiveness of a TSB located directly beneath the load point is examined first, occurring at the midspan of the tested deck. Table 4.1 shows the maximum deflections and values of b_E at the midspan of Timbers 2, 11, and 20 when the load was applied to the east,

center, and west load points, respectively. Because the quarter-point TSBs had almost no effect on the peak displacements at midspan, as discussed in Section 4.1.2, calculations were only completed for the deflections of the bare deck and the deflections after the attachment of the single, midspan TSB.

Effects of the Midspan TSB on the Outer Timbers of the Deck

The effective width of the deck when loaded on the east or the west sides of the deck was quite low, 20% of the deck width of 7 ft. The west side of the deck remained consistently softer than the east side of the deck due to the reduced number of nails, even after the addition of a TSB. However, the improvement in stiffness with the TSB, as shown by the change in effective width, was equal on both sides, indicating that the initial deflections did not have much effect on the ability of the TSB to reduce deck deflections.

Even though only the west side was subject to cyclic loading, the entire deck lost some stiffness after cycling according to the effective width calculation. The change in stiffness due to cycling appeared to be localized to the west side of the deck, as discussed in Section 4.1.3; however, the decrease in b_E on the west side of the bare deck after cycling was equal to the decrease in b_E on the east side of the deck, at approximately 0.5in.

However, the east and the west sides of the deck did behave differently with the attachment of the midspan TSB after cycling. The final values of b_E after cycling were slightly higher at both the east and west locations, but the changes in the final deflections from before to after cycling at these locations were small. This apparent increase in performance of the TSB is most likely a result of the uncertainty of the torque applied to the TSB connecting bolts. The TSBs were hand tightened as snug as possible by the same person in both cases. Although this act places the variation of torque in a reasonably small range, the exact torque applied was not measured. Because the changes were small, they seem to lie within the range of error of this uncertainty.

Still, the west side of the deck experienced a greater increase in b_E with the addition of the midspan TSB than did the east side of the deck from before to after cycling. Before cycling, the TSB had a greater impact on the east side, with Δb_E at 3.5 in., than on the west side, with Δb_E at 3.0 in. After cycling, Δb_E was almost the same on the east and west sides of the deck. The

slight increase in the tightness of the TSB bolts may have contributed to a more uniform effect of the TSB to reduce deflections across the deck width.

Effects of the Midspan TSB on the Interior Timbers of the Deck

The deflections of the center timbers of the deck due to a load at the center of the deck resulted in significantly larger values of effective width than the outer timbers of the deck. The resistance to deflection had contributions from timbers on either side of the center load point, and therefore, had twice as many nails and timbers to resist the imposed loads than were present when the edge of the deck was loaded. As was expected, the value of b_E in the center of the deck was approximately twice the value of b_E calculated on the edges of the deck.

The effects of the TSB, however, were almost three times as great on the center of the deck. The value of b_E in the center of the deck increased by 10.7 in. after the addition of one TSB on the virgin deck, while the value of b_E for the outer timbers increased approximately 3 in. The TSB contributed stiffness from both sides of the load location. It may have also acted to increase the friction forces between timbers, an effect that would also be doubled in the center as compared to the edges. In both instances, the beneficial effects from the TSB were amplified as compared to the effects at the edge loading positions.

After cycling, the loading at the center of the bare deck resulted in a slightly lower b_E than before cycling, even though the effective stiffness at this location was shown to remain constant (Section 4.1.2). There was considerable improvement when the midspan TSB was attached, but the response was very similar to that before cycling. As a result, the final value of the effective width calculated in the center of the deck was lower after cycling, whereas the final value of b_E calculated for the outer timbers of the deck was higher after cycling. The tightness of the TSB to the deck affected its performance more on the outer deck timbers than on the interior deck timbers.

Although the attachment of the midspan TSB had a greater impact on the interior deck timbers than on the exterior timbers, the TSBs were effective in reducing deflections across the entire deck width when located directly beneath the applied load.

4.1.5b. Deck Response at a Length of *L*/8 from the Applied Load and TSB

The previous section dealt with measurements taken at points directly beneath the locations of load applications and at the location of one of the attached TSBs. However, in a field application the load would be moving along the deck, so it is relevant to consider the deflections away from the loading locations and the TSBs. The line of instrumentation at 2.5 ft. (*L*/8) from the deck midspan was used. The loads were applied at midspan; the LVDTs at *L*/8 lie halfway between the midspan and quarter point TSB locations. In this discussion, the cases of zero, one, and three attached TSBs will be considered in order to see the reduction effects between the TSB and support and also between two stiffeners. In the following discussion the results presented in Table 4.2 are quite informative.

Effects of TSBs on the Outer Timbers of the Deck

The deck behavior at these locations was similar, but not identical to, the behaviors observed at the deck's midspan. The west side of the deck still had a lower initial stiffness than the east side of the deck, but the relative difference in calculated effective widths on the bare, virgin deck was smaller when considering deflections at *L*/8 from midspan than for deflections at midspan, even though nails were missing on the west side along the entire deck span. Because the timbers were not subject to direct loading at this point, the slip between Timbers 17 and 18 was apparently less acute.

As at midspan, the increase in b_E after the addition of one TSB was the same on both the east and west edges of the deck, indicating that the initial stiffness did not have any affect on the ability of the TSB to reduce deflections. The additional TSB attached at the quarter-point (5 ft. from midspan) resulted in very little change in deflections at these locations.

After cycling, the initial values of b_E did not change on either the east or the west sides, which is consistent with the very small change in effective stiffness observed during cycling at this point on Timber 20 (Section 4.1.2). Nevertheless, as at midspan, the attachment of TSBs produced greater values of b_E after cycling. Apparently, the effects of tightening the TSB connection bolts were still present away from the TSB location. The midspan TSB had more effect on the west side of the deck than on the east, resulting in increases in b_E of 6.2% and 4.9%,

respectively. Although the initial deflections of the outer timbers were not changed by cycling, the reductions in deflections due to the TSB were. The behavior of the deck timbers at $L/8$ from the load and TSB was very similar to the behavior directly beneath these points.

With the attachment of the quarter-point TSB, the final calculated values of b_E on the east and west sides of the cycled deck were exactly the same. The extra quarter-point stiffener did not change the deflections much, but it brought the deck into a state of transversely symmetrical behavior. Although this seems like a desirable effect in that the load sharing between timbers was more uniform across the deck width, the additional TSB may not be worth this small benefit.

Effects of TSBs on the Interior Timbers of the Deck

The observed behaviors of the center, interior timbers at a distance $L/8$ from the deck midspan were very similar to those at the midspan of the timbers. Calculations of b_E were almost three times higher in the center of the deck than on the edges, and about 1 in. greater than those at the midspan of the same timbers.

The addition of the TSB at midspan increased the value of b_E at this location by about 11 in., which is very close to the increase calculated at midspan of 10.7 in. The quarter-point TSBs increased b_E more in the center of the deck than on the edges of the deck, but the percent of increase was still small at only 2.4%.

As at midspan, the center of the bare deck experienced more deflection after cycling even though there were no recorded changes in the effective stiffness of Timber 11 during cycling. In this case, the midspan TSB did not completely compensate for the increase in deflections due to cycling, and the value of b_E remained lower than it had been for the virgin deck. The differences between the behavior at the center midspan and in the center of the deck at length $L/8$ from the midspan were small. Although the values of deflections were smaller and of the effective widths were higher at $L/8$ from midspan, the changes due to the attachment of a TSB were approximately the same.

4.2. Numerical Results.

4.2.1. Comments on Assumptions Made in Numerical Analysis.

Before discussing the results obtained experimentally we present some comments on additional assumptions made in numerical analysis, which complement those presented in Section 2:

a. It has been assumed that the simple support of the deck is bi-directional, i.e. the supports prevent the bridge deck from lifting up.
b. There is a perfect fit between the TSBs and the deck at the nodes where the two components of the structure are connected by bolts. This assumption was translated into the requirement that the TSB' and the bridge deck have the same degrees of freedom at the connecting nodes.
c. Torsional stiffness of the TSBs was assumed to be negligible.

It was, of course, recognized early on that all of those assumptions (and, in fact, the whole model) are only more or less justifiable approximations of reality. However, considering the fact that the model development takes a lot of time and had to start at the beginning of the project, well before the experiments performed, the quality of those approximations could be ascertained only at a later stage of the project, when the experimental and numerical results became available.

Computations performed within this project used no adjustable coefficients. The modulus of elasticity was taken from the manuals to be E=1,900ksi, and the stiffness of the nail connections were obtained in independent experiments. Those experiments and the resulting values of the stiffness in the nail axial and shear directions are presented in section 3.1. Some difficulties were encountered in identifying the correct value of the shear modulus of elasticity for the planks in direction parallel to grain, which is needed to evaluate torsional stiffness of the planks. It has been assumed that the shear modulus is equal to 1/10 of the modulus of elasticity, i.e., 190ksi.

For the purpose of numerical computations it has been assumed that the nail spacing is 1ft. and that at each nail connection two nails are present (top and bottom). However, as described in section 3.2.1, the nail location is more complicated. The nails are staggered; they penetrate only three planks and, therefore, it is practically impossible to ascertain at what location the nails have developed full load caring capacity. This is perhaps the main reason for lack of symmetry about longitudinal axis of the deck in experiments. With this in mind the assumption made about location of connections is perhaps the best one can do, without going into technical sophistication that would appear unwarranted for this type of project.

4.2.2. Numerical Results for the Load at the Center of the Deck.

Two sets of results for the case not involving a TSB are included in this report: one for the load located at the center of the deck and the other for the load on one side. The location and magnitude of the loads are exactly like those used in experiments. Since the model used is perfectly symmetric, the numerical results for the loads on either side of the deck would be identical.

Deck Without TSB.

Displacements for the load located at the center of the deck are shown in Fig. 4.12. The maximum numerical value of the deflection is about 1.009 in. which should be compared to about 1.05 obtained experimentally and shown on Fig 4.3. Given the complexity of the system (nails location, nonuniformity of the support, weakening resulting from drilling) and uncertainty about the material properties used in computations (connection stiffness was obtained independently, under somewhat different conditions), this should be regarded as a remarkable agreement. The agreement is not as good at the edge of the deck where numerically obtained value of displacement is about 0.1 in. while the experimental value is about 0.2 in. However, this is a small value in both cases and, for the load located at the center, its significance is small.

Figures 4.13, 4.14, and 4.15 show distribution of the plank-bending moments, torsional moments, and resultant shear forces in the nails (which are the same in top and bottom nails).

These results could not be obtained experimentally and are shown here to indicate what kind of additional information can be extracted in the process of computations. This information is critical in the design process.

Deck with One TSB.

The primary variable of interest, transverse displacement, is shown on Fig. 4.16. Its distribution over the area of the deck is markedly different from the distribution not taking the TSB into account., and it is much more uniform in direction perpendicular to the planks. So the TSB does seem to participate in the overall load bearing mechanism in the anticipated way. Unfortunately, the maximum value of the displacement, about 0.52 in., is significantly below the experimental value of about 0.78, cf. Fig.4.3. The error is about 50%. Given the fact that without the TSB the numerical and experimental results were in very close agreement, and the fact that the TSB was modeled in exactly the same fashion as planks, this discrepancy should be attributed to modeling aspects of the interaction between the TSB and the deck itself. Discussion of the numerical results presented in the next section provides some insight regarding that side of modeling and analysis.

For comparison, the distribution of the bending moment in planks and resultant shear forces in the nail connections are shown in Figures 4.17 and 4.18, respectively. Even accepting some inherent inaccuracy in modeling, significant reduction in the magnitude of those quantities, as compared to the deck without the TSB, is evident. The reduction would remain very significant even if it is cut in half. This outcome was anticipated and it was the basis for suggesting TSB as a viable method leading to the reduction of the high maintenance cost. Particularly noteworthy is the reduction in the nail shear forces when TSB is added, as seen from Figs (4.15) and (4.18). Since the nail shear forces are directly proportional to the relative (differential) movements between the neighboring planks, their reduction clearly signifies the corresponding reduction in the differential displacements. This, in turn, should slow the asphalt deterioration process.

4.2.3. Numerical Results for the Edge Load on the Deck Without TSB

Displacement distribution obtained for this case is shown on Fig. 4.19. The maximum value recorded there is about 0.823 in., which is different from the value of about 1.0-1.1in obtained experimentally. The error is not as large as for the case of center load on a deck with TSB, but it is significant -- about 20%. In addition, displacement at the center of the edge opposite to the loaded one, has the opposite sign in the experimental investigations and the same sign (or is close to zero) in numerical analysis. This can be explained by the experimental observation, described in Section 4.1.2, that the edge load caused separation of the deck from the support in the vicinity of the opposite edge. The effect of such separation is sign change for the displacement on the edge opposite to the loaded edge as well as overall stiffening of the system resulting in larger displacement under the load. Given the high accuracy of the result for center load on the deck without TSB and identical modeling procedures, the separation of the deck from the support is the only reason for the large error in this case.

For completeness, Figures 4.20 and 4.21 show distribution of the bending moments in the planks and distribution of the resultant shear forces in the nails, respectively.

4.2.4. Discussion of Numerical Results

Center Load on Deck with One TSB

As mentioned earlier, the most likely reason for this error was the modeling of the interaction between the TSB and the deck. Ideally, this interaction should be considered as a contact problem in which both contact between two involved parts of the system is possible, but their separation is also allowed. For this approach to be meaningful and effective the entire profile of the initial gap between each TSB and the deck should be measured along the entire beam and provided as data for individualized analysis of that kind. In the tested bridge section, gaps like that did exist, and they mainly resulted from the unevenness of the deck surface; jumps as high as about 1/3 of an inch have been observed from one plank to the next. They also resulted from overall slight difference in the shape of the TSB and the shape of the deck.

While the analysis incorporating contact, as described above, is possible to perform, it would take substantially more effort than what was anticipated for the purpose of this project. In addition, the numerical tool that was going to be developed within the framework of this project was to serve designers and those who need it to maintain existing wooden bridges. For them this kind of analysis would be rather useless, since the initial gaps between the TSBs and the deck are random, and they are not known at the design stage of the bridge. Under those conditions, it seems that the only reasonable approach is to assume full connection between each TSB and the deck. This is exactly what has been done in this project by assuming that the degree of freedom of the TSB and of the deck at the points where they are connected by the screws are identical

In the subsequent paragraphs of this section the hypothesis that the interaction between the TSBs and the deck is responsible for the discrepancy between the numerical and the experimental results will be supported by more rational arguments. These arguments will approximately quantify the relationship between the magnitude of the gaps existing between the deck and the TSB and the magnitude of the bridge deflection. However, we would like to note that those initial gaps can be eliminated by additional planing of the deck at the locations where a TSB is to be attached to the deck. Other ways of eliminating the gap may be found to be more cost effective and equally good.

Two types of simplified analyses were conducted to investigate effects of inaccuracies in modeling contact between the TSBs and the deck. The first assumes no initial gap, but weakens the connection between the TSB and the deck. The second analysis assumes existence of initial gasp and estimates its magnitude needed for the experimental displacement at the center to agree with the analysis based on the assumptions made in the course of this project.

To weaken the connection between the TSB and the deck it has been assumed that, at the three points where the TSB is connected to the deck, only the transverse displacements are identical while the rotations are totally independent. Since in the computer program rotations are also identical, computation with the weakened connections required special intervention in the program and cannot be done automatically. Distribution of the transverse displacements with weakly connected TSB is shown in Fig. 4.22. It is clear that the modified solution is much closer to the experimental results shown on Fig 4.3. This time the maximum value of the displacement is 0.693 in. (versus 0.517in obtained before), which is much closer to the experimentally obtained value of about 0,78 in. (cf. Fig 4.3).

From the theoretical point of view there are more logical arguments to assume identical degrees of freedom for the TSB and the deck (as has been done in the computer program) than to assume the weak connection, so the above modification is not advised to follow. However, since the weakly connected TSB is more likely to move independently of the deck, and since this independent motion is also facilitated by the initially existing gaps, the above simplified analysis points to the benefits of eliminating possible initial gaps between the TSB and the deck.

One more approximate analysis, combining numerical results and simple hand calculations, was performed to estimate if the gaps that have been observed to exist in the system could cause discrepancies between numerical and experimental results of the magnitude found in this project. This analysis is based on the following:

a. We suppose that, when the TSB is attached to the deck, there is no gap at the location of the two side screws, and there is a gap "x" at the center screw.
b. We know that, for perfectly connected one TSB (without any gaps, that is), the load P=34kips causes displacement d= 0.5173 in. at the center of the deck, Fig. 4.16.
c. We also know that, if there is no TSB attached, the same force P=34kips causes displacement d_n= 1.00857in at the center and displacement d_s = 0.4 in at the location of either of the side screws, Fig. 4.12.
d. Finally, we know that, with one TSB attached, center displacement obtained experimentally was found to be about d_e= 0.78 in.

It turns out that the magnitude of the gap "x" needed to match the experimental results and numerical results can be estimated based on the following logic: In the process of gradual loading there is an initial stage, up to some magnitude of the load S, during which the gap will be gradually closing, and the transverse beam will not be bent - it will be moving downward as a rigid body. At that stage the pattern of deformation (not the magnitude, though) will be like that in Fig.4.12. The magnitude S of the force when the gap closes can be found from a simple relationship of proportionality. For the load greater than S, the TSB and the deck will be interacting and the pattern of additional deformation will be like the one on Fig. 4.16. This

additional deformation will be related to the difference "P-S". The condition that the sum of central displacements obtained in those two stages of the process, both determined analytically, should agree with the displacement obtained experimentally gives the following expression for the size of the initial gap "x":

$$x = \frac{(d_e - d)(d_n - d_s)}{(d_n - d)} \qquad (4.3)$$

For data obtained in the course of this investigations (listed earlier in this section) one obtains x = 0.325 in. This value is of the order of magnitude of the jumps observed in some locations between neighboring planks, so it is very realistic for the gaps of that magnitude to be present. Furthermore, it is believed that this result is an upper bound of the actual value of x since, for the logic used here to be correct, the displacements d_n and d_s should be obtained for the TSB connected by only two outside screws. This case has not been solved, and the required results were not available. The results of d_n and d_s obtained for the case of no TSB, as described in item "c" above, should be a good approximation of the required values. This assumption reflects the expectation that, when the TSB is connected by only two screws (and the gap is present), the TSB mostly moves vertically as a rigid body and plays minimal role in restraining the movement of the deck.

Edge Load on Deck Without TSB.

It has been mentioned earlier (while presenting the results for the case discussed here) that the main problem behind discrepancy between numerical and experimental results involves the lifting of the deck from the supports. By investing sufficient resources and time, this problem can be modeled in a similar fashion as interaction between the TSB and the deck - it is also a contact problem. It seems that, from a practical point of view, it is more logical to prevent such lifting by some sort of anchoring of the deck along the support (if the load so close to the edge is at all possible). Such anchoring would introduce effects similar to the effects caused by attaching a TSB: It would reduce displacements and internal forces in the deck, which is the whole concept behind this project.

Another aspect of the problem, the effects of which are impossible to examine now, since the bridge used for experiments has been disassembled, is the possibility of gaps existing between the deck and the support on both of the bridge's ends. The initial gaps had to be present there, just as those present between the TSB and the deck. Their likely effect would also be overall increase in the deflections of the bridge in experiments, comparing to computation. Such a difference, although small, has been consistently observed in comparisons.

CHAPTER 5
CONCLUSIONS AND RECOMMENDATIONS

The goal of this study was to determine if the use of TSBs on an LNL deck would improve load-sharing across the deck width and ultimately decrease both total and differential deflections. In all cases, the attachment of the midspan TSB had a beneficial effect on the deck response reflected in a decrease of both total and differential deflections. However, the magnitude of these effects varied across the deck width and, to some extent, along its length. The outer edges of the deck benefited the least from the TSB, while the center timbers of the deck experienced the greatest benefit. Furthermore, the TSB was actually more effective in reducing deflections on the deck after it had been subject to cyclic loading. The difference was not very significant, though.

The benefits of the TSBs attached at the quarter-points in addition to the midspan TSB were minimal. At a longitudinal distance from midspan, they improved the transverse symmetry of the deck response, but they did not appreciably decrease transverse deflections over the single TSB case. However, one has to keep in mind that all deflections reported here, were caused by the loads applied at the midspan of the bridge. The observations reported above might be somewhat different for other load locations. Obviously, those other load locations must occur in practice. Thus, additional studies would have to be conducted to determine how the TSBs should be used to provide adequate improvements under loading representing real traffic conditions.

It can be drawn from these results that TSBs would be equally prudent for use on newly constructed LNL decks and as a retrofit for existing decks. The reductions in deflections brought about by a TSB were not proportional to the number of TSBs per unit of deck length. In this case, a single stiffener at midspan was sufficient to make substantial reductions in the transverse deflections of the deck. Therefore, the TSB spacing need be no smaller than 10 ft. on a long LNL deck span. Finally, the exterior timbers of the deck benefited least from the stiffener beams if the load was located at either edge of the deck, so additional supports may be required to improve deflections in these locations. However, if the deck is sufficiently wide that the outer timbers do not regularly experience significant loading, the TSB could provide enough stiffness to maintain the integrity of the deck.

In spite of some modeling problems and discrepancies between numerical and experimental results for certain bridge configurations, the above conclusions are actually supported by both experimental and numerical investigations. One additional conclusion that can be drawn purely on numerical ground has to do with the significance of the preexisting gaps. It seems that effectiveness of the TSBs can be significantly increased by eliminating these gaps. There are several possible ways to achieve that. One of them is additional planing of the deck. However, the actual choice of the method depends on a specific bridge builder, on what he/she finds most cost effective, technically adequate or convenient. The same comments pertain to the gaps between the deck and its end support. In this case, elimination of gaps has to be accompanied by anchoring the deck at the support.

The static response of the deck after the fatigue test was not very different from the one observed for the virgin deck. Thus, although deemed equivalent to 30 years of bridge life, the fatigue test did not seem to produce any significant damage. It seems to lead to an obvious conclusion that, in real field environment, the negative environmental influence on wood products is as significant as (if not more than) the mechanical effects. In addition, the actual load on the real bridges could be higher than the load used in the fatigue test in the lab. This part of analysis could not be examined numerically.

In summary, the research conducted within this project clearly indicates that attaching one or more TSBs significantly reduces differential deflections of the deck. This should delay deterioration of asphalt (and the deck) and reduce the bridge maintenance cost. However, further studies are needed to determine the optimal design configurations for practical applications. It is reasonable to expect that parameters such as thickness of the deck; size, anchoring, and spacing of the TSBs and the nailing pattern are all interdependent. For example, an increase in the TSB dimensions will probably allow for bigger spacing between them to achieve similar effects. Unfortunately, these and other interactions could not be investigated within one project. Nevertheless, the computer program developed and validated (by experiments) as a result of this project allows for such studies. Those could possibly be conducted in the future, particularly if application of the TSBs in practice will be found of interest to industry.

REFERENCES

(1) M. A. Ritter, and J. P. Wacker, *Field Performance of Timber Bridges*. US Dept. of Agriculture, Forest Service, Forest Products Laboratory. Madison, WI, 1992.

(2) *"Ontario Highway Bridge Design Code",* Ontario Ministry of Transportation. Canada. Highway Engineering Division, 1983.

(3) W.W Sanders, F.W. Klaiber and T.J. Wipf. *Load Distribution in Glued Longitudinal Timber Deck Highway Bridges*. Engineering Research Institute, Iowa State University, ERI 85441, Project 1716, 1985.

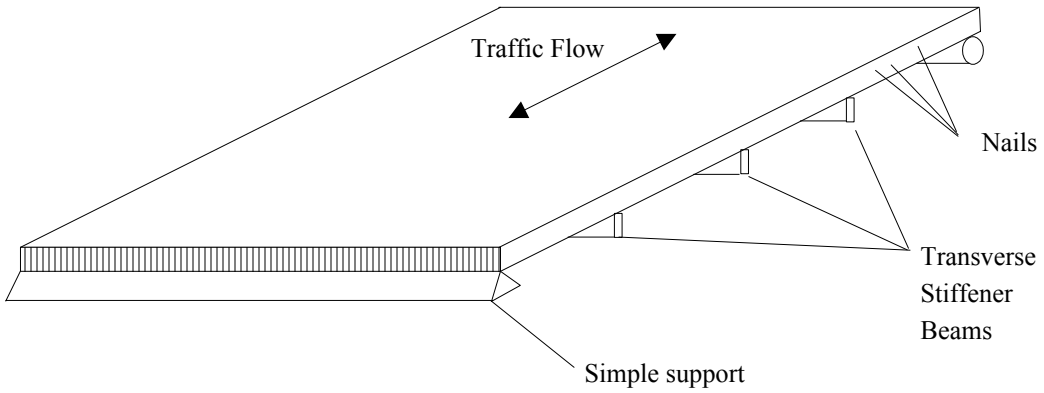

Figure 1.1: Simply Supported LNL Deck with TSBs Attached

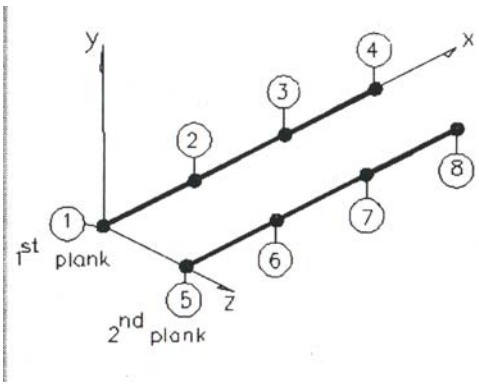

Fig. 2.1a Nodal Numbering.

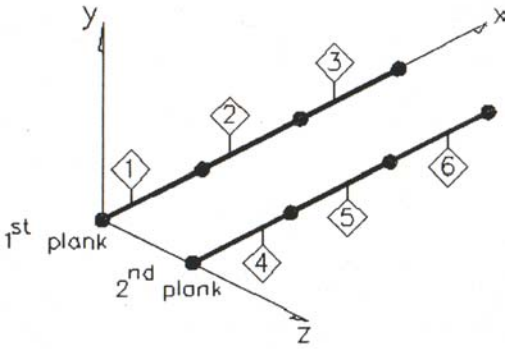

Fig. 2-1b Element Numbering.

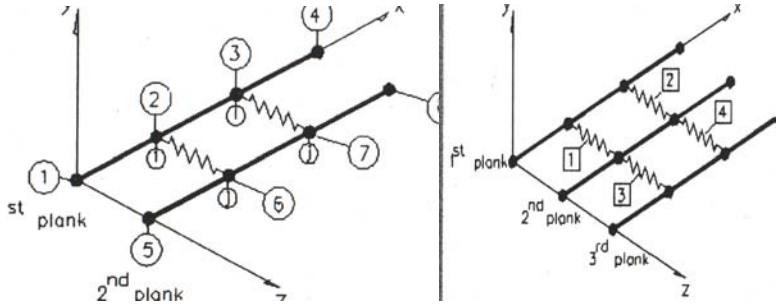

Fig. 2.2 Connector Element Numbering Scheme.

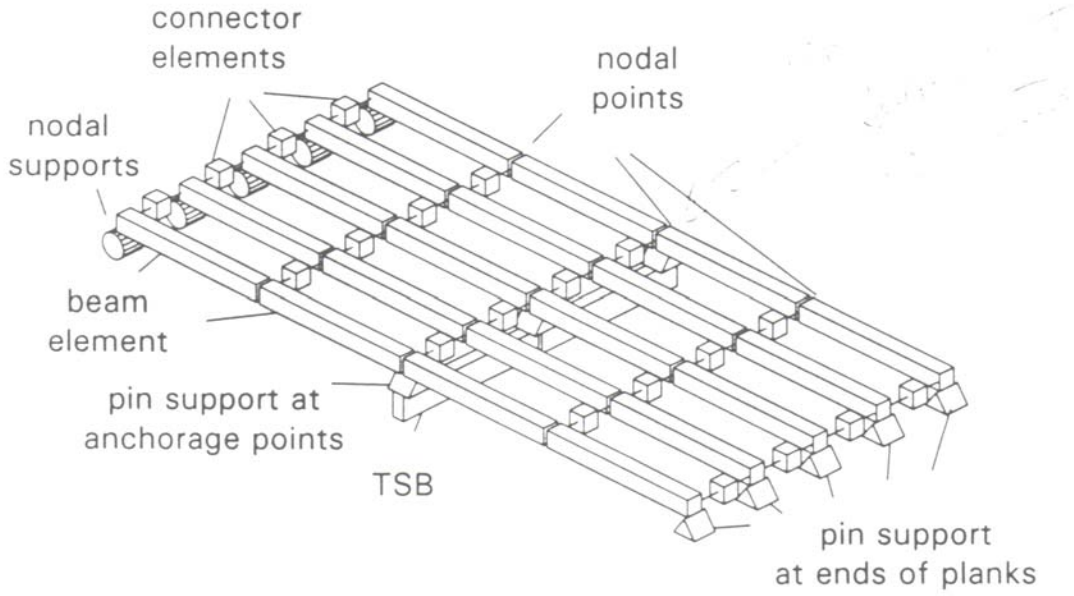

Fig. 2.3. Model of the Bridge Showing Planks, Nails, TSB

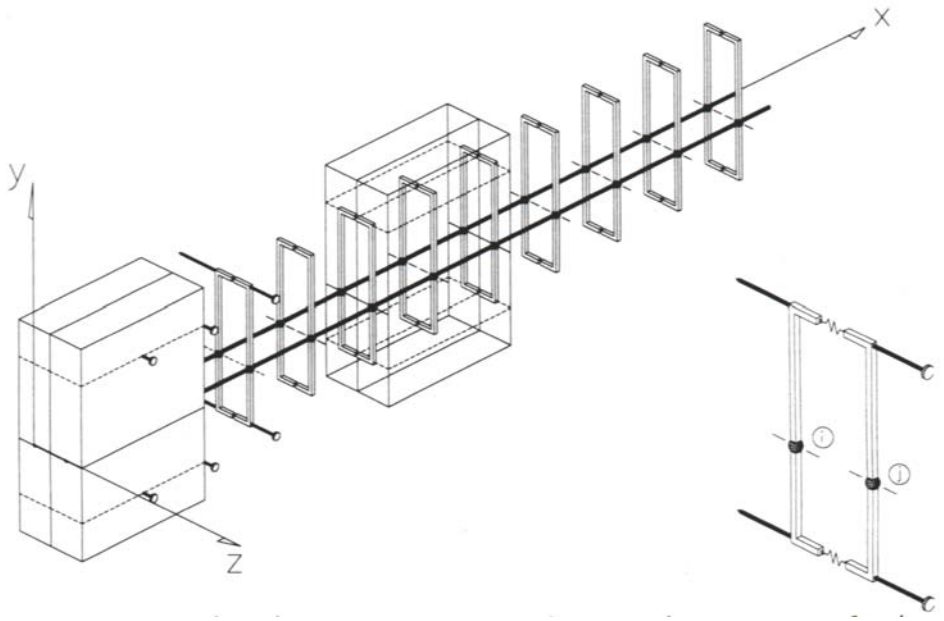

Fig. 2.4. Model for Plank and Nail Connection

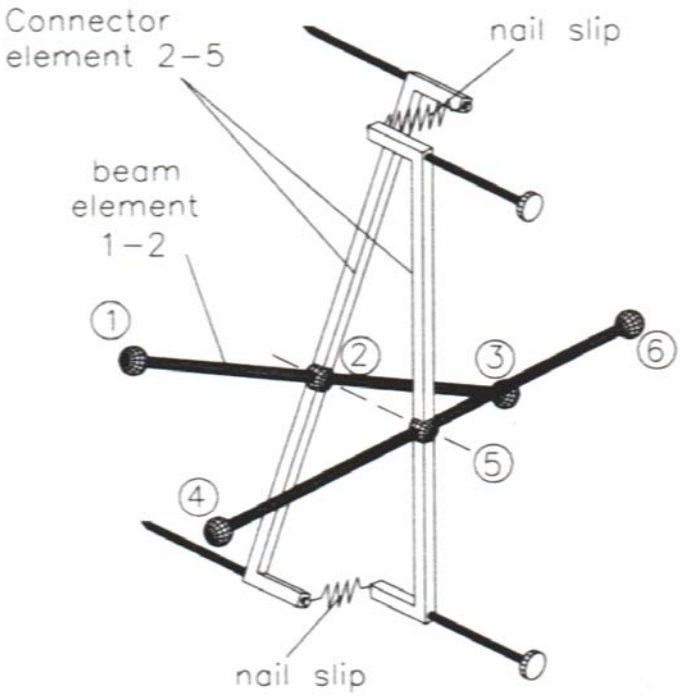

Fig. 2.5. Nail Connector Element.

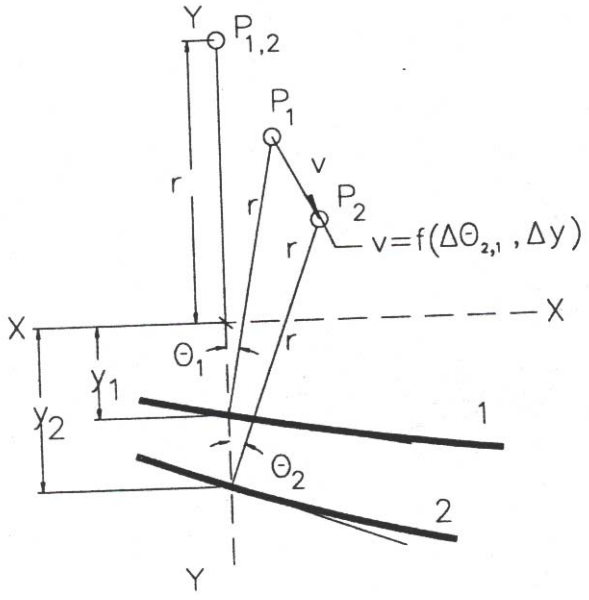

Fig. 2.6 Differential Displacements at Nail Connections.

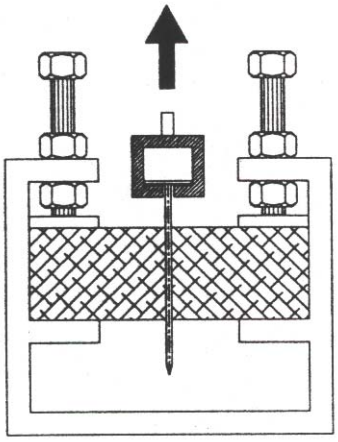

Fig. 3.1 Nail Withdrawal Resistance Test.

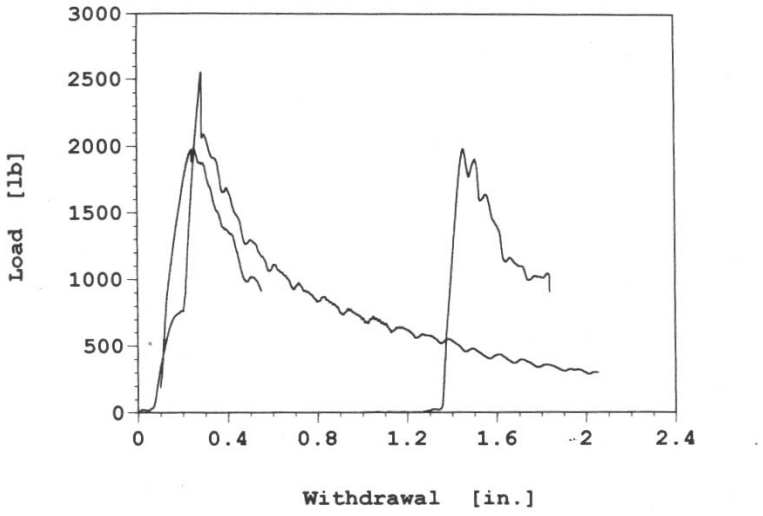

Fig. 3.2 Load Versus Withdrawal Curves from Nail Pull Tests.
(see comments, paragraph 2 of section 3.1)

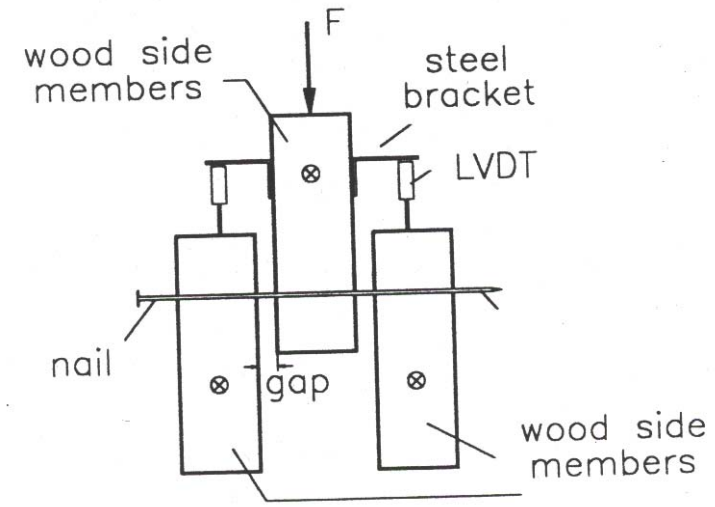

Fig. 3.3 Experiment for Measuring Stiffness in the Direction Parallel and Perpendicular to the Grain.

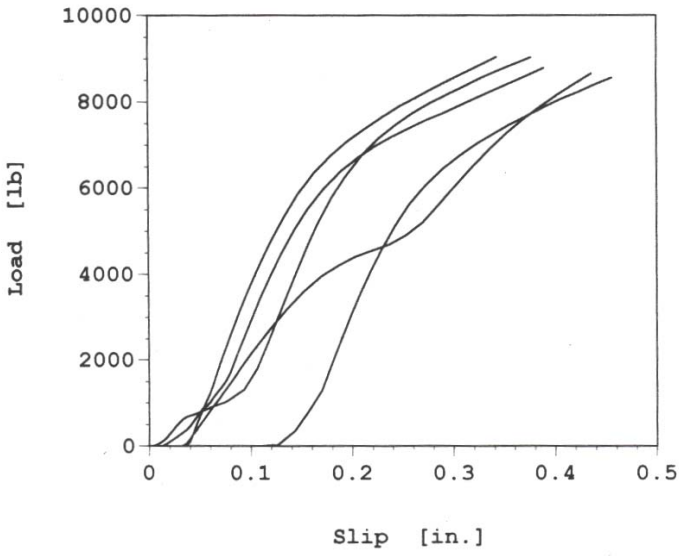

Fig. 3.4 Load Versus Displacement Curves for Shear Loading Parallel to the Wood Grain.
(see comments, paragraph 2 of section 3.1)

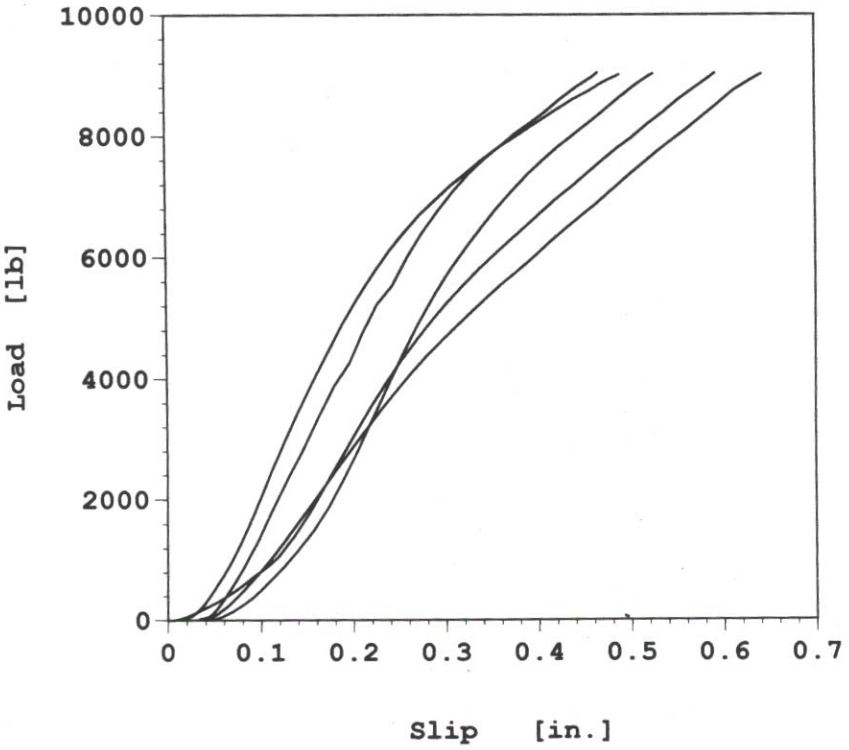

Fig. 3.5 Load-displacement Curves for Nail Shear Tests Perpendicular to Grain.
(see comments, paragraph 2 of section 3.1)

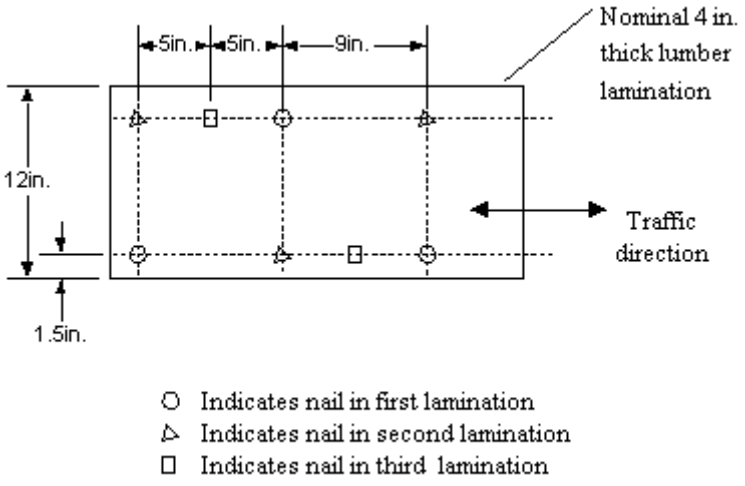

Figure 3.6. Nail Spacing Pattern (elevation)

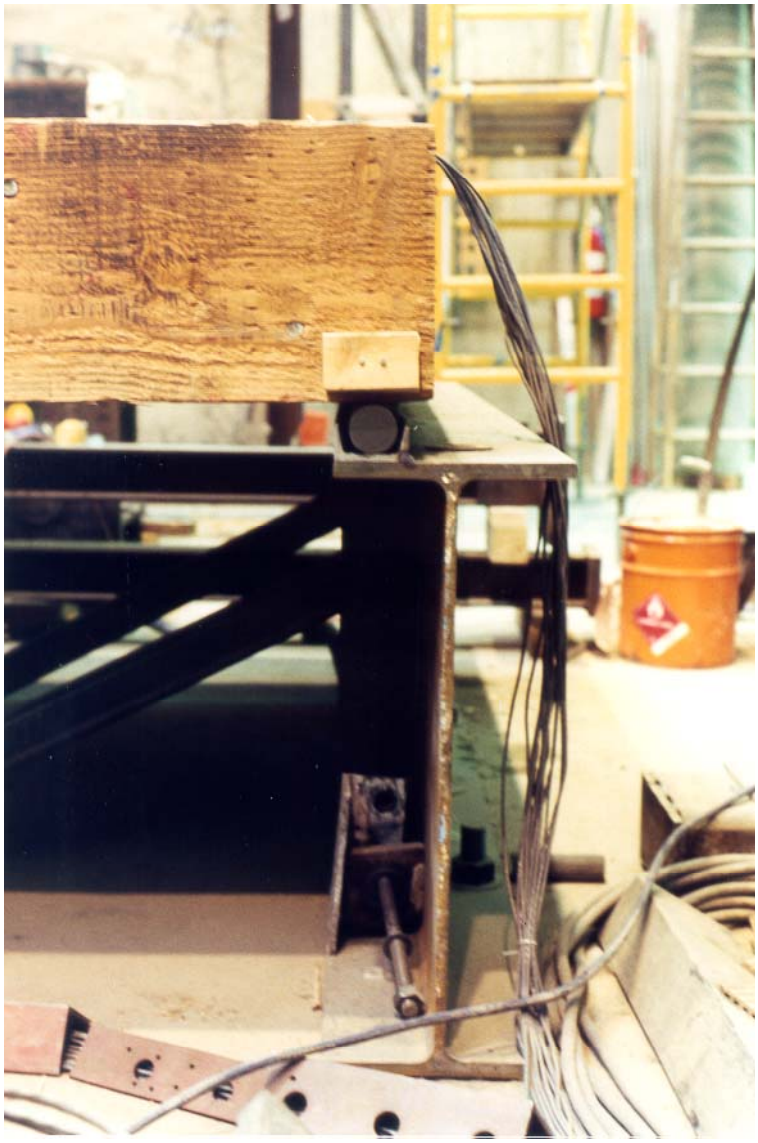

Figure 3.7. Simple Support of Timber Bridge

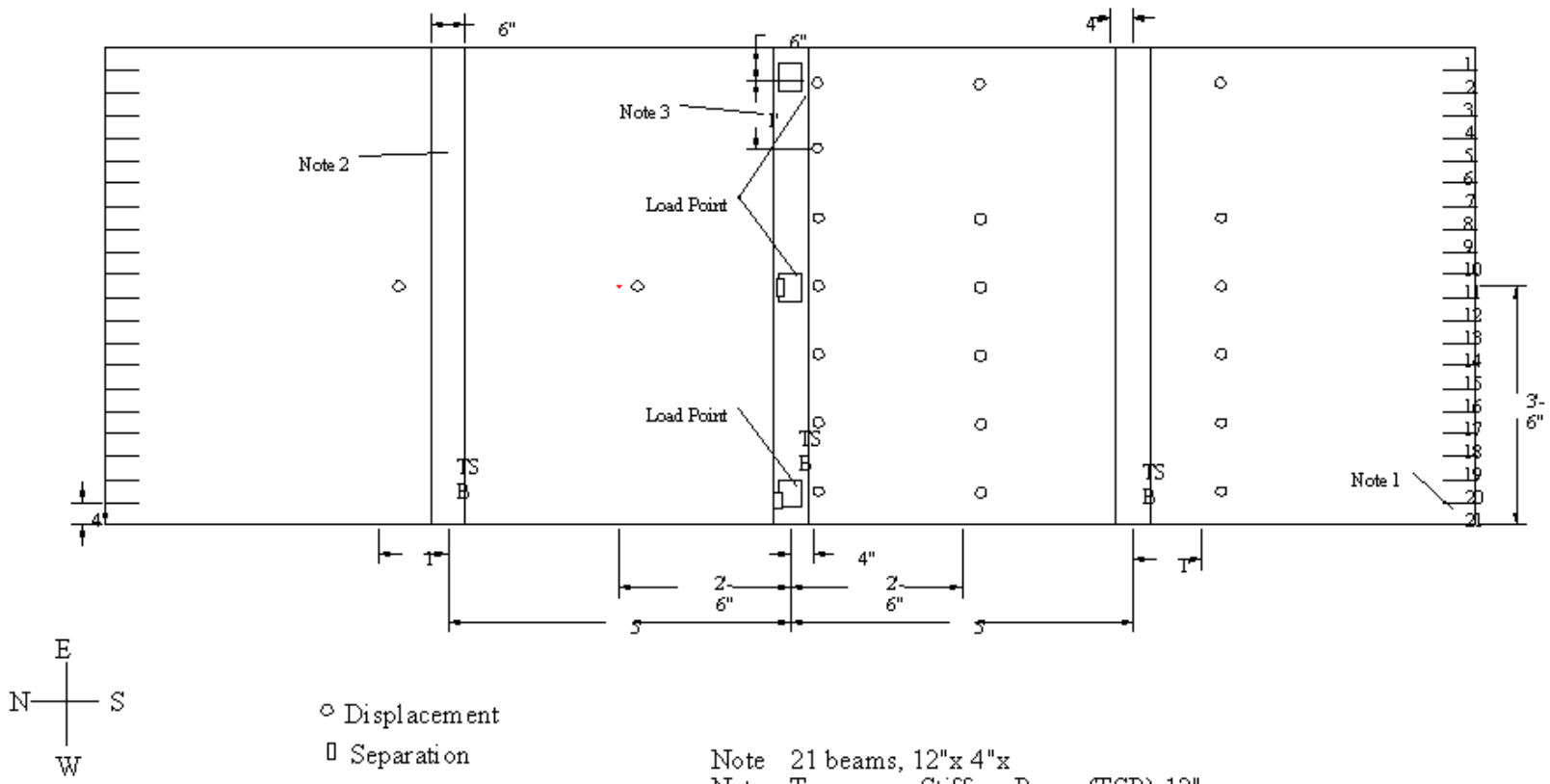

Figure 3.8. Plan view of LNL Deck with TSB locations

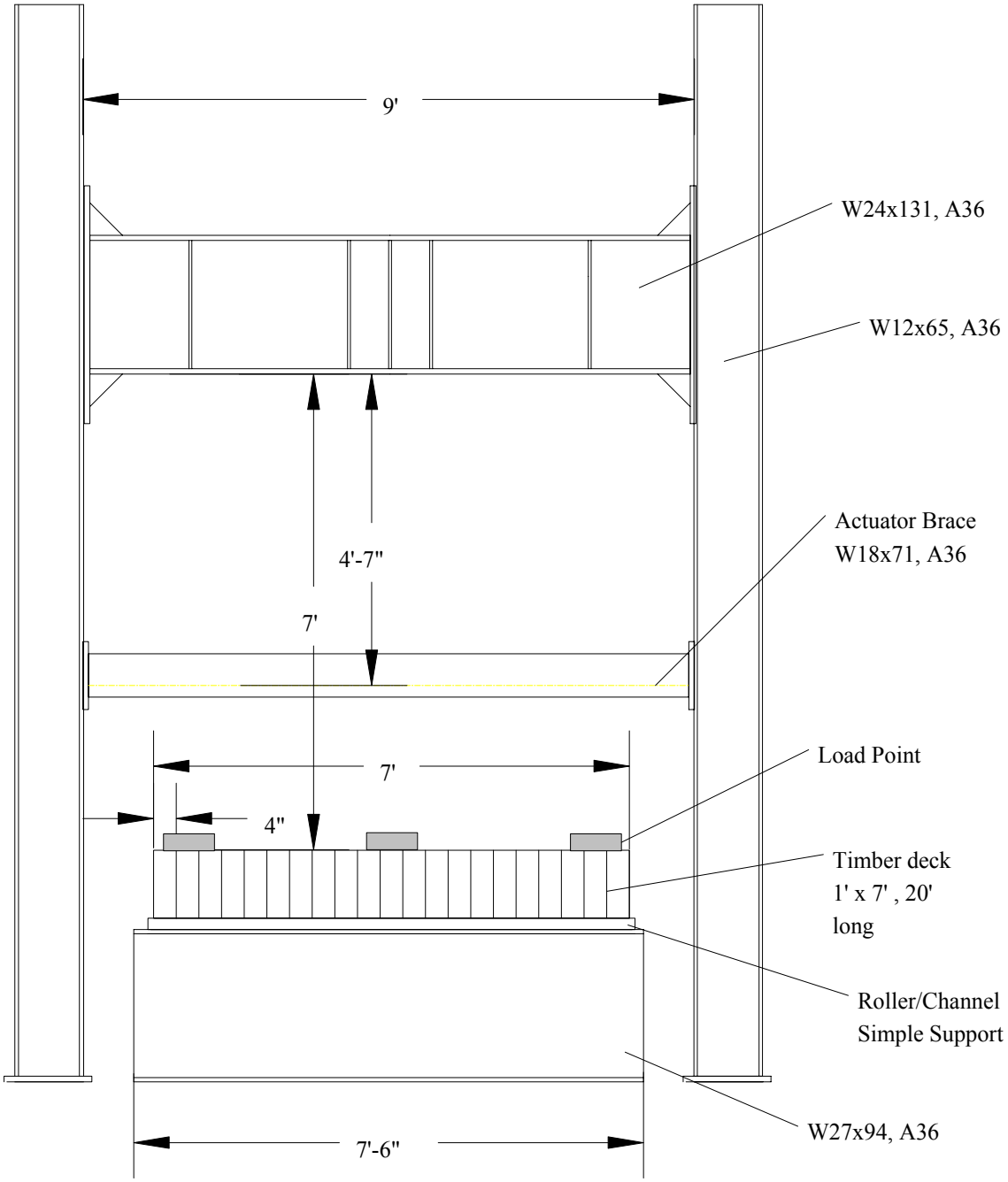

Figure 3.9. Elevation- Load Frame Assembly

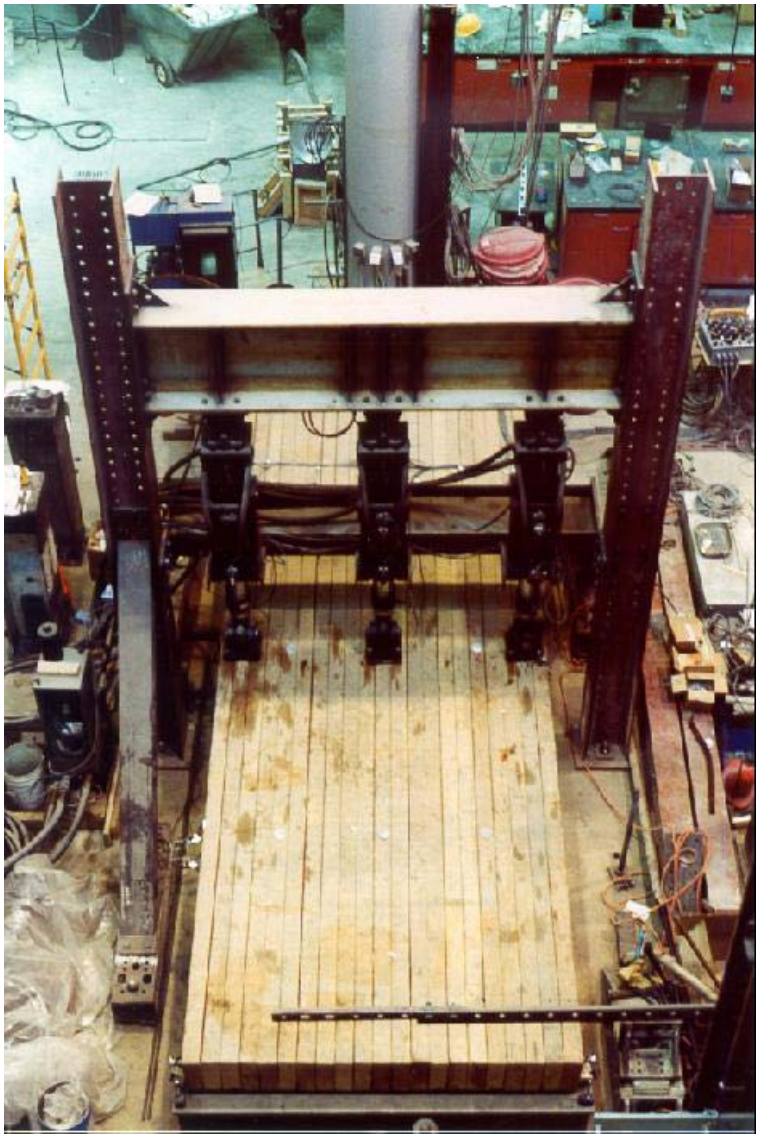

Figure 3.10. Load Frame Assembly.

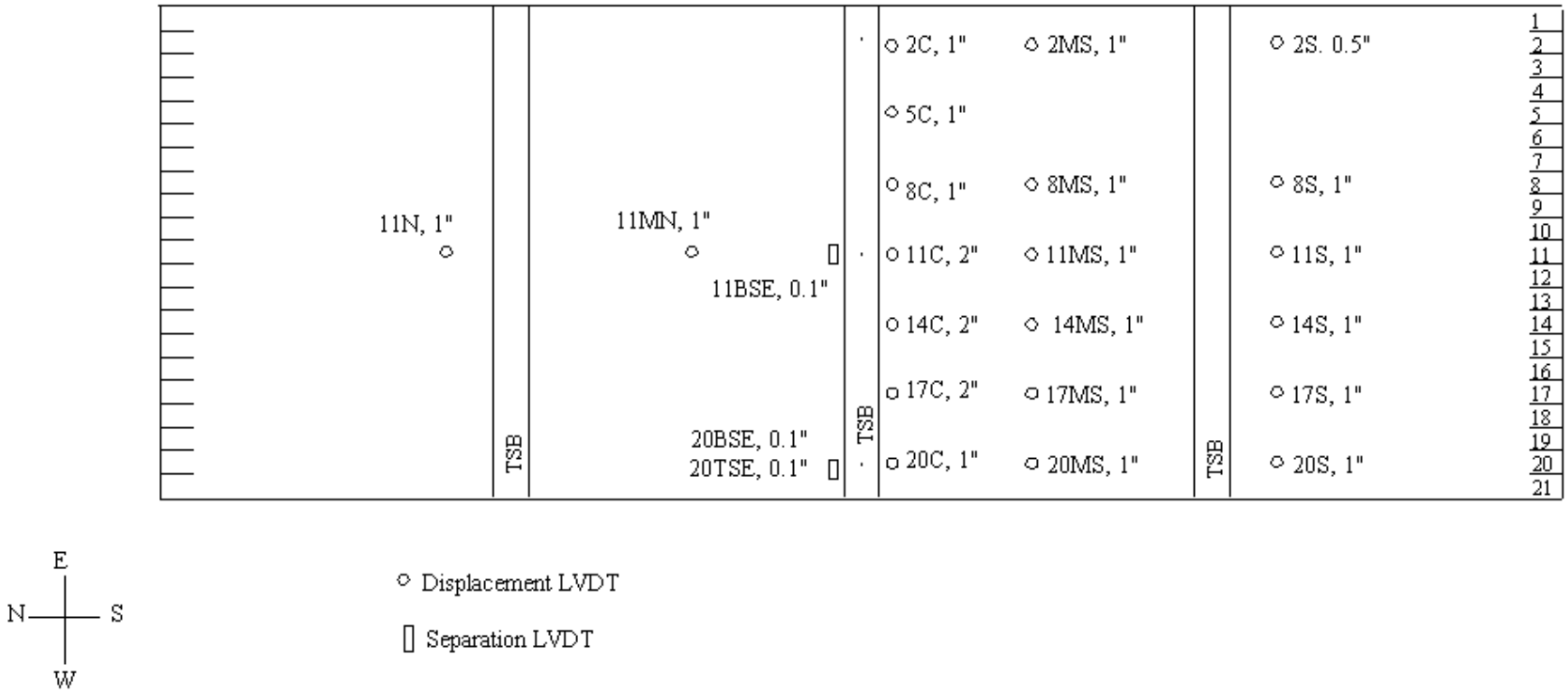

Figure 3.11. LVDT locations, labels, and sizes

Figure 3.12 Displacement LVDT Mounts

Figure 3.13 Separation LVDT Mount

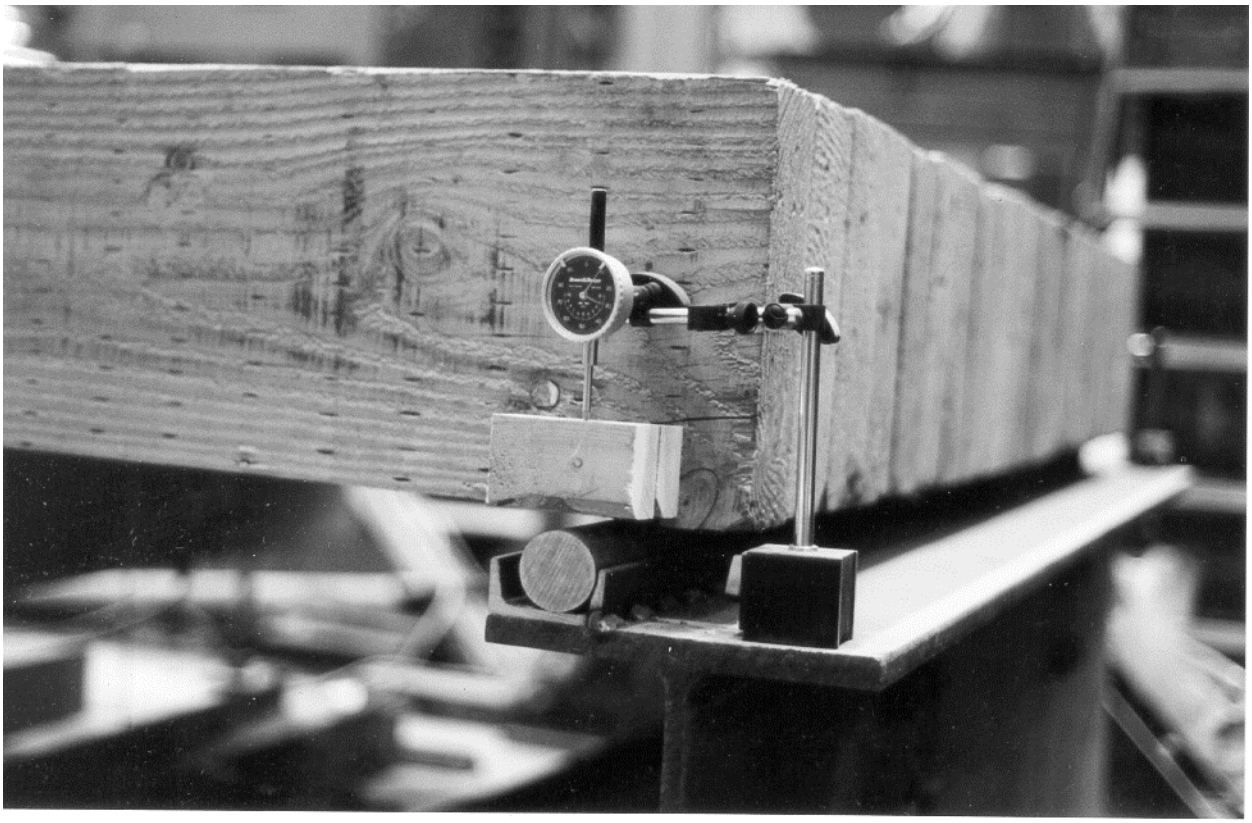

Figure 3.14 Dial Gage

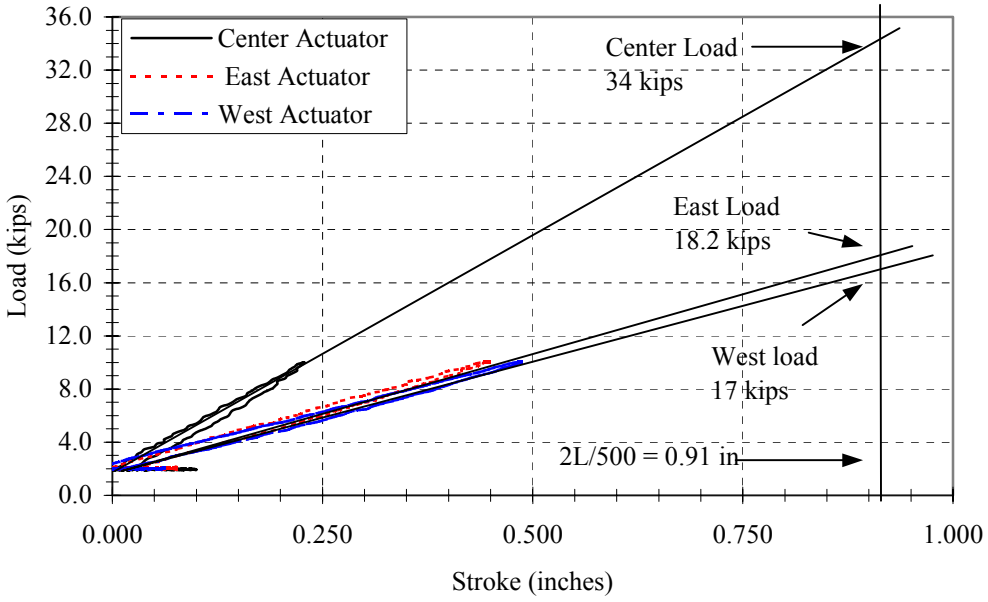

Figure 3.15 Determination of Test Loads

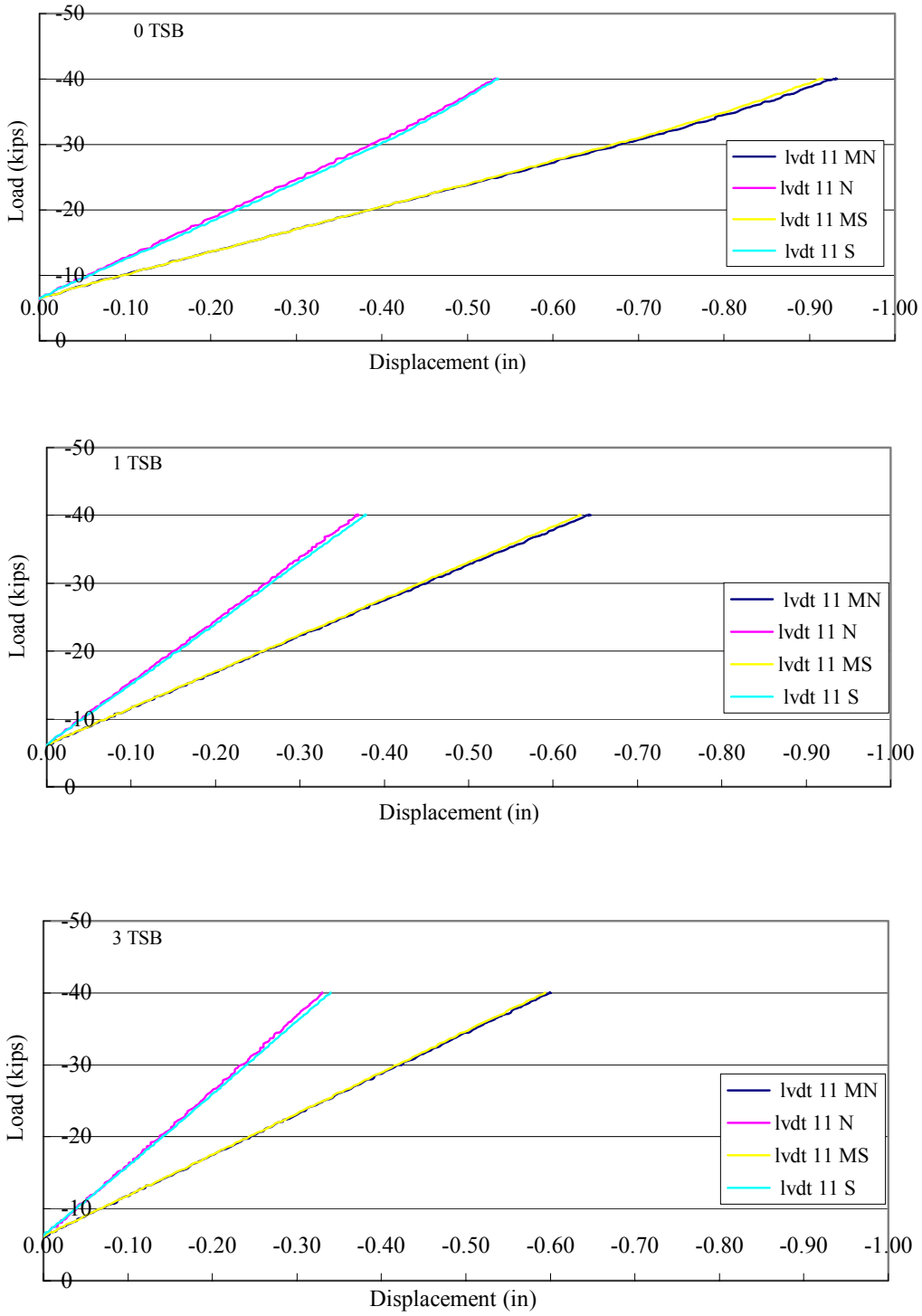

Figure 4.1: Symmetry Comparison on Timber 11

The top chart shows the load-deflection curves on the bare deck, the middle shows the curves after the attachement of one TSB, and the bottom shows the curves after all three TSBs are attached. In all three cases, the deck was loaded in the center.

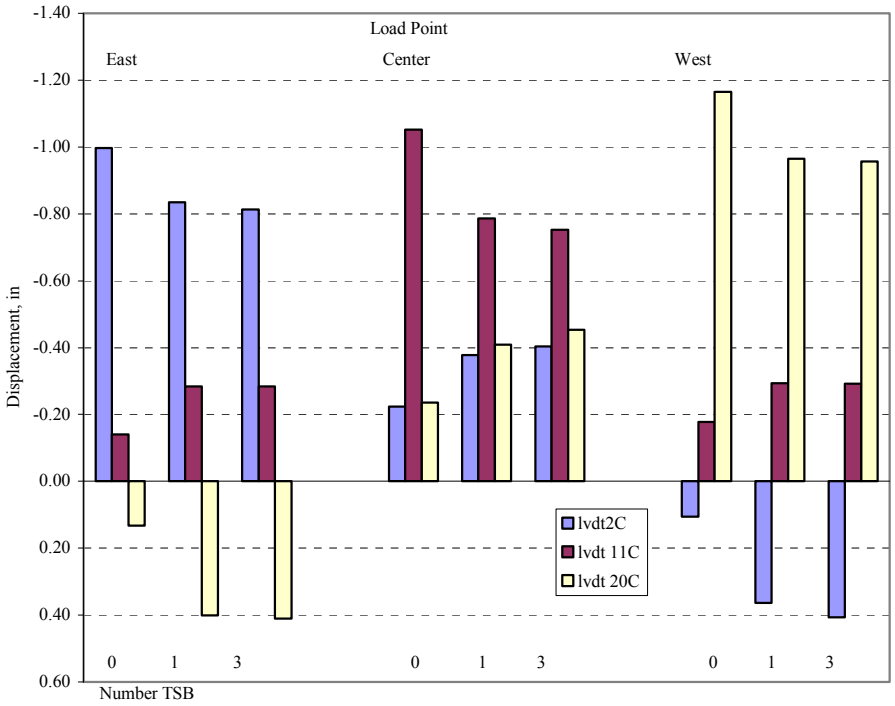

Figure 4.2: Peak Displacements on the Virgin Deck at Midspan

The position of the load is shown on the top axis, while the number of attached TSBs is shown on the bottom axis. The LVDT locations correspond to the points directly beneath the load points.

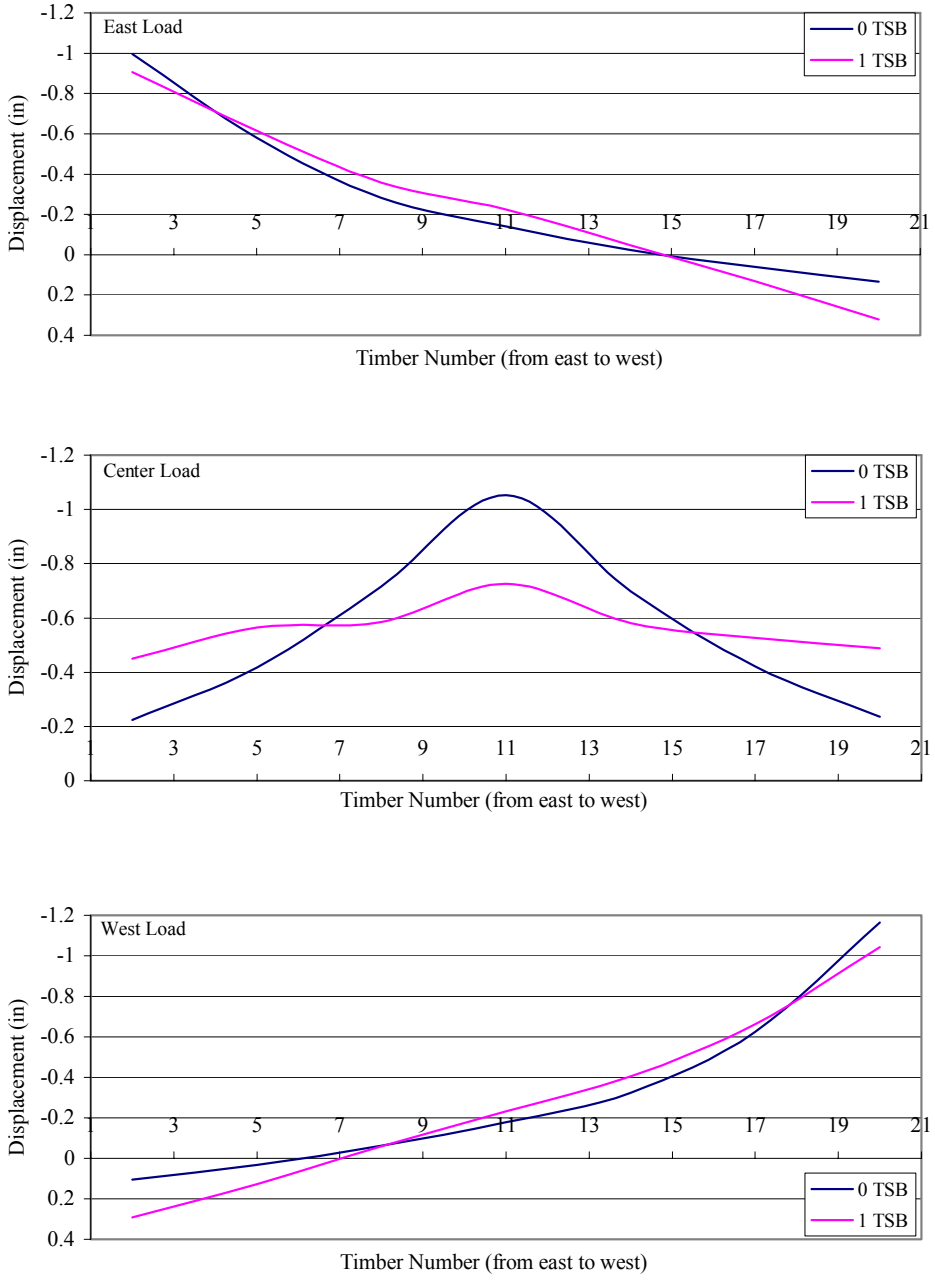

Figure 4.3 Displacements across the Virgin Deck at Midspan

The top graph shows the displacment profile when the load point is on the east side of the deck. The middle chart corresponds to the load in the center, and the bottom chart depicts the west side loading.

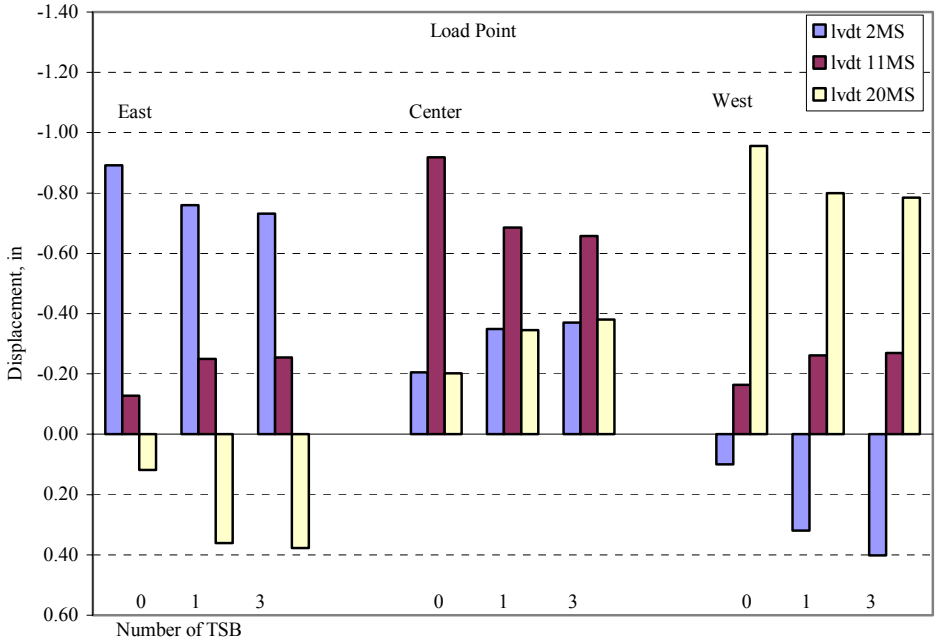

Figure 4.4 Peak Displacments at a Longitudinal Distance of 2.5' (L/10) from Midspan on the Virgin Deck

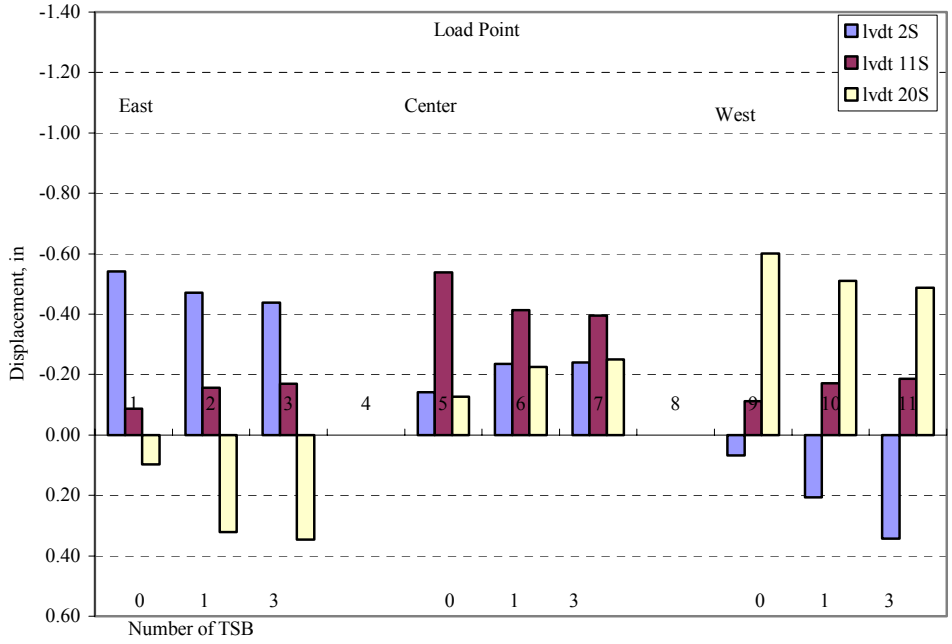

Figure 4.5: Peak Displacements at a Longitudinal Distance of 6' (L/3.33) from Midspan on the Virgin Deck

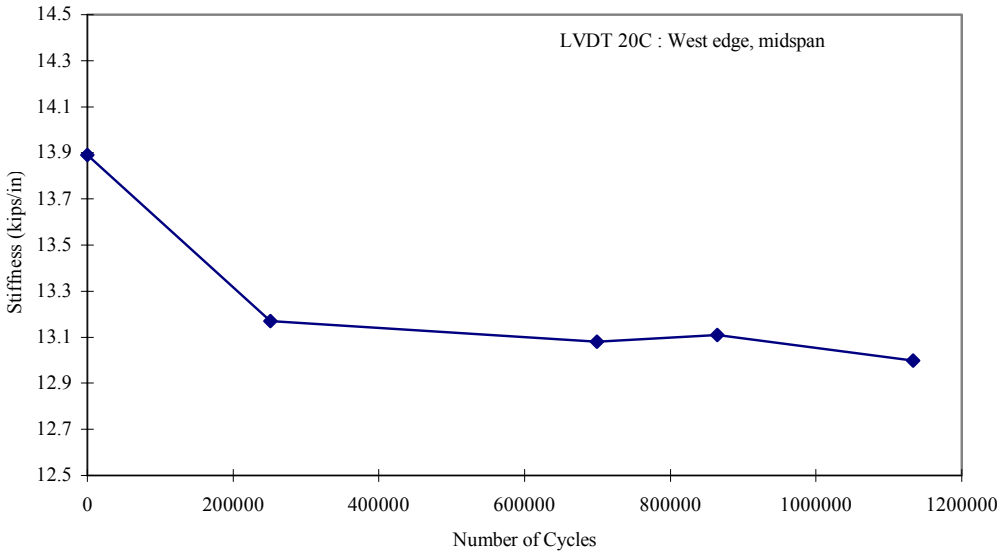

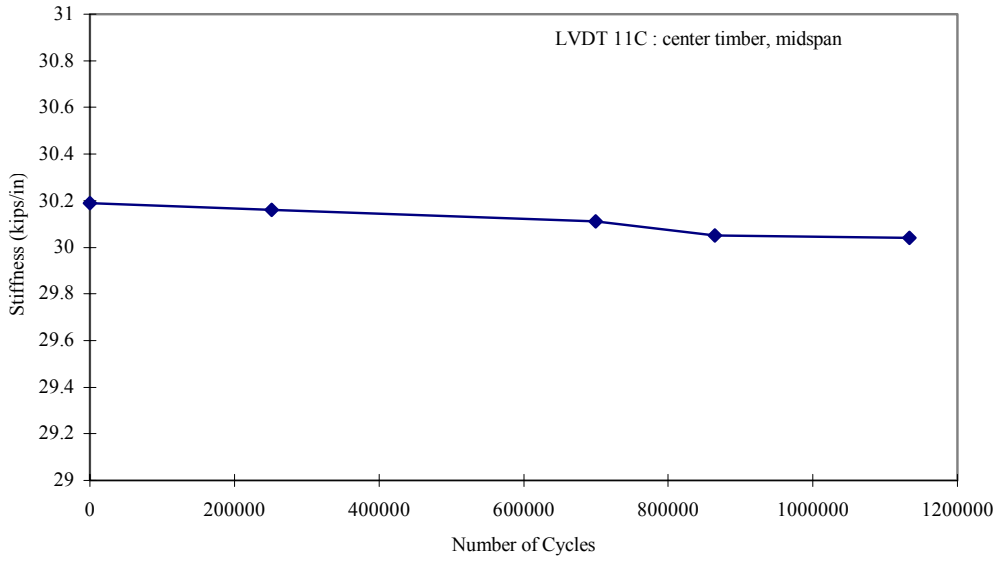

Figure 4.6 : Change in Effective Stiffness during Cycling

The top chart shows the change in stiffness at the point directly beneath the cycling actuator on Timber 20. The bottom chart shows the stiffness of at the midspan of Timber 11.

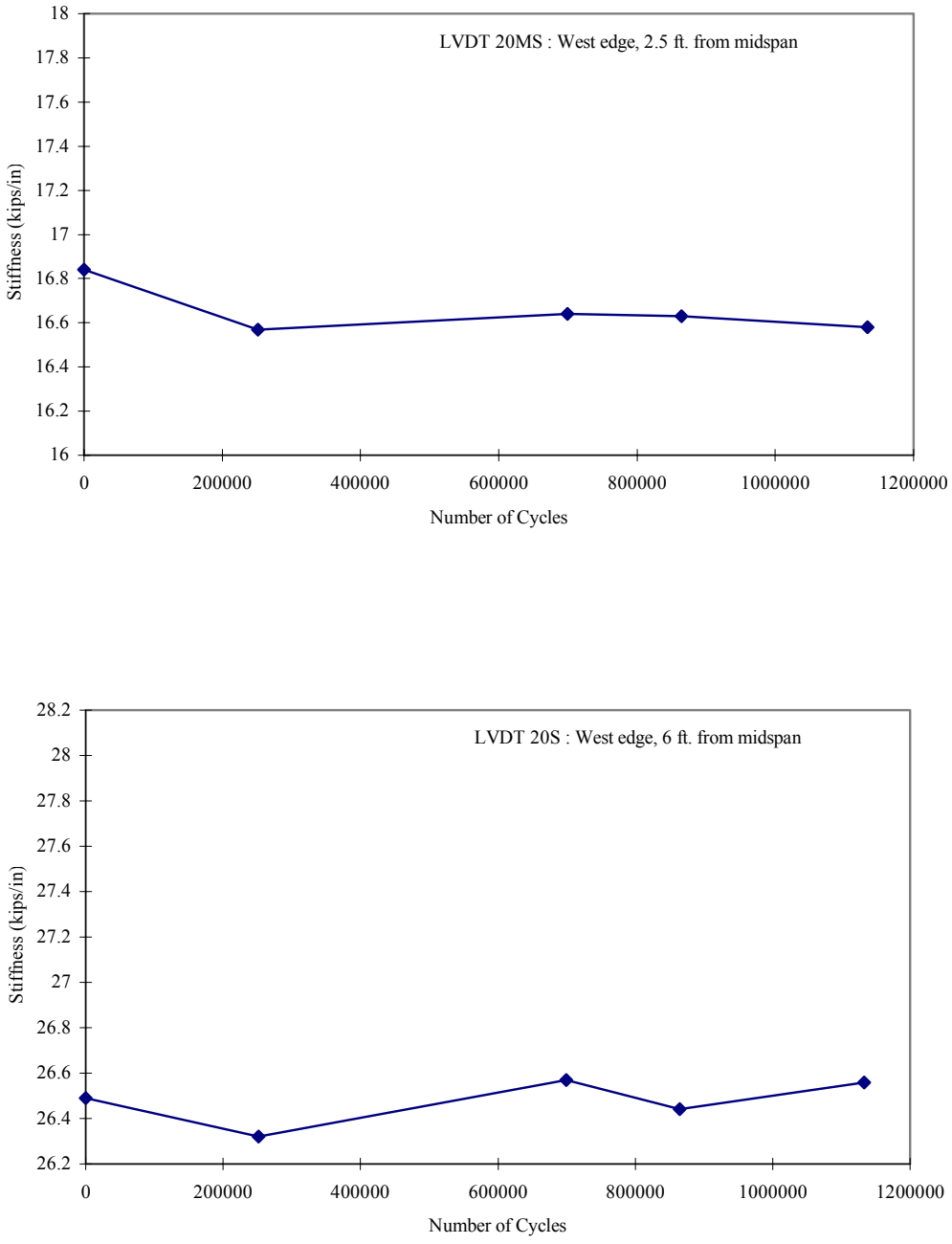

Figure 4.7 : Change in Effective Stiffness during Cycling
The top figure shows the stiffness at a point 2.5' away from the applied load, along timber 20. The bottom shows the point 6' towards the support along timber 20.

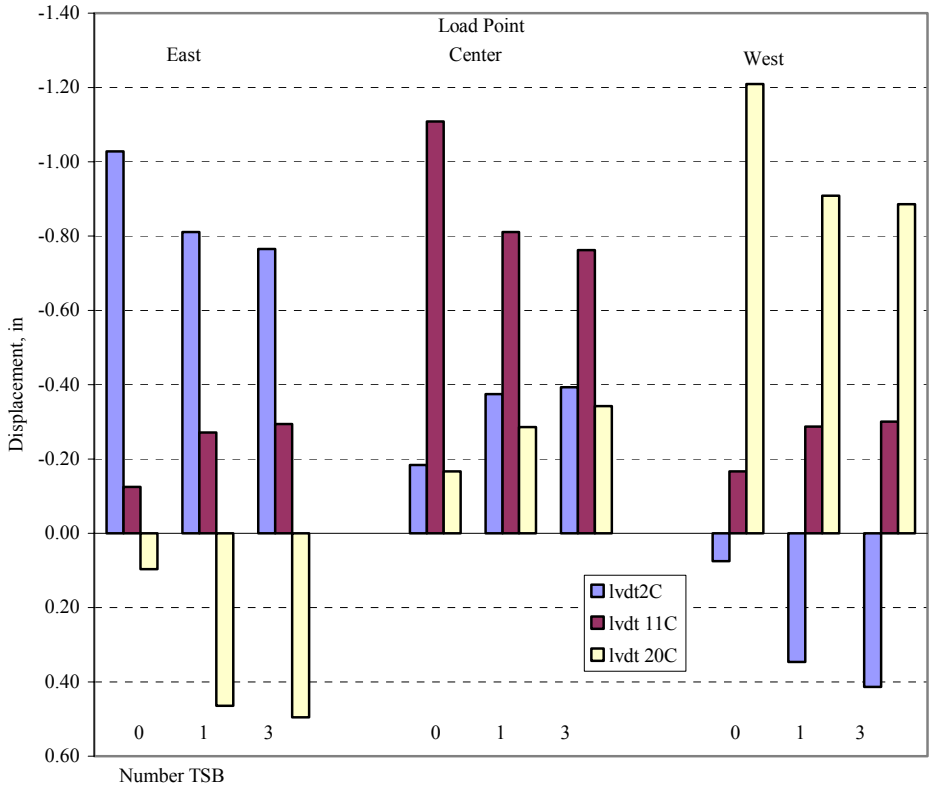

Figure 4.8: Peak Displacements at the Midspan of the Deck after Cycling

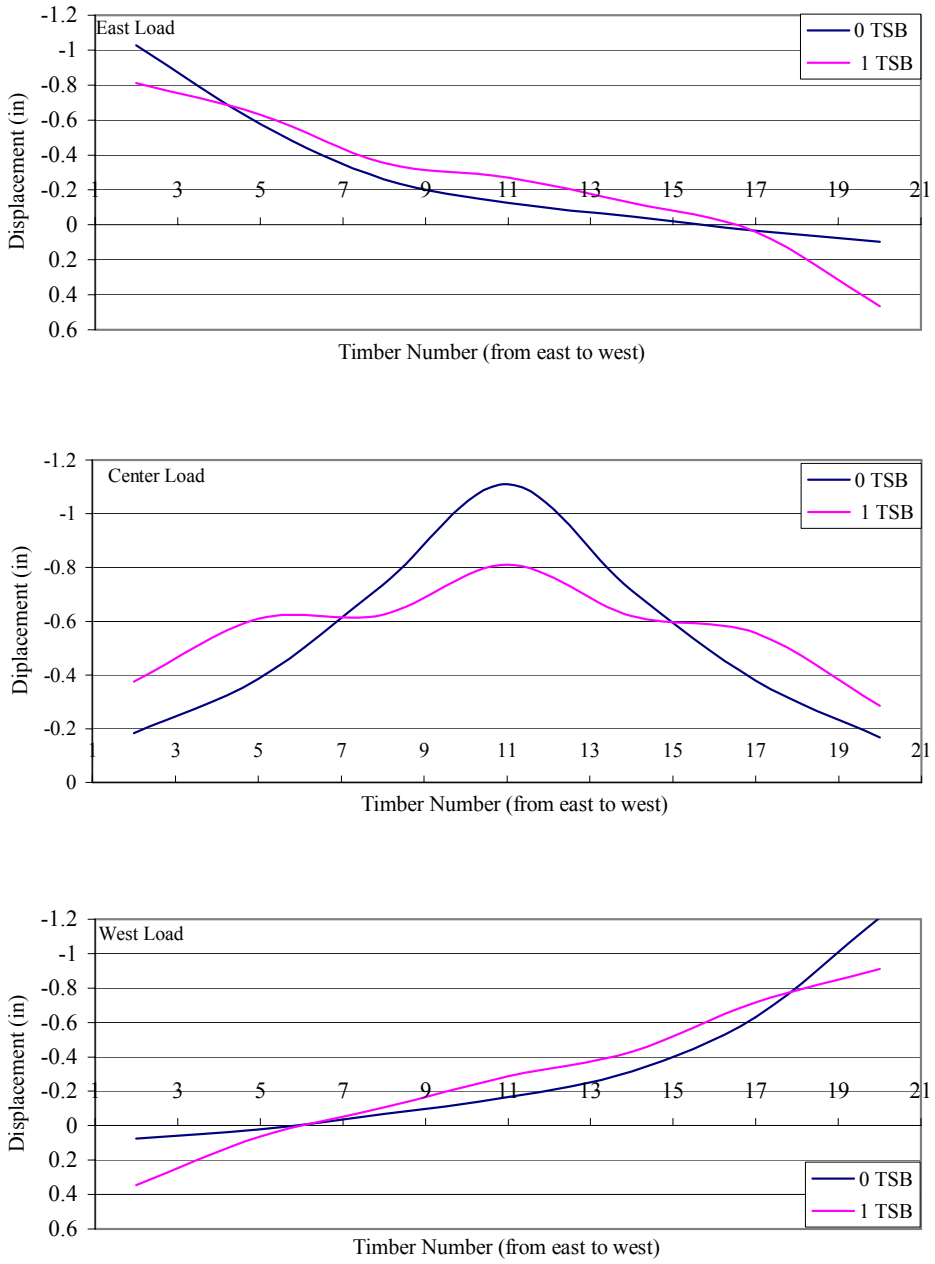

Figure 4.9 Displacements across the Deck at Midspan after Cycling
The top graph shows the displacment profile when the load point is on the east side of the deck. The middle chart corresponds to the load in the center, and the bottom chart depicts the west side loading.

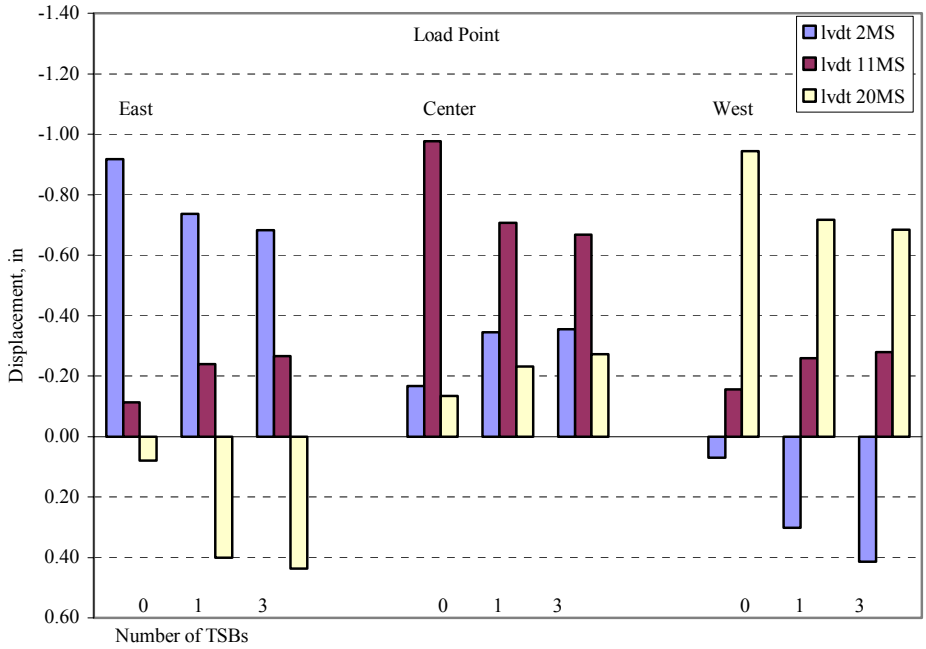

Figure 4.10 Peak Displacments at a Longitudinal Distance of 2.5' (L/10) from Midspan after Cycling

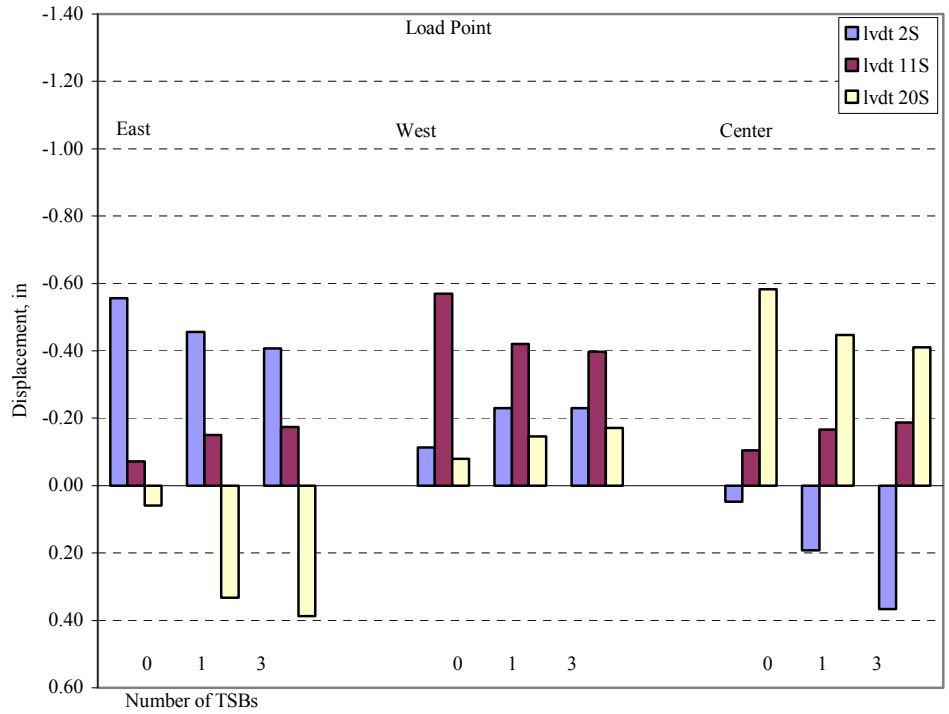

Figure 4.11: Peak Displacements at a Longitudinal Distance of 6' (L/3.33) from Midspan after Cycling

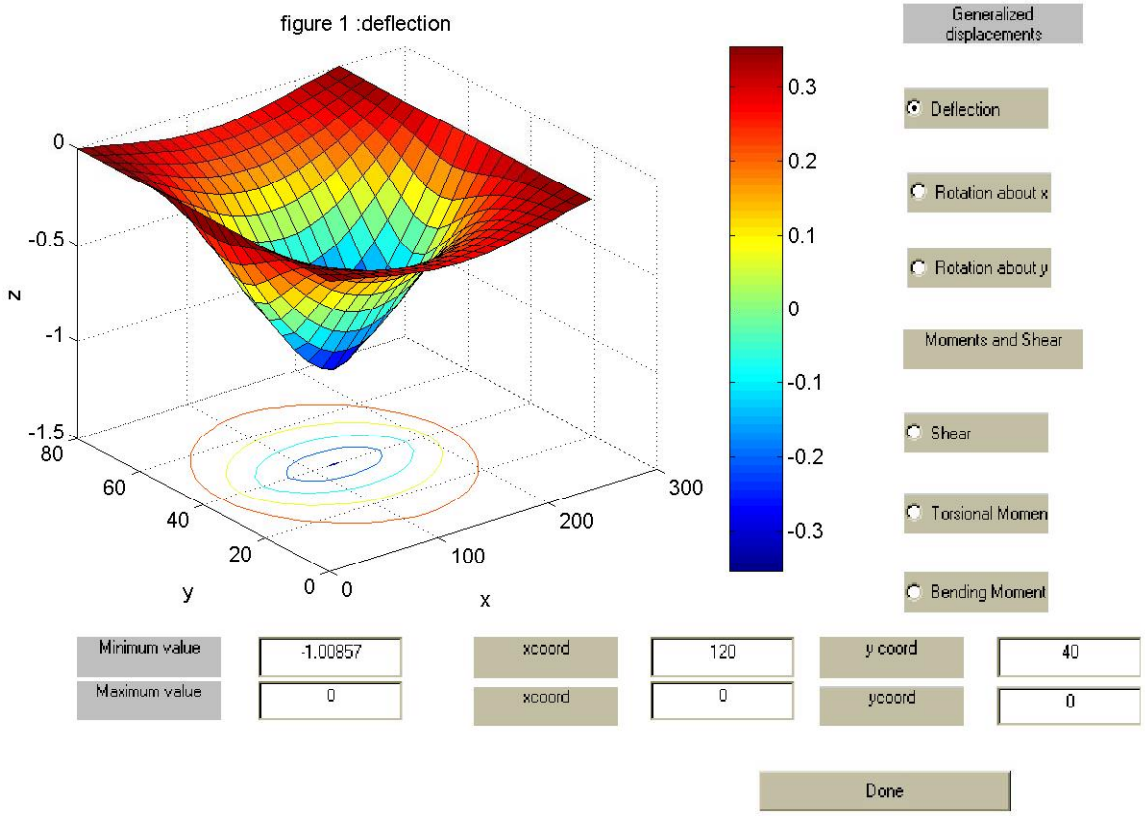

Figure 4.12 Displacements; Center Load, no TSB.

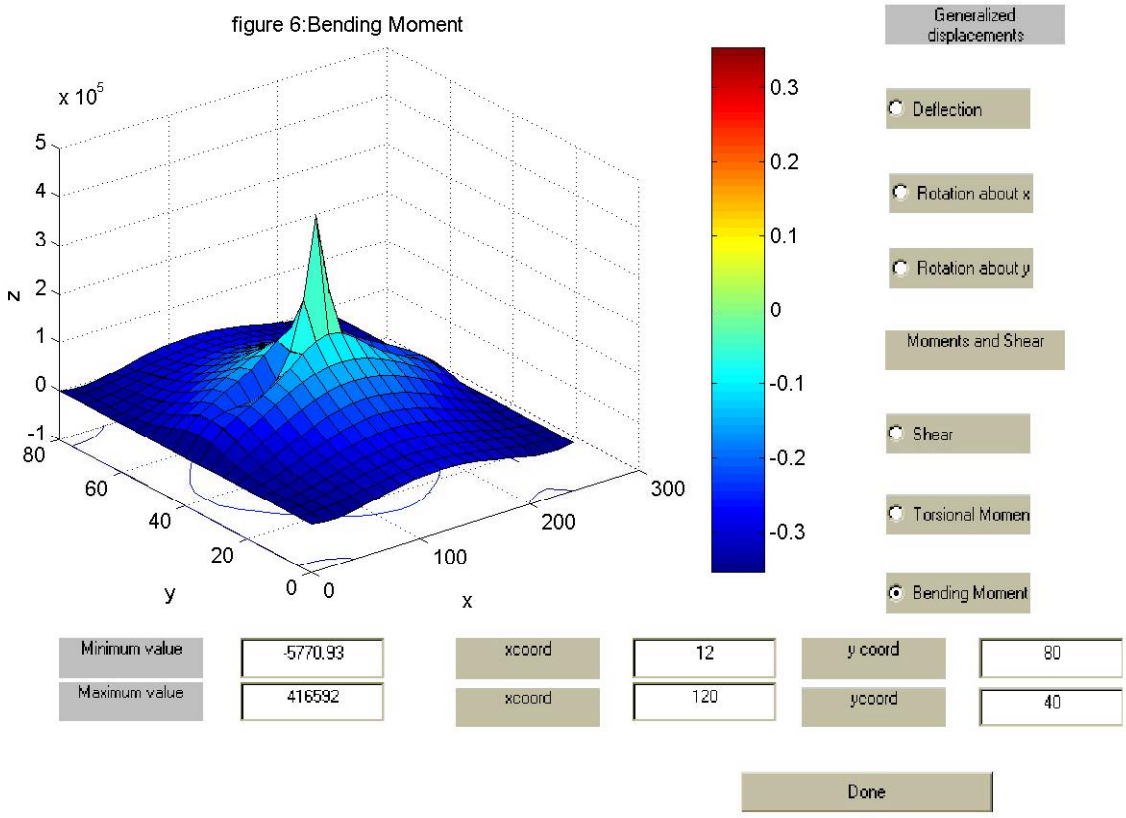

Figure 4.13. Bending Moments in Planks; Center Load, no TSB.

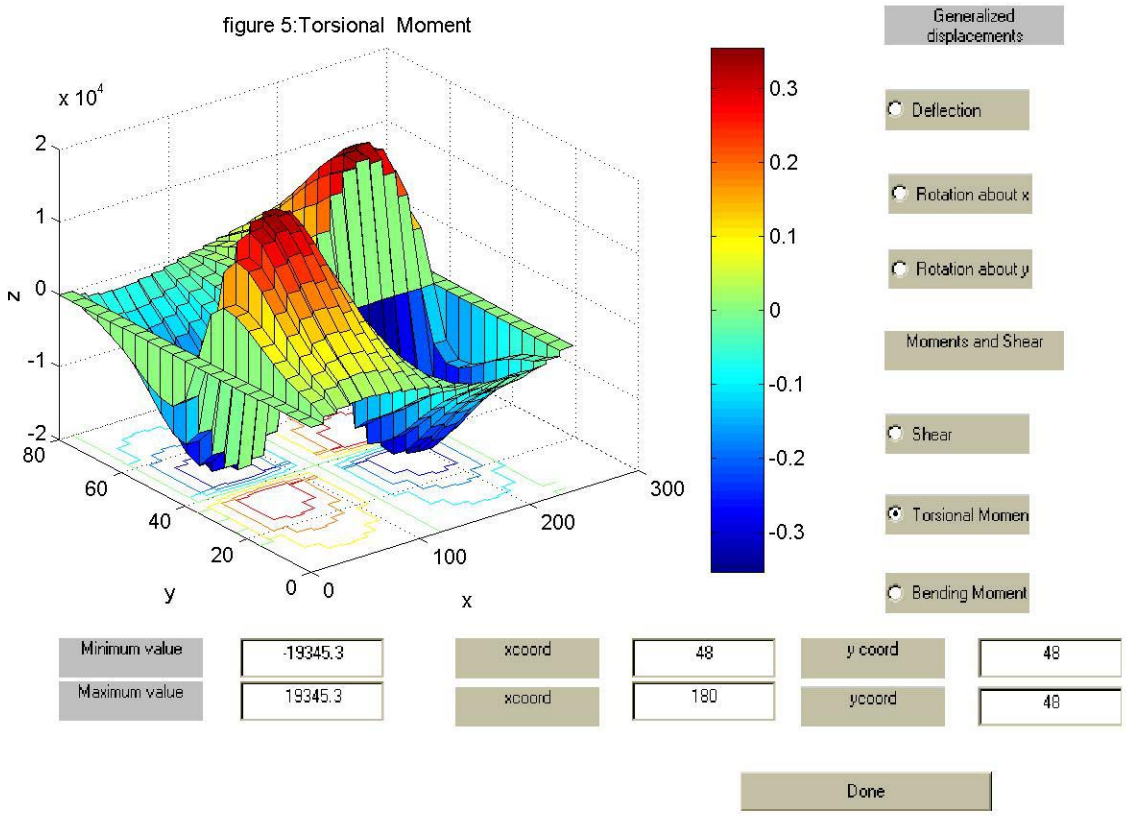

Figure 4.14. Torsional Moments in Planks; Center Load, no TSB.

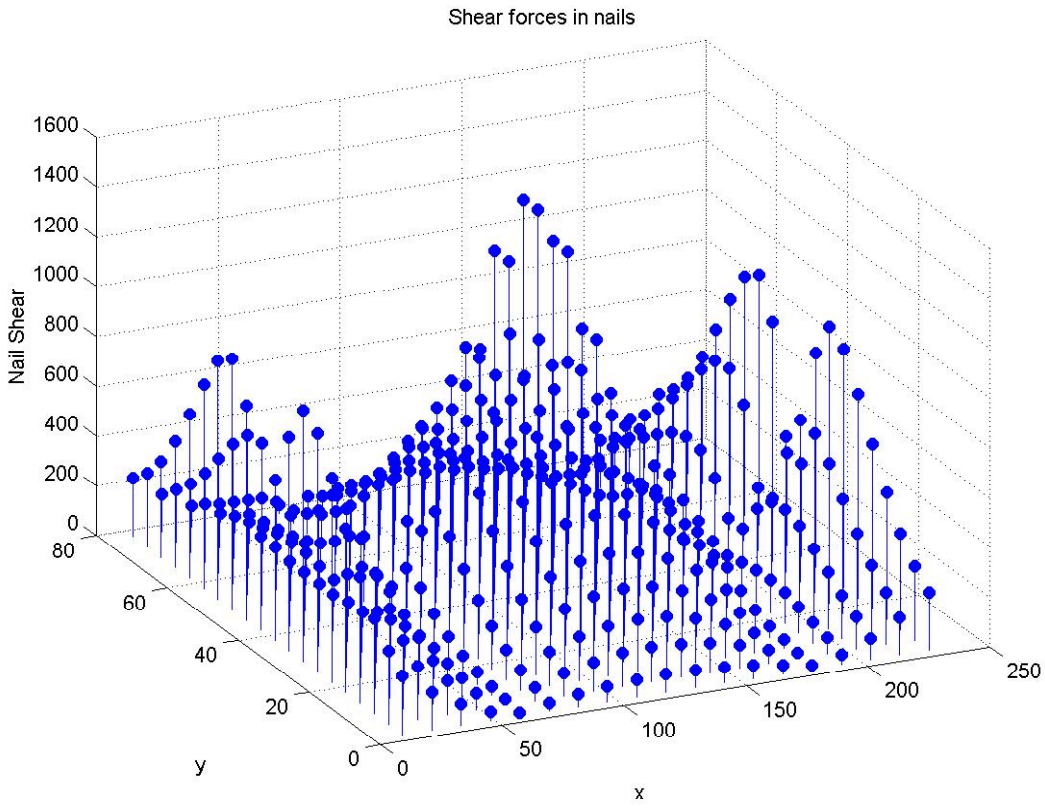

Figure 4.15. Resultant Shear Forces in Nails; Center Load, no TSB.

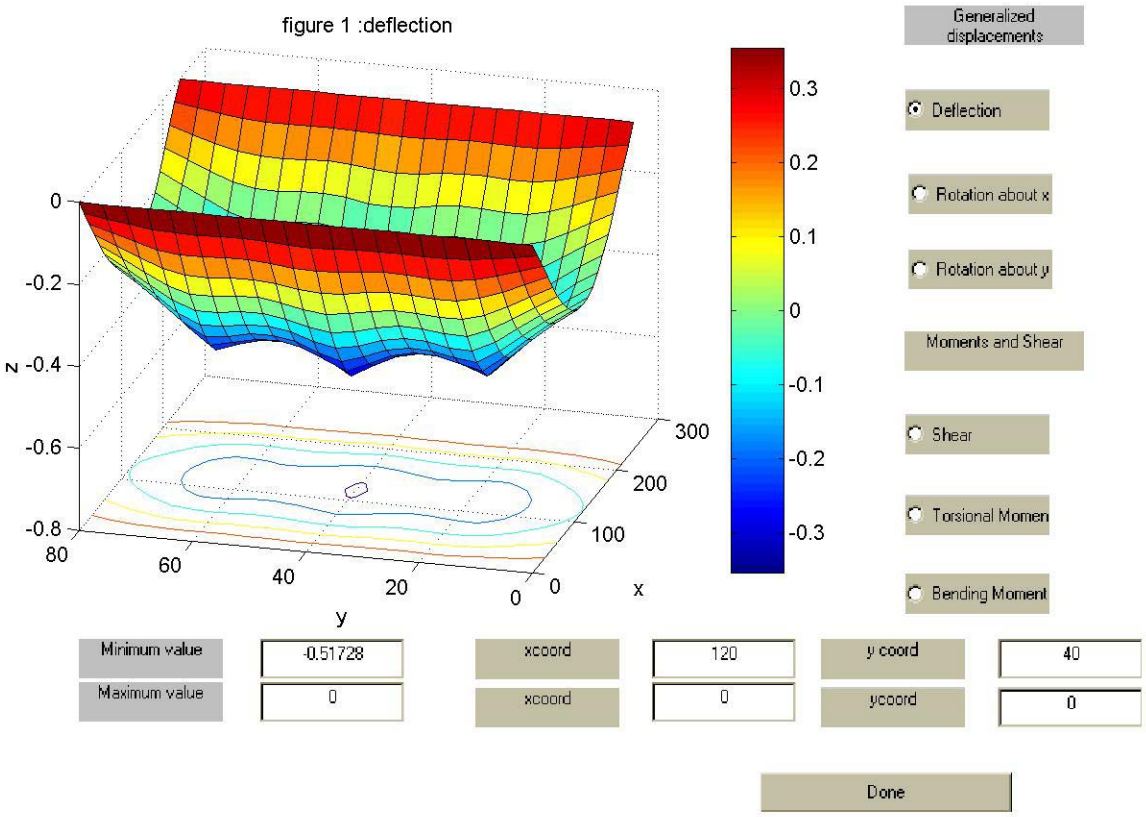

Figure 4.16. Deflections; Center Load, One TSB.

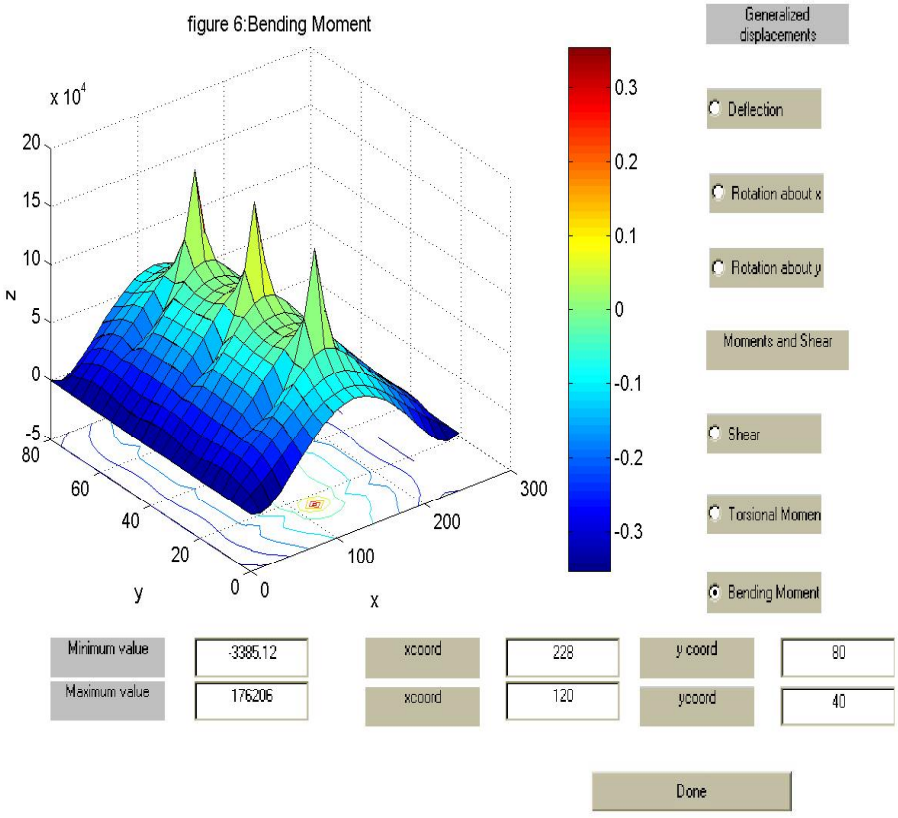

Figure 4.17. Bending Moments in Planks; Center Load, One TSB.

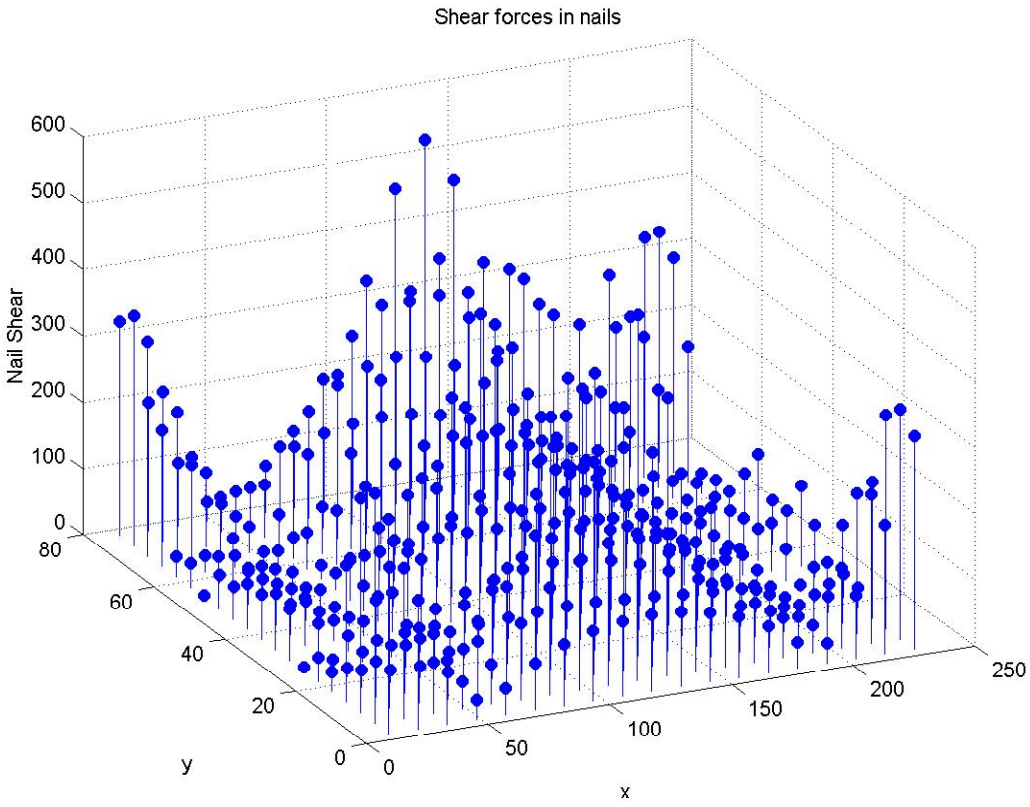

Figure 4.18. Resultant Shear Forces in Nails; Center Load, One TSB.

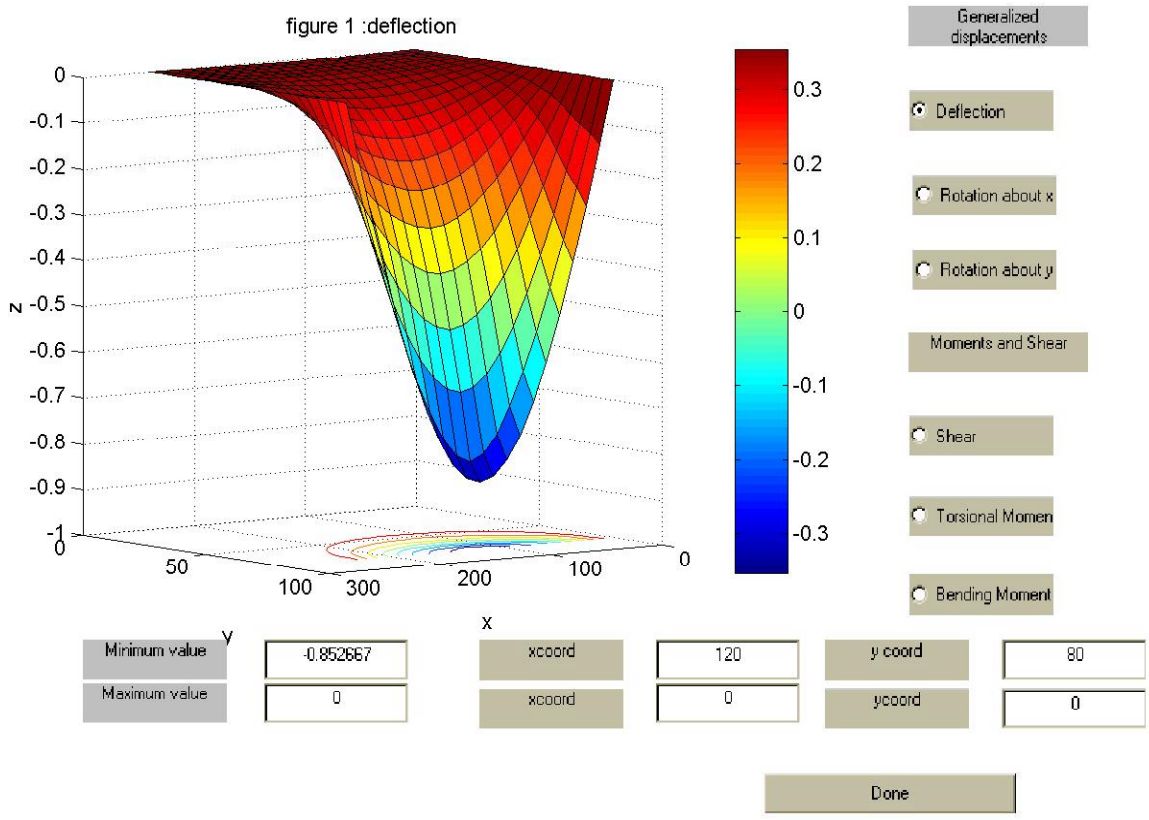

Figure 4.19. Deflections; Edge Load, no TSB.

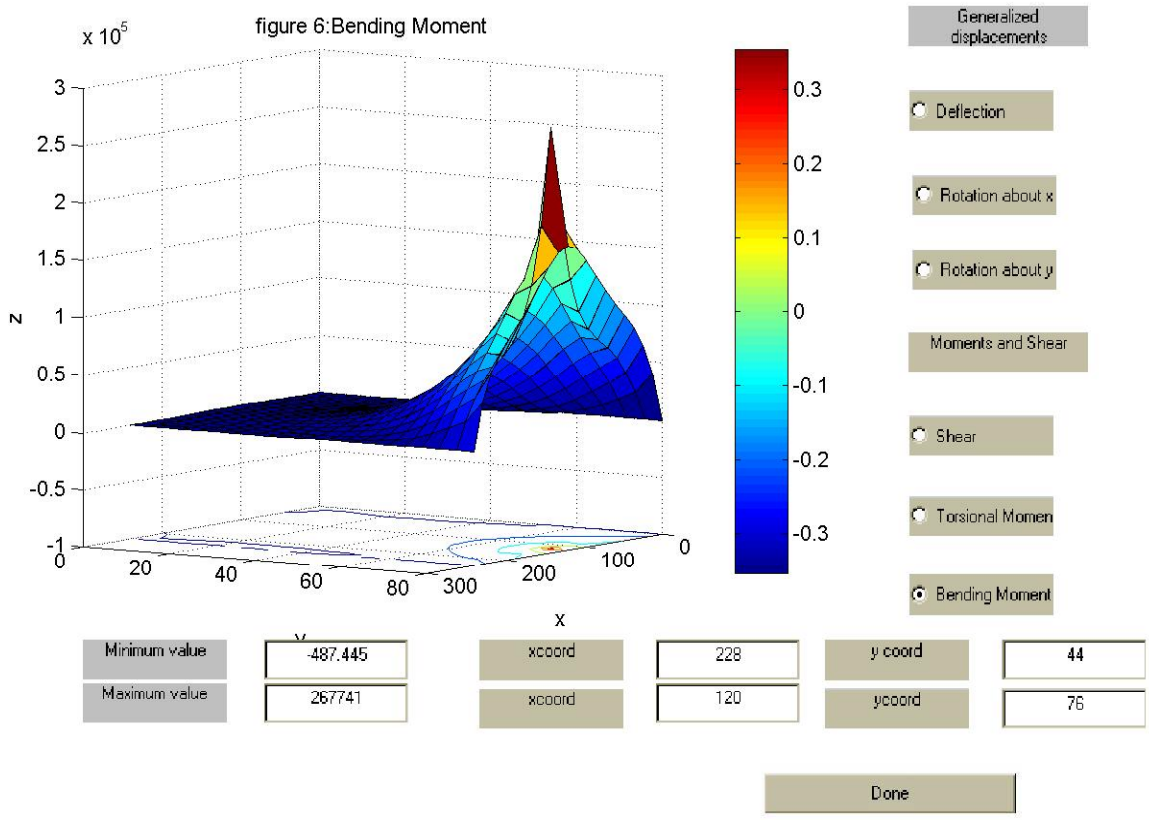

Figure 4.20. Bending Moments in Planks; Edge Load, no TSB.

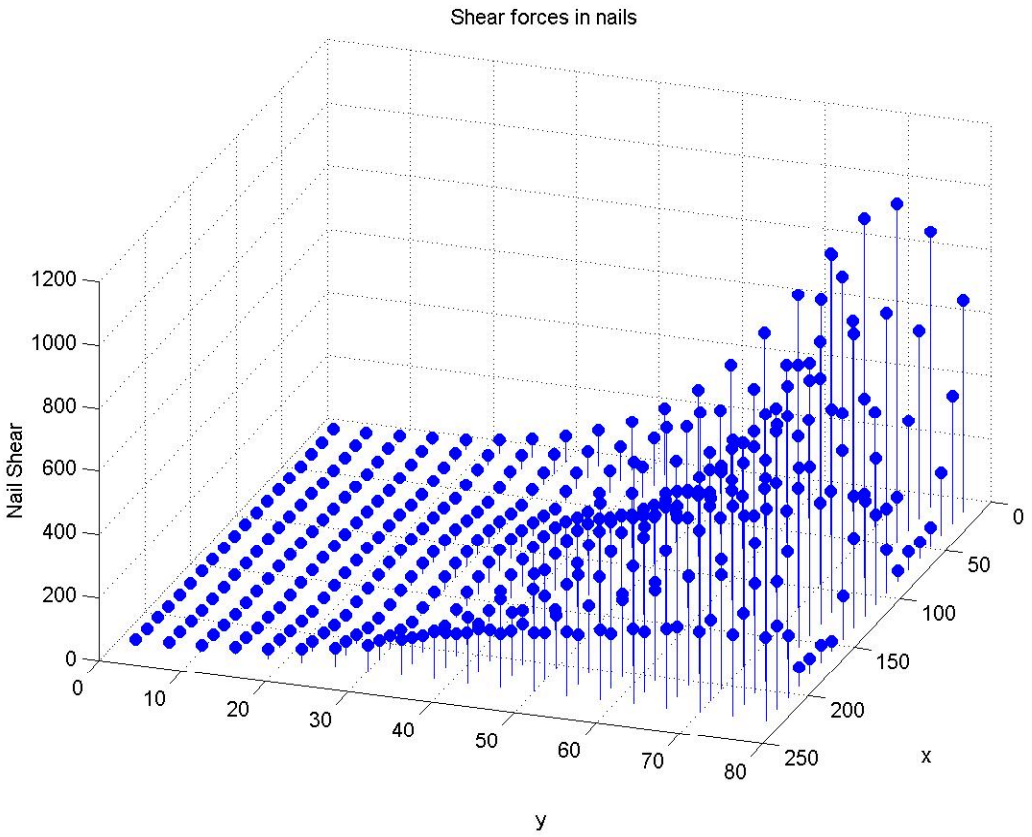

Figure 4.21. Resultant Shear Forces in Nails; Edge Load, no TSB.

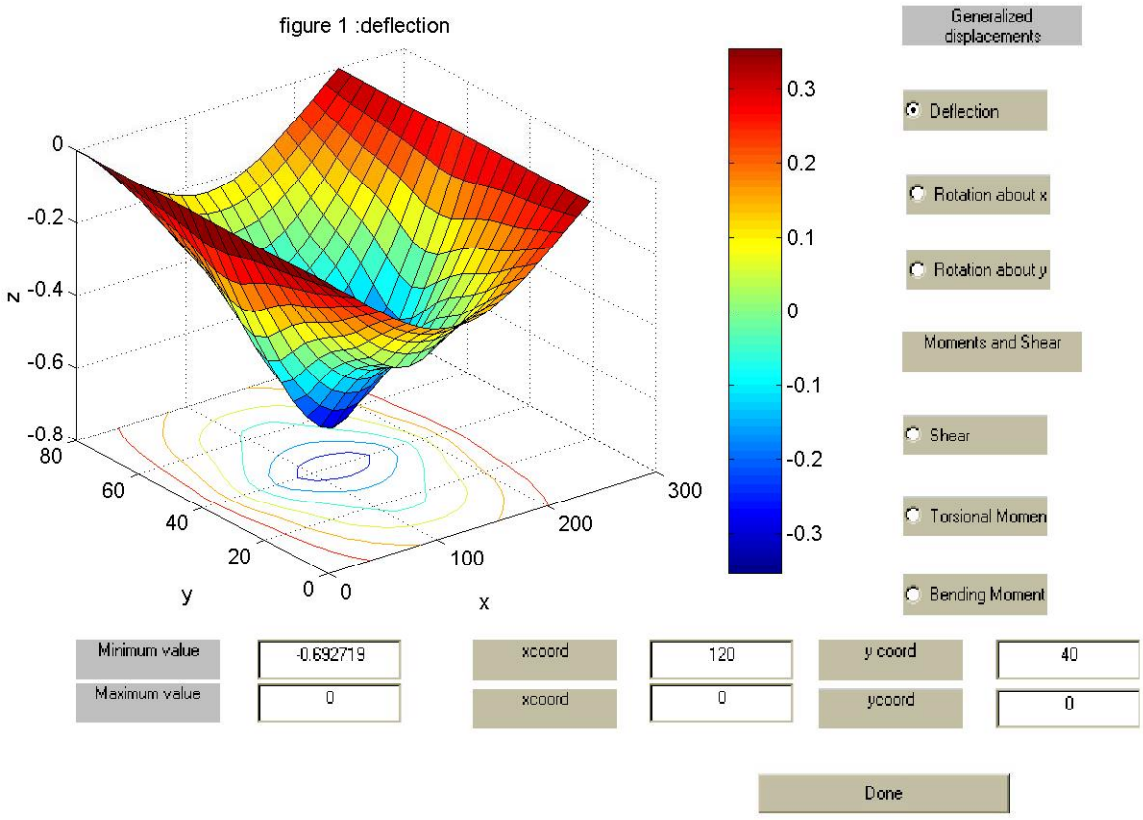

Figure 4.22. Deflections; Center Load, One TSB with no Rotation Compatability

Table 3.1: Testing Sequence

Test Type	Test Number	Load Point	# of TSBs Attached
Static	017	East	0
		Center	0
		West	0
	024	East	1
		Center	1
		West	1
	028	East	3
		Center	3
		West	3
	034	East	0
		Center	0
		West	0
Cyclic	043 - 069	West	0
Static	069	East	0
		Center	0
		West	0
	073	East	1
		Center	1
		West	1
	079	East	3
		Center	3
		West	3
	081	East	0
		Center	0
		West	0

Table 4.1 Effective Widths at Midspan

Virgin Deck

Load	# of TSB	LVDT	δ (in)	b_E (in)	Δb_E (in)	% b_{act}	% Change
E (17k)	0	2C	1	17.0		20.2%	
E (17k)	1	2C	0.83	20.5	3.5	24.4%	4.1%
C (34k)	0	11C	1.05	32.4		38.5%	
C (34k)	1	11C	0.79	43.0	10.7	51.2%	12.7%
W (17k)	0	20C	1.17	14.5		17.3%	
W (17k)	1	20C	0.97	17.5	3.0	20.9%	3.6%

After Cycling

Load	# of TSB	LVDT	δ (in)	b_E (in)	Δb_E (in)	% b_{act}	% Change
E (17k)	0	2C	1.03	16.5		19.6%	
E (17k)	1	2C	0.81	21.0	4.5	25.0%	5.3%
C (34k)	0	11C	1.11	30.6		36.5%	
C (34k)	1	11C	0.81	42.0	11.3	50.0%	13.5%
W (17k)	0	20C	1.21	14.0		16.7%	
W (17k)	1	20C	0.91	18.7	4.6	22.2%	5.5%

Table 4.2 Effective Widths at a Distance L/8 (2.5 ft.) from Midspan

Virgin deck

Load	# of TSB	LVDT	δ (in)	b_E (in)	Δb_E (in)	% b_{act}	% Change
E (17k)	0	2MS	0.89	17.5		20.8%	
E (17k)	1	2MS	0.76	20.4	3.0	24.3%	3.6%
E (17k)	3	2MS	0.73	21.3	0.8	25.3%	1.0%
C (34k)	0	11MS	0.92	33.8		40.2%	
C (34k)	1	11MS	0.69	45.0	11.3	53.6%	13.4%
C (34k)	3	11MS	0.66	47.1	2.0	56.1%	2.4%
W (17k)	0	20MS	0.96	16.2		19.3%	
W (17k)	1	20MS	0.8	19.4	3.2	23.1%	3.9%
W (17k)	3	20MS	0.78	19.9	0.5	23.7%	0.6%

After Cycling

Load	# of TSB	LVDT	δ (in)	b_E (in)	Δb_E (in)	% b_{act}	% Change
E (17k)	0	2MS	0.92	16.9		20.1%	
E (17k)	1	2MS	0.74	21.0	4.1	25.0%	4.9%
E (17k)	3	2MS	0.68	22.9	1.9	27.2%	2.2%
C (34k)	0	11MS	0.98	31.7		37.8%	
C (34k)	1	11MS	0.71	43.8	12.1	52.1%	14.4%
C (34k)	3	11MS	0.67	46.4	2.6	55.2%	3.1%
W (17k)	0	20MS	0.95	16.4		19.5%	
W (17k)	1	20MS	0.72	21.6	5.2	25.7%	6.2%
W (17k)	3	20MS	0.68	22.9	1.3	27.2%	1.5%

APPENDIX A

USER MANUAL
AND GRAPHICAL USER INTERFACE

A1. **Coordinate System and Node Numbering Scheme**

The selection of the coordinate system is closely tied to the numbering scheme for planks, nodes and TSBs. Understanding of that scheme is essential for correct interpretation of the results. This scheme is presented here again for the benefit of the users of the program.

The program is built assuming that the x-axis is aligned with the axes of the planks, y-axis is located in the plane of the bridge deck and is perpendicular to the planks, and z-axis is vertical and such that (x,y,z) form a right-handed system. This is depicted in Fig. A1.

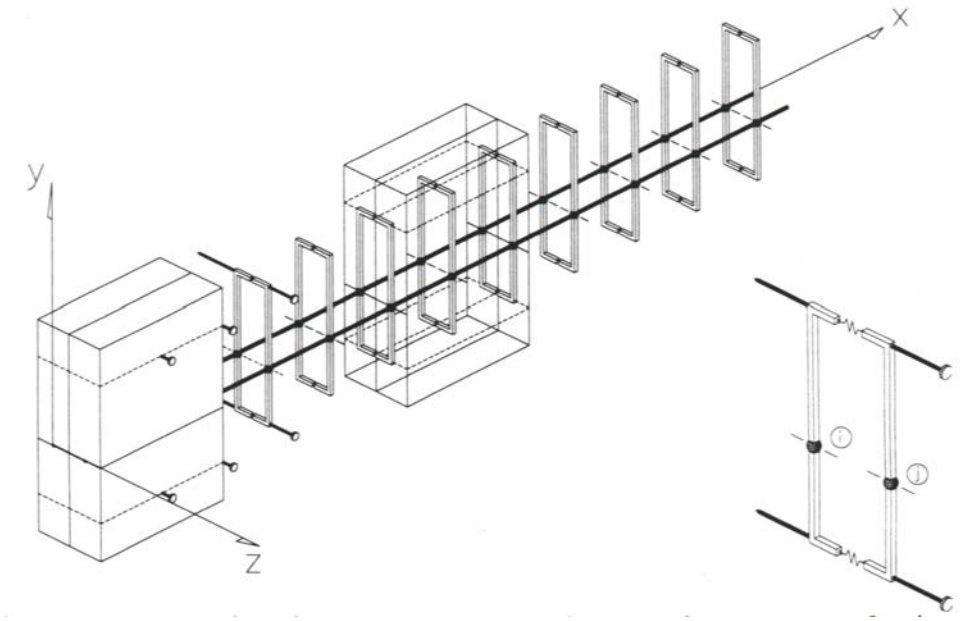

Fig. A1 Coordinate System Used in the Program.

The numbering of planks, nodes, nail connections, and TSBs relates to the selected coordinate system (x,y,z) . Planks are numbered consecutively, starting with the ones whose y-coordinate is the least. Nodes are located at every nail connection and at the ends of the planks. Their numbers increase along each plank with the increasing x-coordinate of the node (see Fig. A2). Node numbering starts with plank 1, then continues along plank 2, then plank 3, etc. A numbering system identical to that used for the nodes is also used for the nail connectors, which are located between the nodes of any two neighboring planks. Two nails, one at the top and one at the bottom, are assumed to exist at each nail connection. TSBs are numbered consecutively starting with the one whose x-coordinate is the smallest.

Sign convention of both input and output, is also related to the assumed coordinate system. On the input side, the load has to be entered as positive if it is directed along positive sense of the z-axis, negative otherwise. On the output side, one displacement and two rotations, at each node, have signs related to (x,y,z) coordinates. Positive displacement is along positive sense of the y-axis, whereas, positive x- and z-rotations are defined by the “right hand rule” and vectors representing those rotations are directed along positive direction of x- and z-axis, respectively.

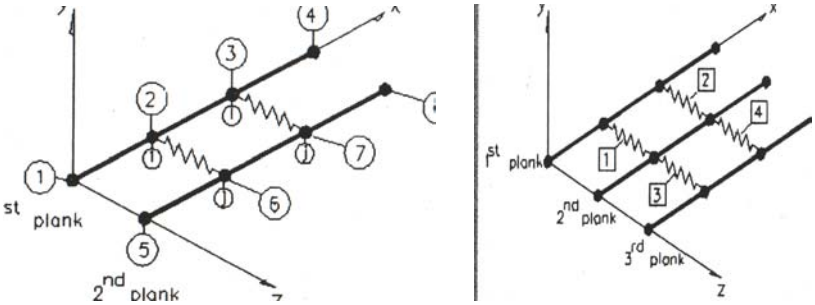

Fig. A2 Nodal and connection numbering

Internal forces in the planks and TSBs are defined applying standard rules of structural mechanics. In particular, positive bending moments are producing tension on the side located on their negative side with respect to z-axis (i.e., at the lower side of the beam).

A2. Input

Before running the program, the user needs to define the directory path for this program. This could be done by typing "**path(path,'a:'),** if the program is run from a disk at drive "**a,**" type **bridge** and the input menus will start.

The first page of the input "Graphical User Interface" (GUI) is for planks and nail connections, and it is shown on Fig. A3.

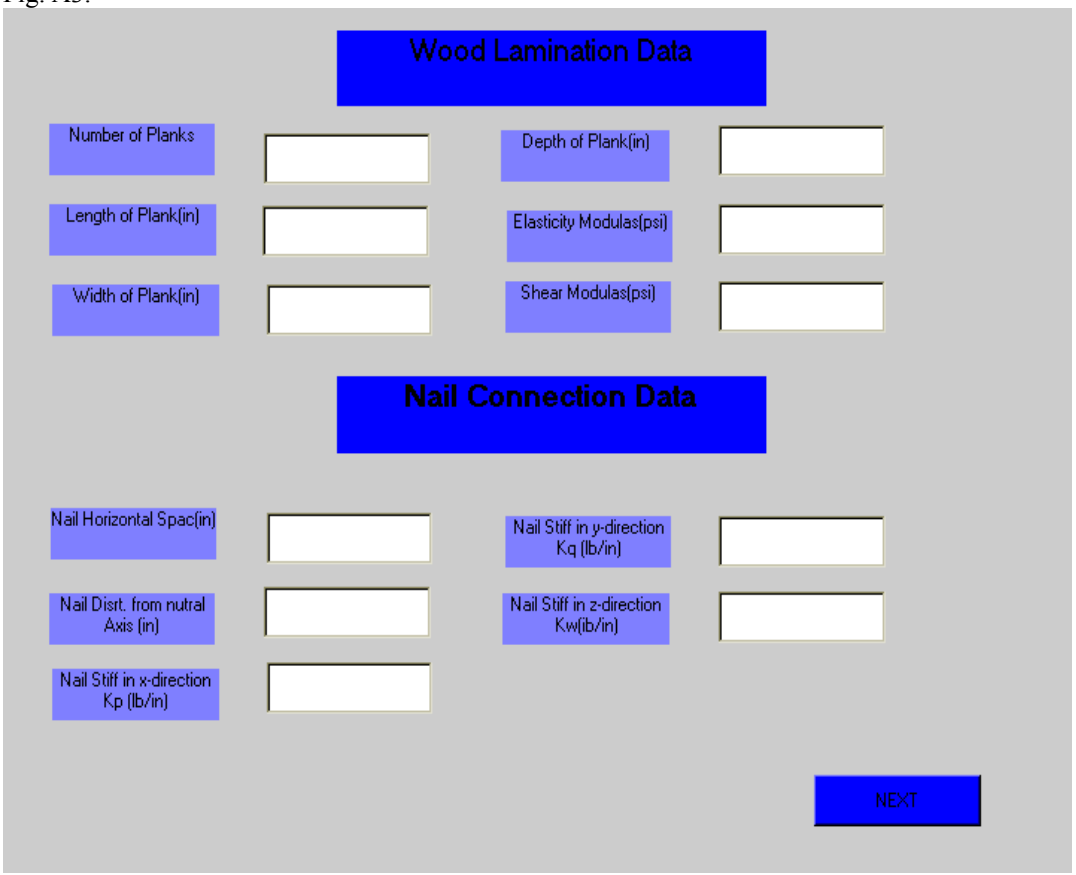

Fig. A3 Wood Lamination Data Page.

Each of the data windows on Fig. A3 is accessed by clicking on it with a mouse button. Units used in the input are arbitrary, but they must be consistent (inches cannot be mixed with feet, for example). After inputing these data, click on "**NEXT**" and the Transverse Beam page will appear next. This page is shown on Fig. A4.

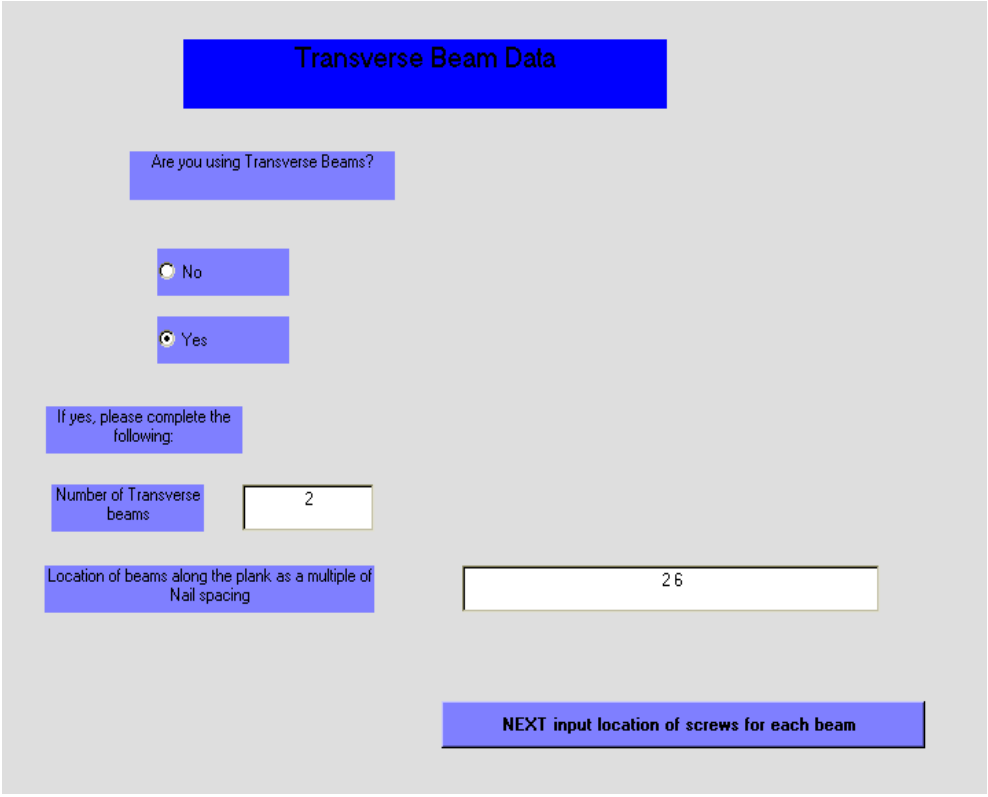

Fig. A4. TB General Data Page.

It requires the input of the number of TB's and the location along the plank where those TSB's are anchored. It is assumed that TSBs run along a sequence of nail connections. So, the location of each TSB is specified in terms of multiplicity of nail spacings from the beginning of the planks. The window "**Location of beams along the plank …**" should describe positions of all TSB's, so we write each position specification separated from the next specification by space. For example, on Fig. A4, we have two beams of which the first beam is located 2 nail spacings from the beginning, and the second is 6 nail spacings from the end.

In some circumstances, a TSB may be set slightly off a nail connection in which case, accepting some small error, it can be assumed to be located at a nearest row of nail connectors.

If there is no transverse beam clicking, "**No**" will take the user to the load page. This page is shown in Fig. A5.

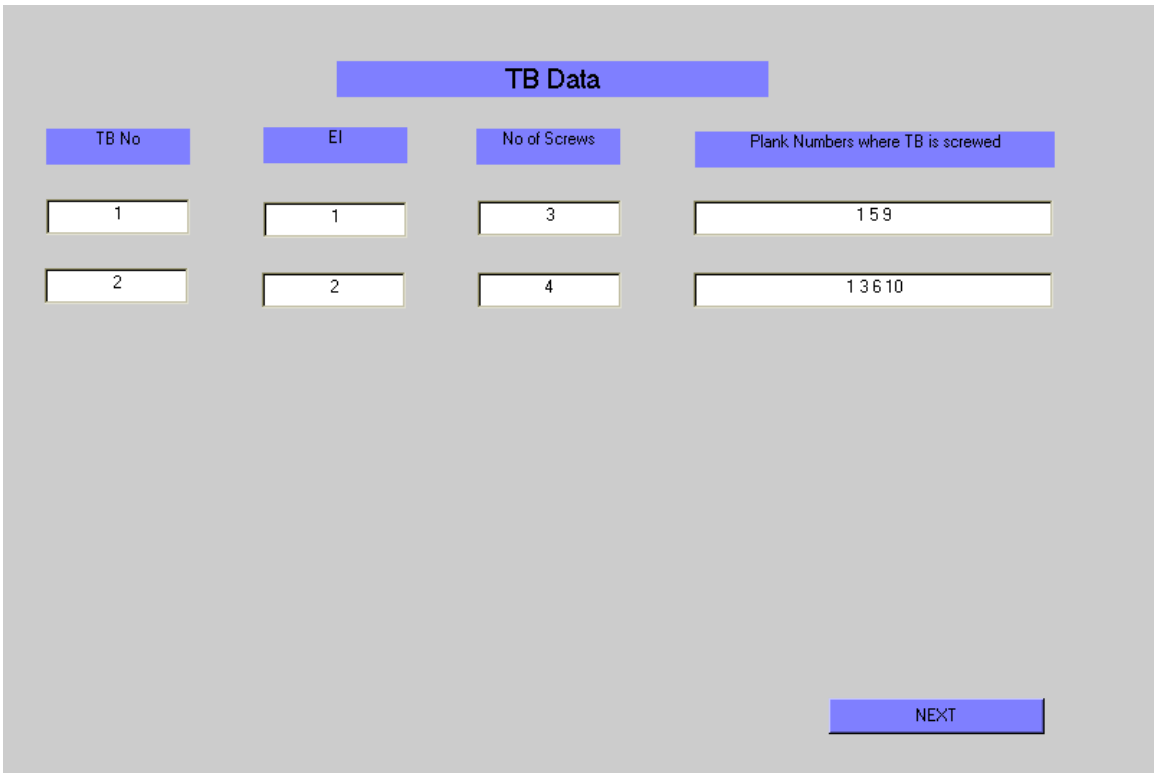

Fig. A5. TSB Data Page.

The plank numbers to which TSB is attached by a screw are listed in the last data window for each TSB; these numbers should be separated by a "space." For example, on Fig. (A), the TSB 2 is connected to the planks 1,3,6 and 10. The number of windows on Fig. A5 will correspond to the number of TSBs specified on the previous page. The next page is the one asking about the number of loads, Fig. 6.

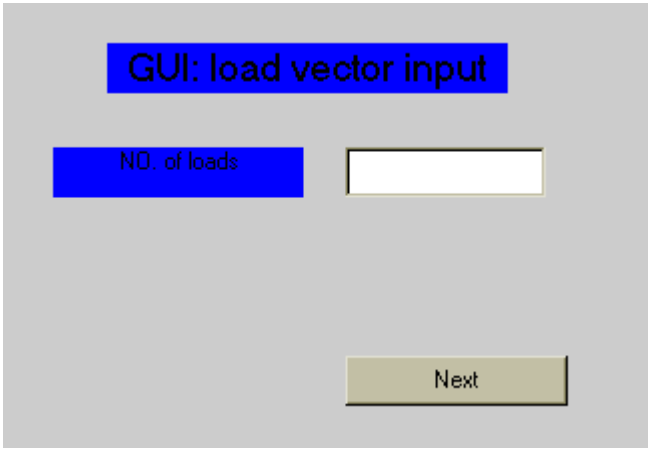

Fig. A6 Load Vector Page #1.

This is followed by a page specifying the magnitude and location of each load, Fig. A7.

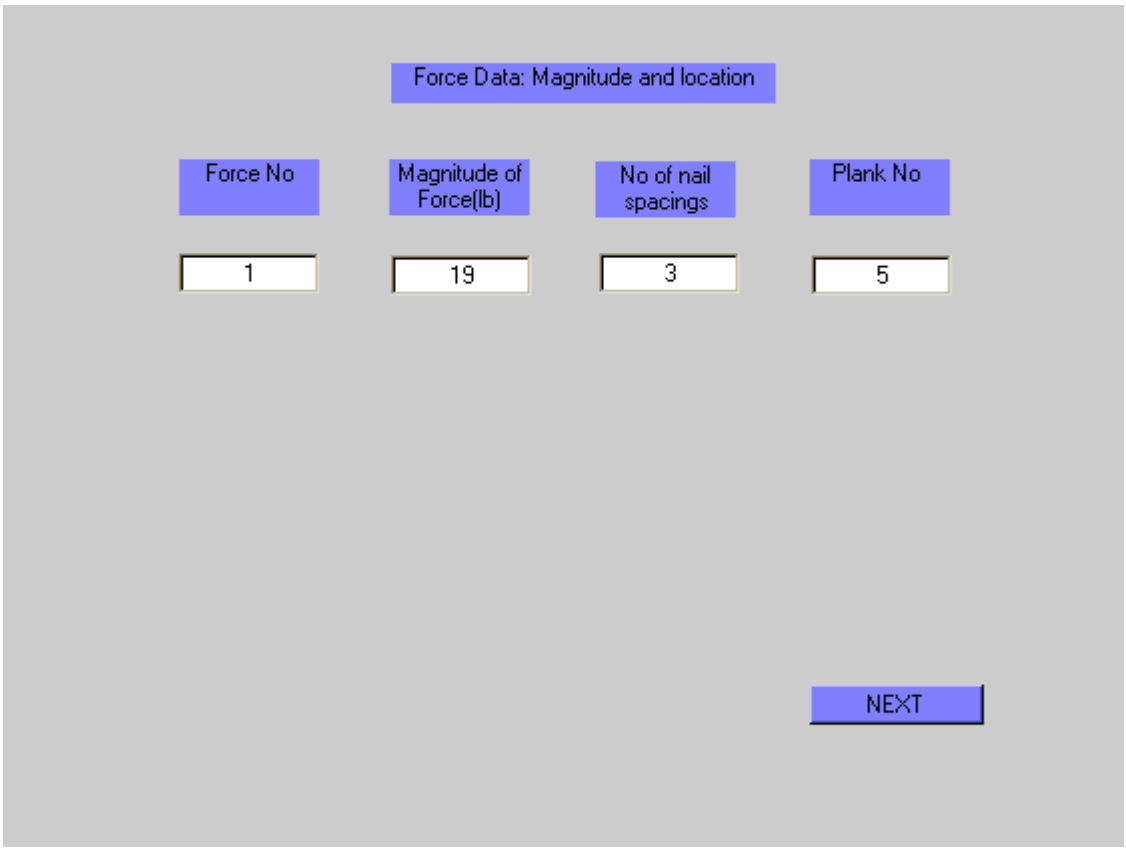

Fig. A7. Load Data Page #2.

As can be seen on Fig. (f), it is assumed that location of a concentrated load is restricted to a node. That is why this location is defined by the plank number and by the number of the nail spacing from the end of the plank (the one having smaller x-corrdinate). There may be a huge number of other loading scenarios, not falling in the iteration described above. In this case, the user has to make a rational, engineering decision about how this load should be assigned to particular nodes. Given the fact that there is no limit on the number of nodal loads, and relatively large numbers of nodes per unit area of the deck, any load on the bridge can be represented by nodal forces with good engineering accuracy.

Page shown in Fig. A7 of the input and will stay on screen until the program finish running.

A3 Output

Any time the user wants to access the output, the user needs to type "**result"** which causes the display of the output master page, Fig. A8.

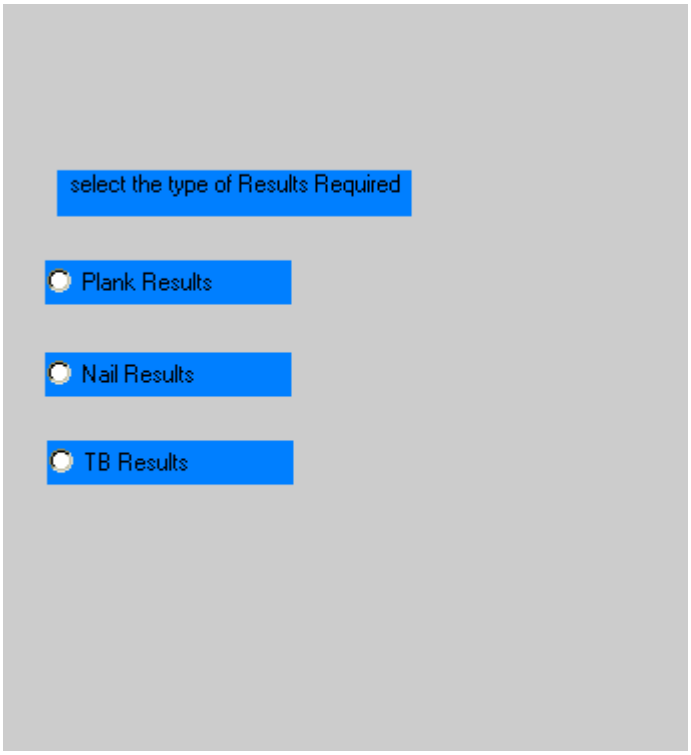

Fig. A8 Master Output Page.

Clicking on the appropriate white dot (radio button) will cause the corresponding output page to appear.
For example, the response to selecting the first radio button which corresponds to the plank output will result in displaying the page shown in Fig. A9.

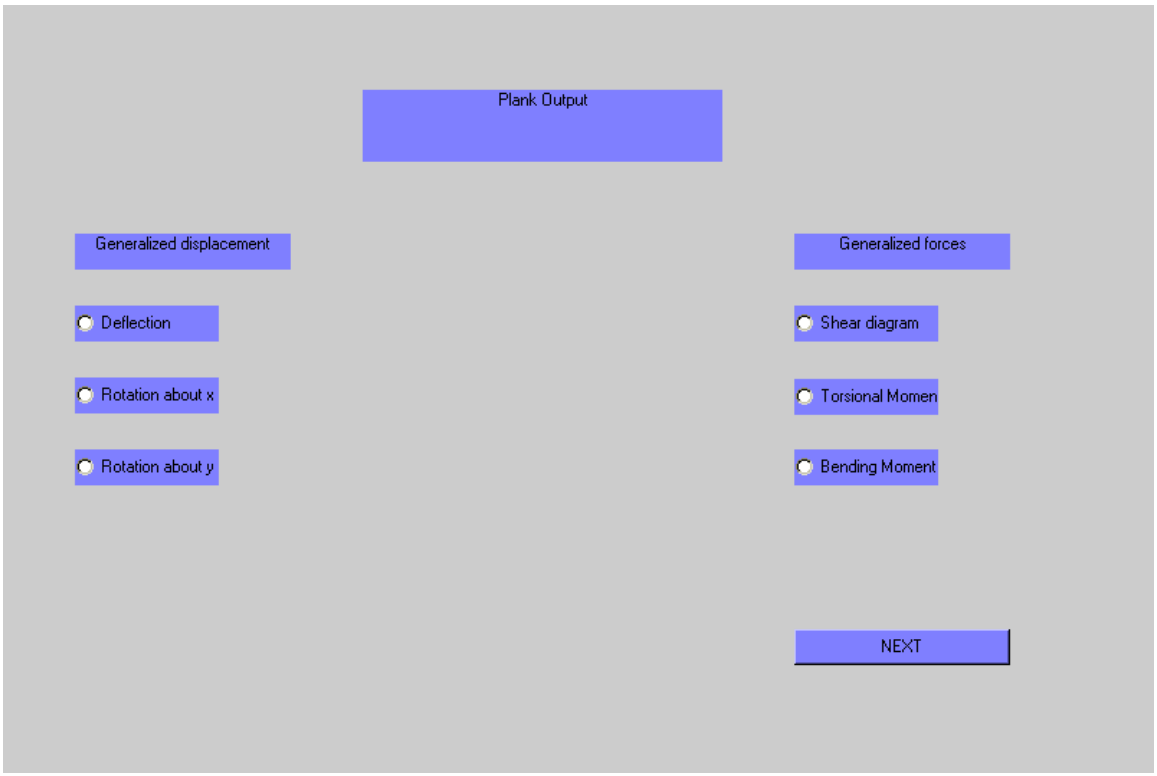

Fig. A9 Plank Output Page.

This page will allow the user to choose the results he needs. For example, selecting "**Shear**" will display the plot of shear force distribution on all planks, as illustrated on Fig. A10. This figure also presents minimum and maximum values on the plot (corresponding to their figures) along with their location.

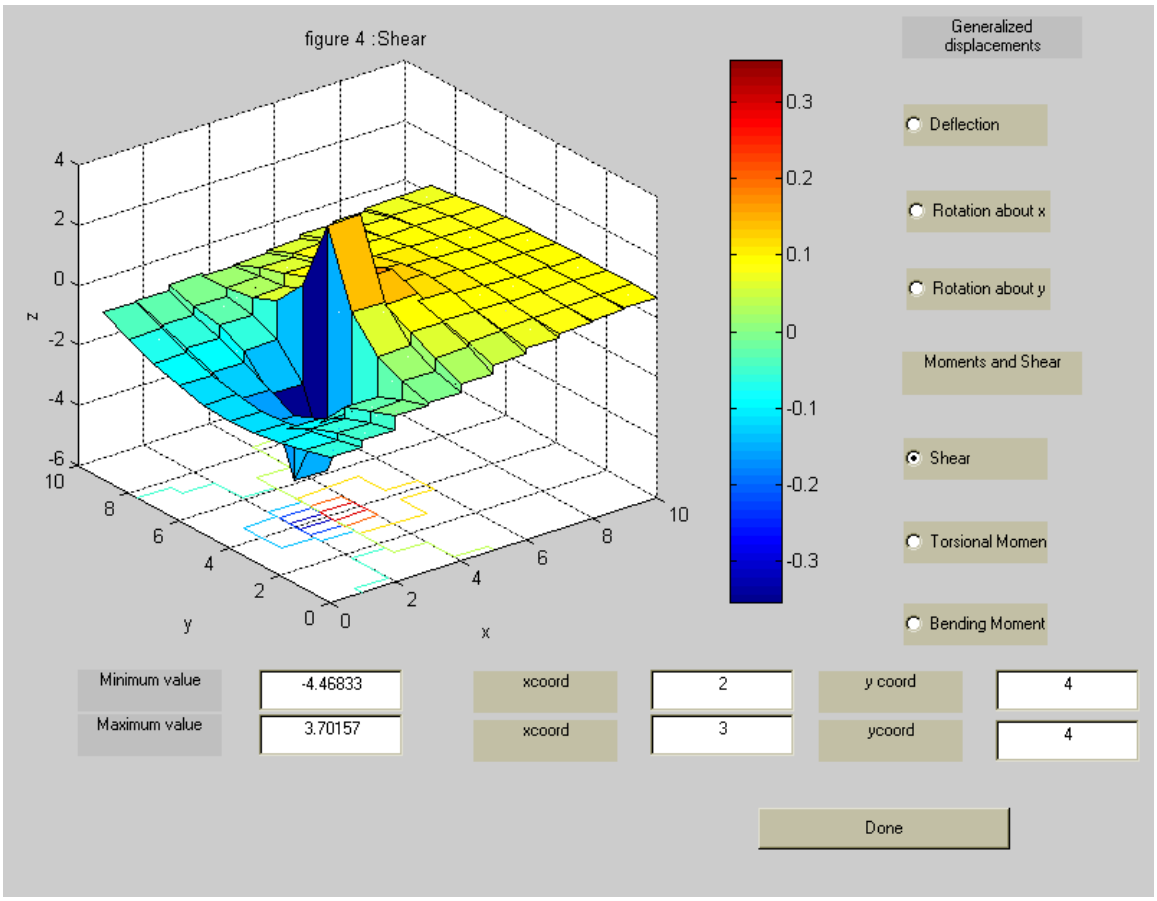

Fig. A10. Shear Force Distribution in the Planks.

It should be noted that one can rotate the figure in three dimensions using the mouse so the user can see the figure from any angle. One can also switch to other results, such as deflection, rotation, moment or torque by clicking on the appropriate choice, shown on the righthand side of the page, like the one shown on Fig. A10.

After selecting nail results the page shown on Fig. A10 will be displayed:

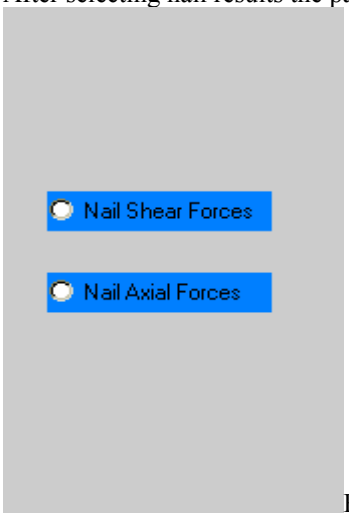

Fig. A11. Nail Output Page.

Selecting, for example the "**Nail Shear Force**" radio button, the following page will be displayed. The values on that page represent total shear force magnitude, which is the magnitude of the resultant of the shear forces in x and z directions. Similar plot, but representing axial forces, is displayed after selecting the other radio button.

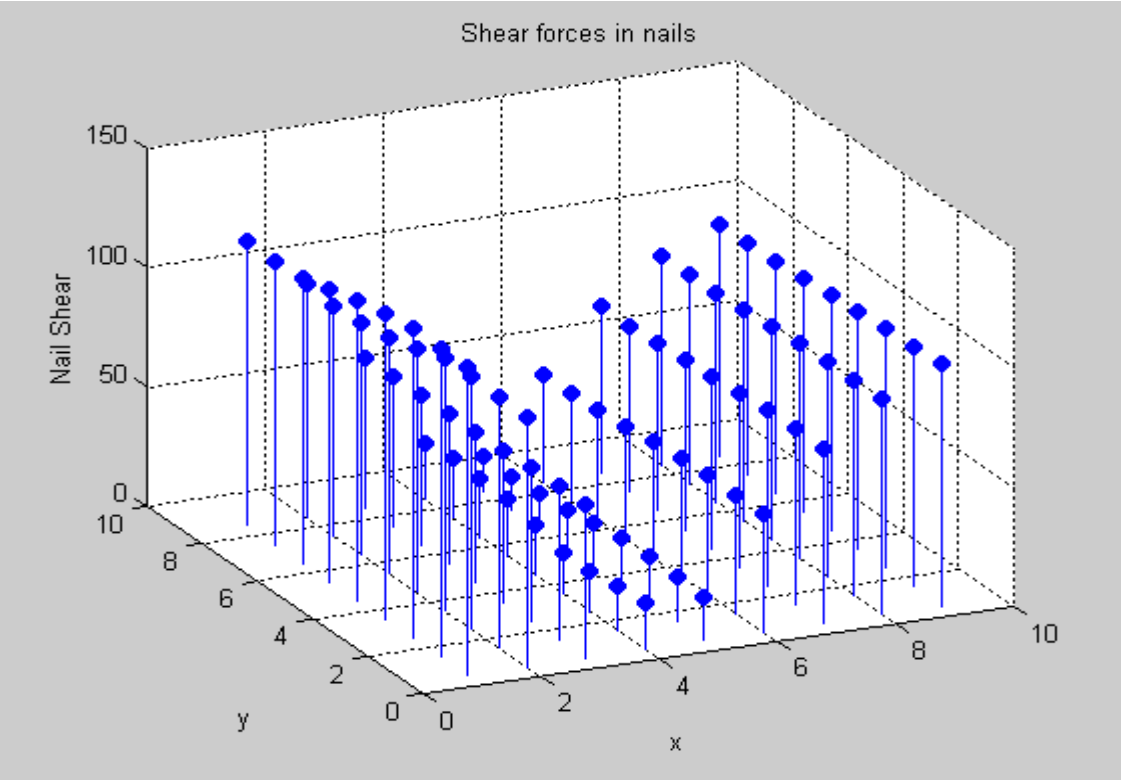

Fig. A12. Nails Shear Forces Output.

By selecting "**TB results,**" the following page, shown on Fig. A12, will be displayed.

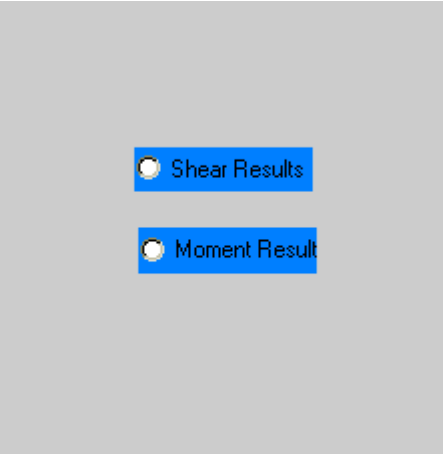

Fig. A13. Master Page for TSB Output.

The "Moment **Results**" radio button leads to the page shown on Fig. A14. This page will be gradually filled up when the specification of the derived plot is made. For example, referring to Fig. A14, after inputting the TB number of the desired beam equal to 1 and clicking "**process,**" Fig. A14 will be modified and will look like Fig. A15.

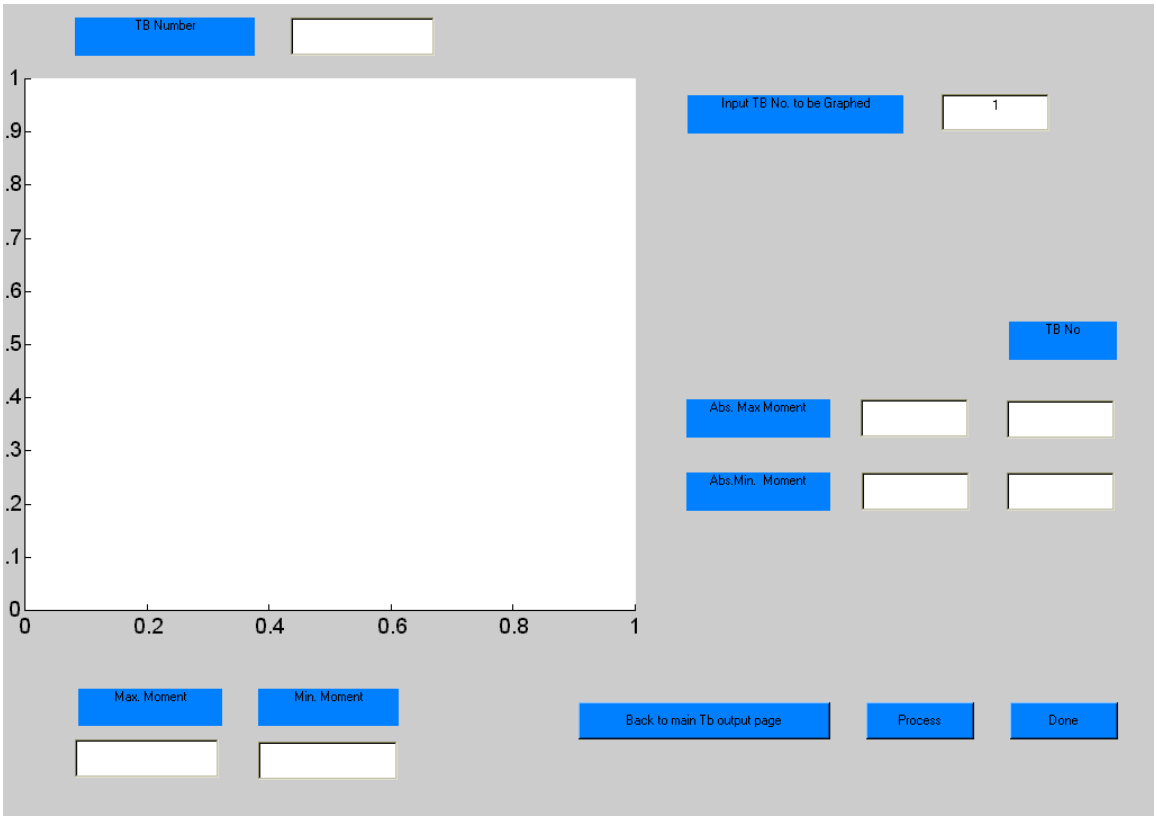

Fig. A14. TSB Plot Page 1.

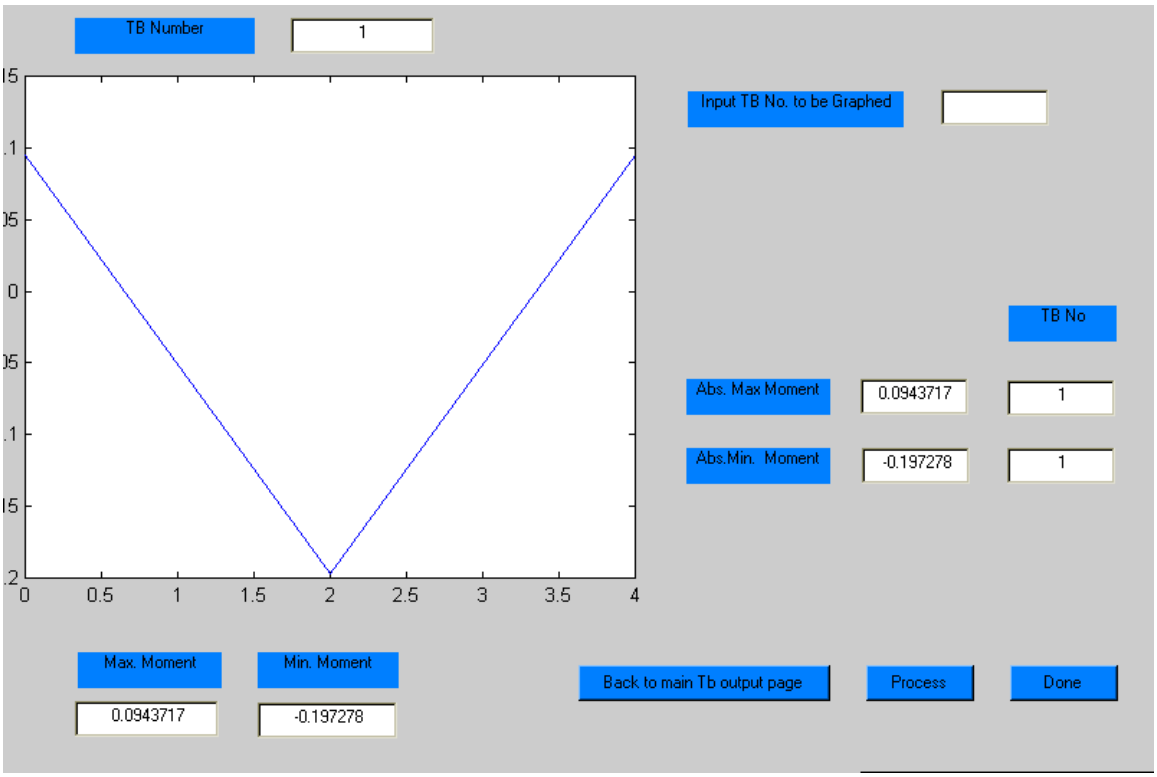

Fig. A15. TSB Plot Page 2.

The above presentation, done only for illustration, involved certain specific choices. Other choices could be made and would result in slightly different outcomes. However, the principles and processes illustrated above apply to all other possible selections. They should be sufficient to obtain any desired output produced by the program.

APPENDIX B

DATA PAGES
FOR THE BRIDGE INVESTIGATED IN THE PROJECT

10. APPENDIX B.

DATA PAGES FOR THE BRIDGE SECTION INVESTIGATED IN THE PROJECT. (CENTER LOAD, ONE TSB CASE)

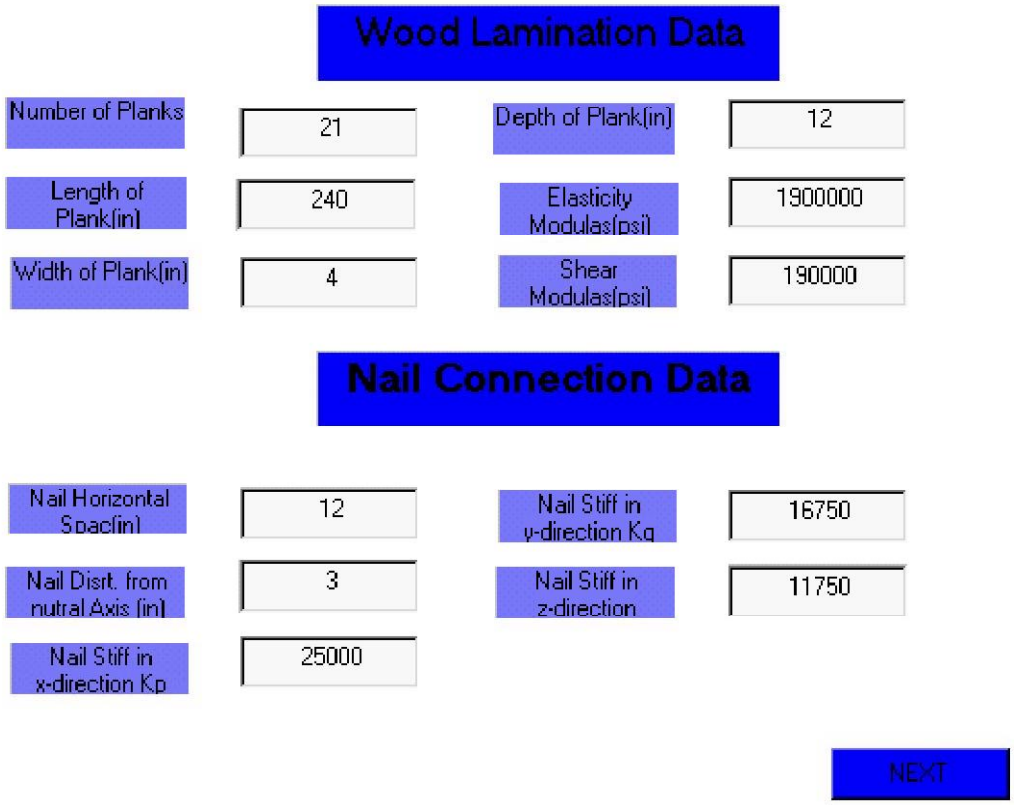

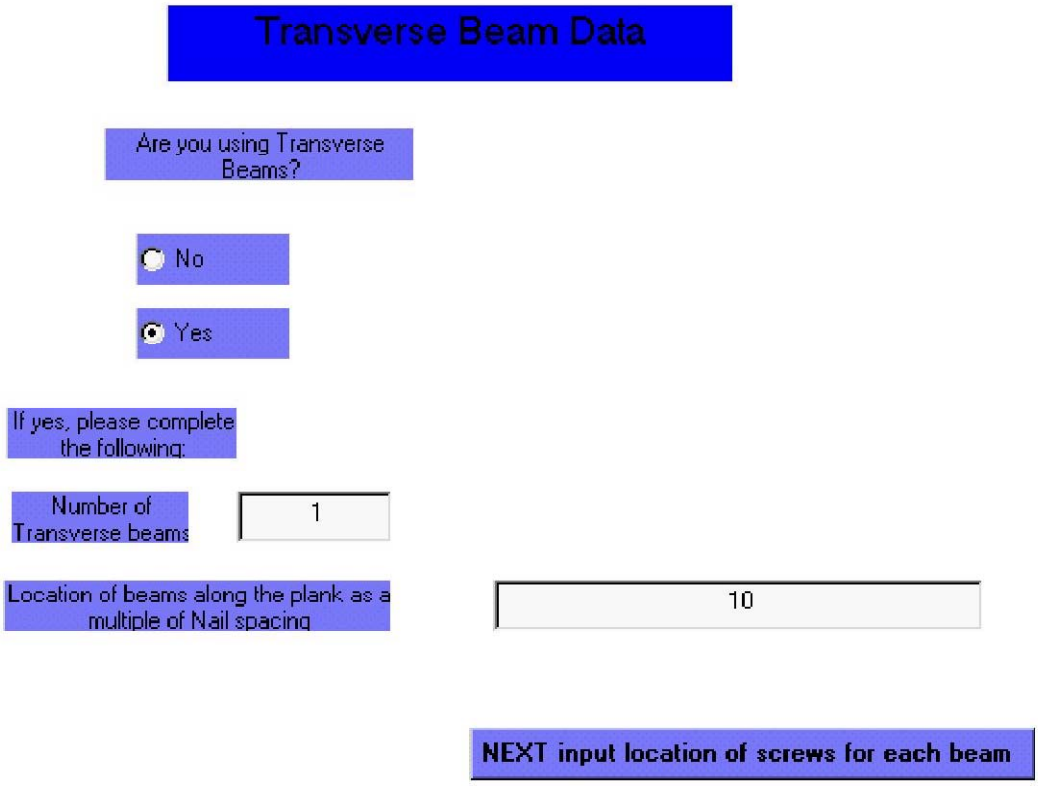
Transverse Beam Data
Are you using Transverse Beams?
No
Yes
If yes, please complete the following:
Number of Transverse beams
1
Location of beams along the plank as a multiple of Nail spacing
10
NEXT input location of screws for each beam

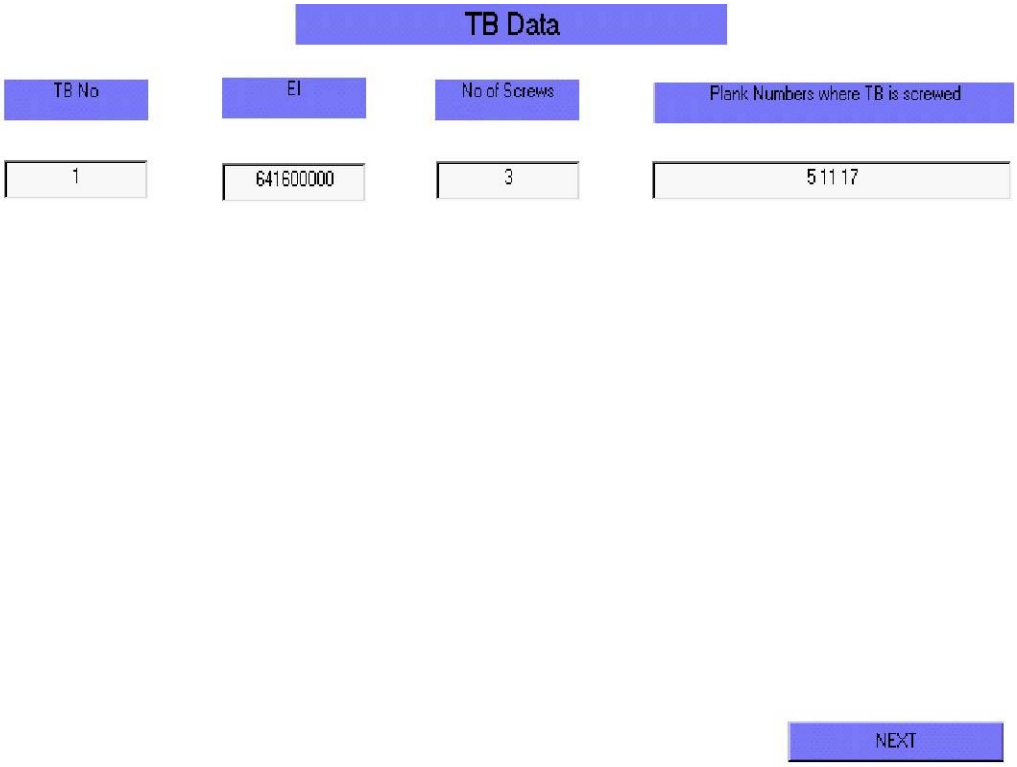
TB Data
TB No
EI
No of Screws
Plank Numbers where TB is screwed
1
641600000
3
5 11 17
NEXT

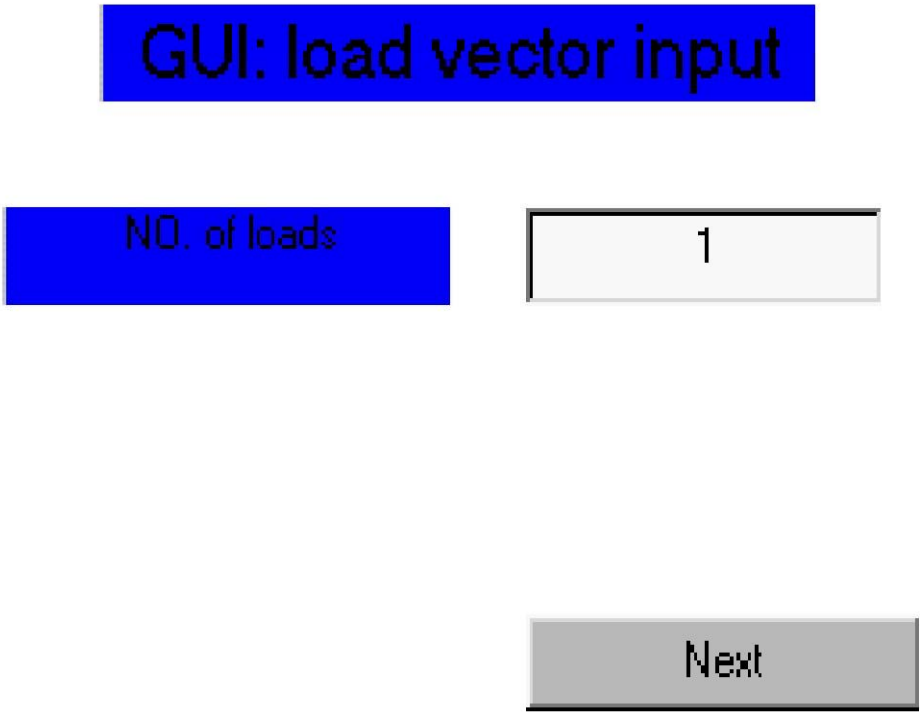
GUI: load vector input
NO. of loads
1
Next

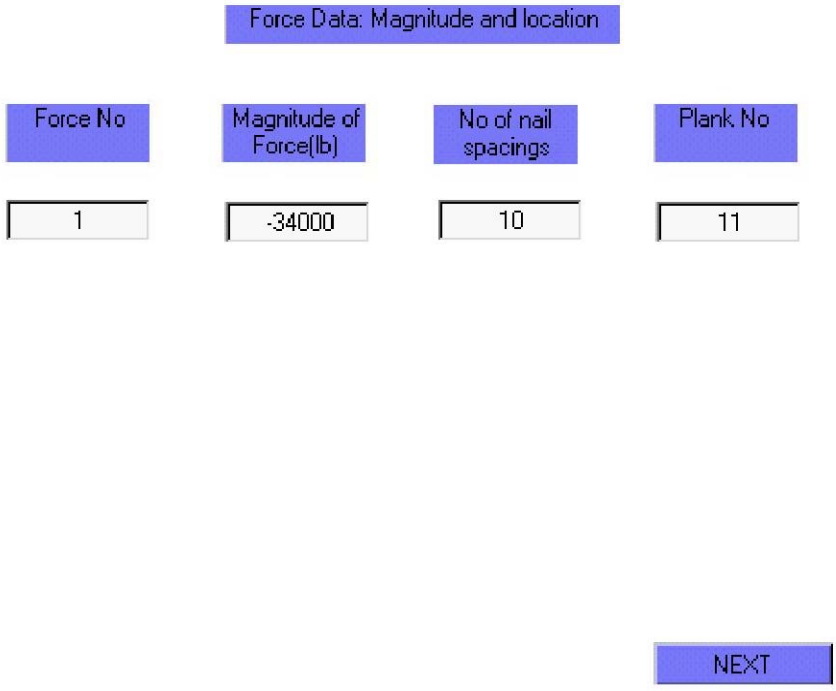
Force Data: Magnitude and location
Force No
Magnitude of Force(lb)
No of nail spacings
Plank No
1
-34000
10
11
NEXT